

GASES

1.1 STATISTICS OF MOLECULES

Historically, “gas,” the gaseous phase of matter, was studied and understood before all other phases. It remains as one of a few rigorously treated systems, and therefore successful statistical interpretation of other phenomena often depends on the possibility of reducing them to a gas model. For example, a solid may be adequately represented by a mixture of electron and phonon gases. Liquids are difficult to describe qualitatively just because they cannot be modeled by a gas.

The idea that matter is composed of atoms goes back to the Greek philosophers, notably Democritus. While the existence of atoms remained just a hypothesis, it was not so easy to develop a molecular model of a gas; however, this was the only direction to take that was at all feasible. The basic features of the model are suggested by the well-known gas properties: a tendency to expand indefinitely in free space and to exert pressure on the walls of a vessel (“container”). An ensemble of infinitesimal solid spheres—point masses—would behave similarly. Having definite translational energy, the point masses would absolutely fly out, if the opportunity arose, and exert pressure on any wall met on their way. This qualitative picture could be made quantitative, if anybody could calculate the equilibrium pressure value to show that it complied with the ideal gas equation of state: $pV = RT$, where V is the volume of one mole of a gas, p is its pressure, T is the temperature, and R is the gas constant.

Pressure

If a gas is an ensemble of randomly moving point masses, then many of them collide with a wall all the time. In the i th collision the wall obtains an elementary momentum Δp_i . According to the law of conservation of momentum this is exactly equal to the change in the molecule's momentum in this i th collision against the wall. The force acting on a wall is the total momentum imparted to the wall by all collisions that happen per second:

$$F = pS = \overline{\sum_i \Delta p_i}, \quad (1.1.1)$$

where S is the area of the wall.

This force is not constant, but varies randomly (“fluctuates”) in time. Similarly, the pressure differs at from moment to moment although it fluctuates around a constant value if the gas is in an equilibrium state. The line above $\sum_i \Delta p_i$ denotes averaging, so by macroscopic pressure we imply the average over all possible values of the random variable. Since a gas consists of a great number of molecules, under equilibrium conditions any measurement, no matter when it is taken, cannot differ essentially from the mean. Noticeable deviations (fluctuations) in any large ensemble are very rare, as, for example, an accidental concentration of passengers in one airport when all other airports are empty. Besides, the sluggish response of measuring instruments smooth out most of the deviations themselves by not following very fast fluctuations of $\sum_i \Delta p_i$. Although the pointer of the instrument still “fluctuates” following slow variations of the value being measured, the obtained result is just the mean about which the readings fluctuate. Any macroscopic value is always the average of many microscopic values. With this in mind, henceforth we shall omit the sign of averaging, and the words “number of collisions” striking the wall, as well as “number of molecules” with a definite velocity, and so on will be used only in the sense of their mean values.

Though identical molecules represented by point masses lack almost any specific features, they should be distinguished by one very important parameter, namely, the velocity of motion. For example, when a molecule moves towards a wall perpendicular to the x axis, its velocity along this axis determines the magnitude of momentum imparted to the wall upon collision. If the collision is elastic: $v'_y = v_y$; $v'_z = v_z$; $v'_x = -v_x$ (the primed symbols indicate the velocity after collision, the unprimed symbols before it), then

$$\Delta p_x = mv_x - mv'_x = 2mv_x. \quad (1.1.2)$$

To calculate the pressure one has to know the number of collisions with the wall that occur per unit time with a velocity v , which is greater than v_x but less than $v_x + dv_x$. If $dN(v_x)$ is the number of such collisions from a total number

of impacts per second $N = \int dN(v_x)$, then the force acting on a wall can easily be determined to be

$$F = pS = \int 2mv_x dN(v_x). \quad (1.1.3)$$

The number of collisions with such a rigidly limited velocity is infinitesimal as compared to N . This justifies the designations dN (not ΔN) and integration, instead of summation, of momenta imparted to the wall by molecules with different “attack” velocities.

Now, if we select the subensemble of molecules with some particular velocity v_x , it becomes evident that number of their collisions with a wall is

$$dN(v_x) = Sv_x dn(v_x). \quad (1.1.4)$$

In the notation accepted here, $dn(v_x)$ denotes “a small fraction of molecules” (from the total number per unit volume n) moving towards the wall with a velocity that lies between v_x and $v_x + dv_x$. The estimate (1.1.4) is similar to counting rain drops falling on the surface of the area S per second. Rain drops which are at a distance of more than v_x from the surface have no time to reach it. Only those confined in a parallelepiped with the base S and height v_x (Fig. 1.1) will succeed. Their number is equal to the volume Sv_x multiplied by the density $dn(v_x)$. As v_x is the same for all drops, it makes no difference whether the rain is slanted or straight. Therefore the molecular “rain” may be classified by only one variable—the value of v_x , because after that we can apply Eq. (1.1.4) to each group of molecules. Using it in Eq. (1.1.3) we find

$$p = \int_0^\infty 2mv_x^2 dn(v_x) = 2mn \int_0^\infty v_x^2 dW(v_x), \quad (1.1.5)$$

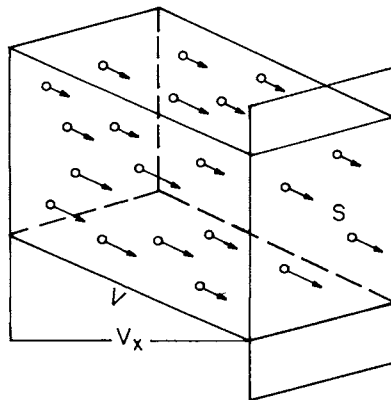


Figure 1.1 Molecules of the same velocity \mathbf{v} , which impact with an element of area S of a wall per second. The arrows are unit vectors with direction of the velocities.

where integration is extended to all molecules moving towards the wall ($v_x > 0$). Of course, v_x cannot exceed the speed of light c . Since such rapid molecules are usually very few, they actually do not contribute to the integral so the integration may be extended to infinity, provided that temperatures are not too high.

Statistical Distribution

Equation (1.1.5) gives a microscopic, kinetic definition of pressure. The quantity involved

$$dW(v_x) = \frac{dn(v_x)}{n} \quad (1.1.6)$$

is a “probability of finding a molecule moving with the velocity v_x .” It denotes the fraction of particles (from the total number per unit volume n) possessing the required property, that is, having a velocity in a small interval dv_x around the defined value. The number of molecules may be different in different intervals of the same size, but having tried all the possibilities, we count all molecules per unit volume: $\int dn(v_x) = n$. Similarly, the probability of finding a molecule with a higher or a lower velocity is not equal, but the detection of a molecule moving somewhere and somehow is an authentic event whose probability is equal to unity:

$$\int dW(v_x) = \frac{\int dn(v_x)}{n} = 1 \quad (1.1.6a)$$

This is a probability distribution normalized to 1. In this sense $dn(v_x)$ may be considered as a distribution of particles normalized by their density. The option of using either the distribution of probabilities $dW(v_x)$ or that of particles $dn(v_x)$ depends on the problem, and, sometimes, on the specific properties of a gas.

In the absence of external fields (electric, magnetic, gravitational, etc.) there is no preference for any direction of motion. Thus molecules moving towards or away from the wall are to be observed equally often, and the probability $dW(v_x)$ of detecting them remains unchanged when v_x reverses sign. Consequently,

$$\int_0^{\infty} v_x^2 dW(v_x) = \int_{-\infty}^0 v_x^2 dW(v_x),$$

and

$$p = 2mn \int_0^{\infty} v_x^2 dW(v_x) = mn \int_{-\infty}^{+\infty} v_x^2 dW(v_x) = mn\overline{v_x^2}. \quad (1.1.7)$$

The Statistical Average

The averaged value of $F(a)$ is by definition

$$\overline{F(a)} = \int F(a) dW(a).$$

In Eq. (1.1.7) this definition was applied to $F(v_x) = v_x^2$. It implies that integration is performed over the whole domain of a random variable: $-\infty \leq v_x \leq \infty$ in our case.

Since there is no preference for any direction, $\overline{v_x^2}$ does not differ from either $\overline{v_y^2}$ or $\overline{v_z^2}$. No axis has an advantage over any another. Therefore,

$$\overline{v^2} = \overline{v_x^2} + \overline{v_y^2} + \overline{v_z^2} = 3\overline{v_x^2}$$

so Eq. (1.1.7) may be written as follows

$$p = \frac{1}{3} mn\overline{v^2} = \frac{2}{3} n \frac{m\overline{v^2}}{2} = \frac{2}{3} n\bar{c}. \quad (1.1.8)$$

To continue further is impossible without ascertaining the form of the probability (1.1.6).

However, by representing n as N/V , we can note the similarity between Eq. (1.1.7) and the ideal gas equation of state $pV = RT$:

$$pV = Nm\overline{v_x^2}. \quad (1.1.9)$$

The statement of the problem follows from the above equality. Its left-hand side coincides with the corresponding side of the equation of state. To calculate the right-hand side it is necessary, first, to know the velocity distribution, and, second, to perform the averaging of v_x^2 using this distribution.

1.2 DISTRIBUTION FUNCTION

To determine the distribution function is the primary goal of statistical physics. However, from where can we get information about it? Up until the mid-nineteenth century an experimental study of the velocity distribution was out of the

question. Even the very existence of atoms and molecules was still a hypothesis. Therefore it is surprising that only these *a priori* assumptions made by Maxwell from the basis of pure thought proved to be sufficient for the determination of this distribution.

Obviously, the number of molecules with a “definite” velocity depends on the accuracy of its determination. The smaller the interval of velocities ($v_x, v_x + dv_x$) the lower the probability of finding molecules moving with such velocities. The probability that a molecule will have a strictly specified velocity ($dv_x = 0$) is equal to zero. With this in mind, we can write for the isotropic space (where no direction is preferable):

$$dW(v_x) = f(v_x)dv_x, \quad dW(v_y) = f(v_y)dv_y, \quad dW(v_z) = f(v_z)dv_z, \quad (1.2.1)$$

where the distribution function $f(\xi)$ is the same for ξ either v_x , v_y , or v_z . The general relation

$$dW(a) = f(a)da \quad (1.2.2)$$

remains valid for any continuous random variable a , whether it be velocity coordinate, angular momentum, energy, etc. If a is a vector quantity, for example, velocity \mathbf{v} , then to find the “probability of detecting a definite velocity” means the determination of the probability that its projections in the intervals dv_x , dv_y , and dv_z are near the given values of the components. In other words, the end of the velocity vector must be within the confines of a cube with the sides dv_x , dv_y , dv_z constructed around the point with the coordinates v_x, v_y, v_z (Fig. 1.2). The less the volume of the cube $d\mathbf{v} = dv_x dv_y dv_z$, the

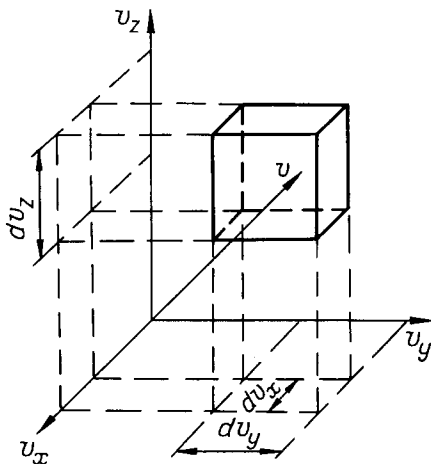


Figure 1.2 An element of velocity space.

more rarely are the molecules encountered whose velocity vector is directed to such a precisely indicated velocity space region. Thus

$$dW(\mathbf{v}) = g(\mathbf{v})dv_x dv_y dv_z = g(\mathbf{v})d\mathbf{v}. \quad (1.2.3)$$

Since all directions are equivalent the distribution function cannot depend on spherical angles of the vector \mathbf{v} (θ and φ). Hence, it must depend solely on its modulus $v = \sqrt{(v_x^2 + v_y^2 + v_z^2)}$, that is,

$$g(\mathbf{v}) = g(v). \quad (1.2.4)$$

The identity of all distributions in Eq. (1.2.1) and the constraint imposed by Eq.(1.2.4) is all the information we can extract from the isotropy of space. Due to these limitations the choice of $f(v)$ and $g(v)$ is not absolutely arbitrary, but we need some additional idea to remove the residual uncertainty.

This idea follows from the concept of independent random motion in any direction. It seems plausible that the probability of detecting a molecule that moves along the x axis with the velocity v_x is completely independent of the projections of \mathbf{v} on the other axes. If the given value v_x admits any v_y and v_z , and gives no preference to any particular value, then the above assumption is valid. This means that the three accidental events, namely, the detection of different values of three velocity components, are independent of one another. The value of one of them says nothing about any other. In this case

$$dW(\mathbf{v}) = dW(v_x) \cdot dW(v_y) \cdot dW(v_z). \quad (1.2.5)$$

This is a mathematical formulation of the probability multiplication theorem: the probability of accidental coincidence of several independent events is equal to the product of their probabilities. For example, the probability that three cubic dice cast at a time will show 1 is $1/6 \times 1/6 \times 1/6 = 1/216$. In general, the probability of getting any three *a priori* specified numbers, for instance, 2,4,1 or 3,5,2 is the same. Accidental detection of three numbers, v_x, v_y, v_z differs from the above example only in that the probabilities of their different values are not equal, and, moreover, are still unknown. However, only the assumption that they are independent makes it possible to use the multiplication theorem (1.2.5) and this is sufficient for their determination.

Substituting distributions (1.2.1) and (1.2.3) into (1.2.5) in view of (1.2.4) yields

$$g(v) = f(v_x) \cdot f(v_y) \cdot f(v_z). \quad (1.2.6)$$

Taking the logarithm of the above equality and differentiating it with respect to v_x , we get

$$\frac{1}{g} \frac{dg(v)}{dv} \frac{\partial v}{\partial v_x} = \frac{1}{g} \frac{dg(v)}{dv} \frac{v_x}{v} = \frac{1}{f(v_x)} \frac{df(v_x)}{dv_x}. \quad (1.2.7)$$

Differentiation with respect to v_y and v_z gives similar results. Together with (1.2.7) they may be represented as

$$\begin{aligned} \frac{1}{g(v)} \frac{dg(v)}{dv} &= \frac{1}{f(v_x)} \frac{df(v_x)}{v_x dv_x} = \frac{1}{f(v_x)} \frac{df(v_y)}{v_y dv_y} = \\ &= \frac{1}{f(v_z)} \frac{df(v_z)}{v_z dv_z} = -2\alpha. \end{aligned} \quad (1.2.8)$$

Here α is a constant, since functions of different arguments may identically coincide over the whole domain only if all of them are equal. Upon integrating Eq. (1.2.8), we obtain

$$g(v) = \frac{1}{Z} \exp(-\alpha v^2), \quad f(\xi) = \frac{1}{Z_0} \exp(\alpha \xi^2), \quad (1.2.9)$$

where $\xi = v_x, v_y, v_z$. By virtue of (1.2.6) there is a simple relationship between the integration constants Z and Z_0

$$Z = Z_0^3. \quad (1.2.10)$$

So if the motion in different directions is statistically independent, then the distribution functions must be of the form (1.2.9) and no other. However, it should be remembered that statistical independence is just a hypothesis, and not so evident as might appear at first sight. If, for example, one of the velocity components is equal to c , the speed of light, then the other components are obviously zero, that is, strictly specified. As a result the velocity distributions of photons are qualitatively different from (1.2.9) as we shall see in the next chapter. The Maxwell hypothesis gives correct results for classical molecular gases just because at ordinary temperatures atoms and molecules cannot move with relativistic velocities. For quantum gases—bosons and fermions—the situation is different. The phonon and electron velocity distributions at low temperatures do not satisfy the functional equation (1.2.6), nor, hence, (1.2.5). Thus there is some element of luck that the idea of independent motion of molecules in different directions proved to be valid for classical (not too cold) but at the same time nonrelativistic (not very hot) gases. This is a happy thought and a great piece of luck for the theory of Maxwell, who had to proceed from more or less arbitrary premises for lack of any other.

It is also remarkable that Maxwell's hypothesis was sufficient to determine the precise shape of $f(\xi)$ and $g(v)$. The uncertainty still remaining in Eq. (1.2.9) is the unknown Z_0 . This uncertainty is easily eliminated by taking into account the normalization condition

$$\int_{-\infty}^{+\infty} dW(v_x) = \frac{1}{Z_0} \int_{-\infty}^{+\infty} f(v_x) dv_x = 1.$$

It gives

$$Z_0 = \int_{-\infty}^{+\infty} f(\xi) d\xi = \int_{-\infty}^{+\infty} \exp(-\alpha\xi^2) d\xi = \sqrt{\frac{\pi}{\alpha}}, \quad (1.2.11)$$

which is the so-called Poisson integral. The following calculations show that it is actually equal to $\sqrt{\pi/\alpha}$:

$$\begin{aligned} Z_0^2 &= \left(\int_{-\infty}^{+\infty} f(\xi) d\xi \right)^2 = \int_{-\infty}^{+\infty} d\xi \int_{-\infty}^{+\infty} d\eta \exp[-\alpha(\eta^2 + \xi^2)] = \\ &= \int_0^{2\pi} d\varphi \int_0^{\infty} e^{-\alpha\rho^2} \rho d\rho = \pi \int_0^{\infty} e^{-\alpha z} dz = \frac{\pi}{\alpha}. \end{aligned} \quad (1.2.12)$$

By substitution of (1.2.11) into (1.2.9) and (1.2.1), we obtain

$$f(v_x) = \sqrt{\frac{\alpha}{\pi}} \exp(-\alpha v_x^2), \quad dW(v_x) = \sqrt{\frac{\alpha}{\pi}} \exp(-\alpha v_x^2) dv_x. \quad (1.2.13)$$

The remaining freedom in choosing the parameter α is by no means the drawback of the theory. This degree of freedom actually exists in the system under study. The smaller is α , the more frequently molecules with high velocities, and, therefore, with high kinetic energies, are observed (Fig. 1.3). The measure of the kinetic energy of a substance is evidently its temperature. So the smaller is α , the greater is T . To make the character of this dependence clearer, it is necessary to carry out the second part of our plan: to perform the averaging of v_x^2 and use it in Eq. (1.1.9) to compare the equation obtained with the familiar gas equation of state.

1.3 IDEAL GAS EQUATION OF STATE

Let us calculate the root-mean-square velocity using Eq. (1.2.13)

$$\overline{v_x^2} = \int_{-\infty}^{\infty} v_x^2 \sqrt{\frac{\alpha}{\pi}} e^{-\alpha v_x^2} dv_x = -\sqrt{\frac{\alpha}{\pi}} \frac{d}{d\alpha} \int_{-\infty}^{\infty} e^{-\alpha v_x^2} dv_x. \quad (1.3.1)$$

This result shows that the desired average may be obtained by differentiating Z_0 as defined in Eq. (1.2.11):

$$\overline{v_x^2} = -\sqrt{\frac{\alpha}{\pi}} \cdot \frac{dZ_0}{d\alpha} = \frac{1}{2\alpha}. \quad (1.3.2)$$

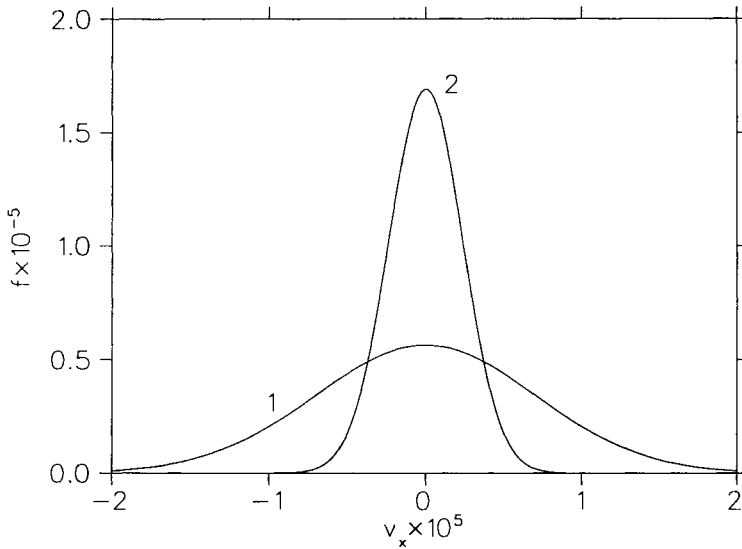


Figure 1.3 The Maxwellian distribution of a component of the molecular velocity at different temperatures: (1) $\alpha = 10^{-10}$, (2) $\alpha = 9 \times 10^{-10}$.

Substituting (1.3.2) into (1.1.9) gives

$$pV = \frac{Nm}{2\alpha}. \quad (1.3.3)$$

If we deal with one mole of a gas, then N is equal to N_0 , the Avogadro number. In this case, the equation $pV = N_0m/2\alpha$ is equivalent to the equation $pV = RT$, and the required exact correspondence between α and T follows from the identity of the two definitions of one and the same law

$$\frac{N_0m}{2\alpha} = RT, \quad \alpha = \frac{m}{2kT}, \quad (1.3.4)$$

where $k = R/N_0 = 1.38 \times 10^{-16}$ erg/K. According to Avogadro's law, N_0 is a fundamental physical constant. So k , the ratio of two fundamental constants, is also a fundamental constant—the Boltzmann constant. In view of (1.3.4), we can obtain instead of (1.3.2)

$$\frac{m\overline{v_x^2}}{2} = \frac{m\overline{v_y^2}}{2} = \frac{m\overline{v_z^2}}{2} = \frac{kT}{2}, \quad \bar{\epsilon} = \frac{m(\overline{v_x^2} + \overline{v_y^2} + \overline{v_z^2})}{2} = \frac{3}{2}kT, \quad (1.3.5)$$

It is seen that the value $3kT/2$ defines the average kinetic energy of translational motion of gas molecules. At $T = 300$ K it is equal to

6.2×10^{-14} erg = 4×10^{-2} eV. For comparison, it should be noted that the bonding energy of an atom in a molecule is greater by two orders of magnitude. The difference between room thermal energy of molecules and the energy of electrons in atoms, or that of accelerated particles is even more impressive. Still, the thermal energy of molecules is sufficient for them to move at rather high velocities. For example, for *oxygen*: $(\overline{v^2})^{1/2} = \sqrt{2\epsilon/m} = (12.4 \times 10^{-14}/5.3 \times 10^{-23})^{1/2} = 4.8 \times 10^4$ cm/s while for *hydrogen* the velocity is four times greater.

Finally let us return to the previous discussion and analyze the assumptions made, in particular, the model of an “ideal” gas. Purely qualitative property of a gas—the tendency to disperse in all directions, if no walls prevent the expansion—has been considered as an indication that gas molecules are not linked by intermolecular forces. In such a strong statement this assumption is not quite justified. A gas will disperse provided that the average kinetic energy ϵ exceeds the attraction energy when molecules are at the average distance from one another. In fact, the energy of intermolecular interaction is not negligible, as it is responsible for the condensation of a gas into a liquid or solid. This fact, as well as the finite sizes of molecules which were previously considered as point masses, leads to the conclusion that the equation of state is essentially different from $pV = RT$. For most gases the ideal gas law holds only approximately and only at rather low pressures and high temperatures. However, the limited applicability of the ideal gas model does not remove its advantages. Due to its simplicity, an exact mathematical treatment is possible. The model of non-interacting point masses provides information about the most important features of molecular motion in a gas and sheds light upon the basic distinctions between the classical gas and ideal photon and phonon gases which will be considered later. The theoretical basis of the model is consistent and clear. It may be used as a skeleton upon which to build models suited to reveal the specific features of real objects. Abandoning ideal model simplifications one after another, we shall discover effects or phenomena omitted in the simplest scheme. Transfer phenomena are associated with finite sizes of molecules, chemical reactions—with molecular destruction, electric conduction—with their ionization, and so on. The advantages of the ideal model are elegance and strictness, while the advantage of the real models is their applicability to a variety of phenomena and physical situations.

According to (1.3.3) and (1.3.4), in an ideal gas

$$p = nkT. \quad (1.3.6)$$

In a real gas nonlinear corrections in n appear which become dominant in condensed phases.

1.4 MAXWELL DISTRIBUTION

Substituting (1.2.9) into (1.2.3) in view of (1.2.10) and (1.2.11), we find

$$dW(\mathbf{v}) = \left(\frac{\alpha}{\pi}\right)^{3/2} e^{-\alpha(v_x^2+v_y^2+v_z^2)} dv_x dv_y dv_z, \quad (1.4.1)$$

where $\alpha = m/(2kT)$. The probability of detecting the velocity defined by the value and direction cannot depend on the shape of an elementary volume in velocity space which contains the end of the vector \mathbf{v} . Thus (1.4.1) may be recast as

$$dW(\mathbf{v}) = \left(\frac{\alpha}{\pi}\right)^{3/2} e^{-\alpha v^2} d\mathbf{v}, \quad (1.4.2)$$

where by $d\mathbf{v}$ (or d^3v) we mean the volume of the element of arbitrary shape in the velocity space containing the group of molecules we are interested in. In particular, if we wish to know the probability of finding a molecule with the definite velocity \mathbf{v} whose orientation in the space is specified by spherical coordinates θ and φ , it is necessary to calculate the volume $d\mathbf{v}$ defined by the increments dv , $d\theta$, $d\varphi$. As is seen from Fig. 1.4a, this volume is equal to the product of the height of the spherical layer dv and the area of its base: $(v \sin \theta d\varphi) v d\theta$, so that $d\mathbf{v} = v^2 dv \sin \theta d\theta d\varphi = v^2 dv d\Omega$, where $d\Omega$ is a spherical angle limiting the direction dispersion of velocities. Thus in these coordinates the Maxwell distribution is of the form

$$dW(\mathbf{v}) = \left(\frac{\alpha}{\pi}\right)^{3/2} e^{-\alpha v^2} v^2 dv d\Omega = \left(\frac{\alpha}{\pi}\right)^{3/2} e^{-\alpha v^2} v^2 dv \sin \theta d\theta d\varphi. \quad (1.4.3)$$

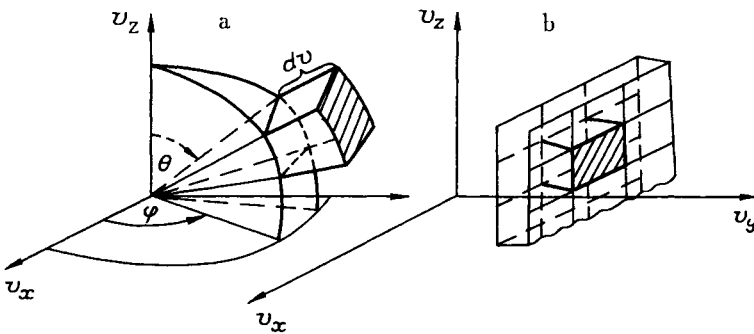


Figure 1.4 Elements of velocity space in (a) spherical and (b) Cartesian coordinates.

Summation of Probabilities

Sometimes, only part of the information obtainable from (1.4.1) or (1.4.3) is necessary to solve a problem. For example, in calculating the pressure, we need only know the velocity of a molecule moving towards the wall along the x axis, independent of its projections on the other axes. What is wanted for the calculation of $\overline{v_x^2}$, and, hence, p , is the distribution $dW(v_x)$. How can this particular distribution be obtained from the general Maxwell distribution (1.4.1)?

The recipe is given by the summation theorem: the probability of observing one of a number of incompatible events, no matter which of them, is equal to the sum of probabilities of these events. To appreciate the physical meaning of the theorem, just remember that the probability of a state is the relative number of particles in this state: $dn(v_x, v_y, v_z)/n = dW(\mathbf{v})$. For the given value v_x other projections are not essential: they may be identical, different, great or little. All molecules with the same v_x which differ only in other projections should be counted. The ratio of their total number to the corpuscular density n gives the desired probability

$$dW(v_x) = \frac{1}{n} \int_{v_y} \int_{v_z} dn(v_x, v_y, v_z) = \int_{v_y} \int_{v_z} dW(v_x, v_y, v_z) = \sqrt{\frac{\alpha}{\pi}} e^{-\alpha v_x^2} dv_x. \quad (1.4.4)$$

Substituting (1.4.1) into (1.4.4), we can readily see that this equality is valid. The summation theorem also has a clear geometrical meaning. The quantity $dW(\mathbf{v})$ is the probability that the end of the velocity vector will find itself in one of a number of equal cubic elements $d\mathbf{v}$ confined between two planes $v_x = \text{const}$ and $v_x + dv_x = \text{const}$, while $dW(v_x)$ is the probability that it will be found in any of these cubes, that is, in any point of the infinite plane layer (Fig. 1.4b).

Reasoning similarly, it is easy to calculate the probability that a molecule will move at the absolute velocity v (which is greater than v and less than $v + dv$), irrespective of the direction. Obviously, all points of a spherical layer confined between two spheres of the radius v and $v + dv$ fit the criterion thus formulated. At whichever point the end of the vector \mathbf{v} finds itself, its modulus will meet the requirement, while the direction may be arbitrary. The probability of moving with the same velocity but in a strictly specified direction—within the limits of the spherical angle $d\Omega$ —was defined by the general distribution (1.4.3). To find from it the required probability, it is necessary to integrate over all angles, taking into account the entire volume of the spherical layer:

$$dW(v) = \int_0^{2\pi} d\varphi \int_0^\pi d\theta dW(\mathbf{v}) = 4\pi \left(\frac{\alpha}{\pi}\right)^{3/2} e^{-\alpha v^2} v^2 dv. \quad (1.4.5)$$

Statistical Weight

Let us consider the origin of the multiplier v^2 which appears in Eq. (1.4.5) but was not involved either in (1.4.1) or in (1.4.4). Through the following analogy we can deduce that it is associated with different definitions of the “states” whose probability is being sought. Compare a many-storied pyramid-shaped building with a box-like skyscraper, assuming that all living units inside are of equal size and quality (Fig. 1.5). If they are inhabited uniformly the probability of finding a tenant in any apartment in the daytime is one and the same regardless of the story or the architecture. However, the probability of finding a person in a particular story is less, the nearer the story to the top of the pyramid house. This is because the greater the number of apartments on the story, the greater the probability of a successful search. As far as a box-like house is concerned, the apartment distribution over stories is uniform, and the probability of finding a person in any of them is the same.

The unit volumes of the velocity space may be associated with “apartments.” The number of units in a spherical layer increases with distance from the origin of coordinates as $4\pi v^2 dv$. The probability of finding the end of the vector \mathbf{v} in the layer of the width dv is proportional to statistical weight $4\pi v^2$. On the other hand, the number of units between two parallel planes remains unchanged when the planes are shifted together either to the right or to the left. Thus the corresponding statistical weight is invariant with respect to the position of a flat layer (see Fig. 1.4).

The previous analogy is not quite precise. The probability of occupancy of equal elements of the volume $d\mathbf{v}$ at different spherical “stories” is not the same: it decreases exponentially as $e^{-\epsilon/kT}$. Imagine that most of the rooms in a hotel are vacant and the few visitors occupy apartments as they like. If there is no escalator in the hotel, then the visitors will prefer those on the lower floors, even though the rooms are equal in size. The statistical weight $\rho(v)$ is a measure of the “state” (spherical layer) capacity while the Boltzmann factor $e^{-\epsilon/kT}$ relates the attendance of each unit in the state to its energy.

By the “state” whose probability is given by (1.4.3) we mean the element defined by the increments dv , $d\theta$, $d\phi$, which is the spherical layer delimited by two close meridional cross-sections. Its volume increases the nearer it is to the equator and is equal to zero at the poles. Correspondingly, the statistical weight is $\rho(v, \theta) = v^2 \sin \theta$. Using the summation theorem, we can find the

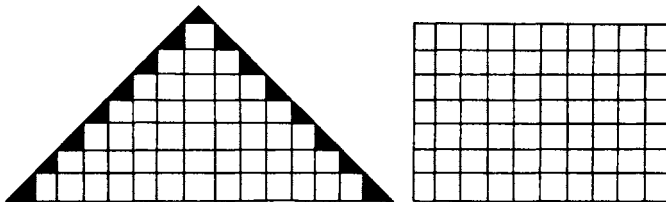


Figure 1.5 Illustration of the concept of statistical weight.

probability of moving in a definite direction irrespective of the absolute value of the velocity:

$$dW(\Omega) = \int_{\nu} dW(\mathbf{v}) = \frac{\sin \theta d\theta d\varphi}{4\pi} = \frac{d\Omega}{4\pi}. \quad (1.4.6)$$

This is just what we expected, due to the space isotropy.

From (1.4.5) we can also derive the probability “to be in a definite energy state,” that is, to have kinetic energy greater than ϵ , but less than $\epsilon + d\epsilon$. Substituting $\nu = \sqrt{2\epsilon/m}$, Eq. (1.4.5) is brought to the form

$$dW(\epsilon) = 2\pi \left(\frac{2\alpha}{\pi m}\right)^{3/2} \exp\left(-\frac{2\alpha\epsilon}{m}\right) \sqrt{\epsilon} d\epsilon = \left(\frac{m}{2\pi kT}\right)^{3/2} \exp\left(\frac{\epsilon}{kT}\right) \rho(\epsilon) d\epsilon, \quad (1.4.7)$$

where

$$\rho(\epsilon) = 2\pi \left(\frac{2}{m}\right)^{3/2} \sqrt{\epsilon} \quad (1.4.7a)$$

is the statistical weight.

The general definition of the statistical weight following from the above examples is given by the equality

$$d\nu = \rho(q) dq, \quad (1.4.8)$$

where q is any variable or a set of variables expressed in terms of ν_x , ν_y , ν_z , and $\rho(q)$ is the statistical weight.

Mean Values

The probability density that enters the Maxwell distribution $dW(q) = g(q) dq$ is as follows

$$g(q) = \frac{1}{Z} \exp[-\alpha\epsilon(q)] \rho(q),$$

where Z is the normalization constant (*partition function*). As the exponential factor and statistical weight change inversely with q , $g(q)$ has a sharply defined maximum (Fig. 1.6). The most probable velocity ν_e and the most probable energy ϵ_e may be determined from the conventional condition $dg/dq = 0$. Using Eqs. (1.4.5) and (1.4.7) one can get

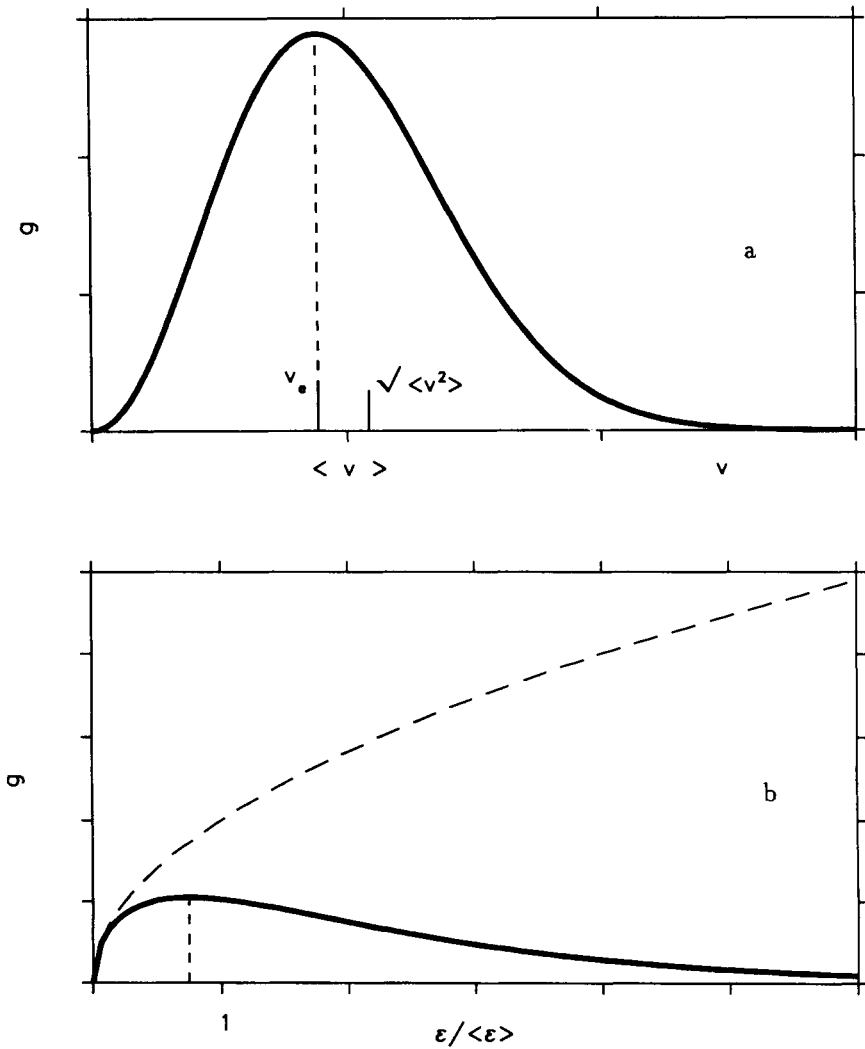


Figure 1.6 Distribution of (a) the molecular speed and (b) kinetic energy.

$$v_e = \sqrt{\frac{2kT}{m}} \quad \text{and} \quad \epsilon_e = \frac{kT}{2}. \quad (1.4.9)$$

Note that $\epsilon_e \neq mv_e^2/2$. This is hardly surprising: an ensemble of molecules with different velocities is poorly described by a simplified model that divides all particles into three groups moving with equal velocities along the coordinate axes. This model is often used for rough kinetic estimates, but it is only within this model that the relations between energy and velocity of a single particle

remain valid both for extreme and average values. What actually happens after averaging over the Maxwell distribution is that \bar{v} coincides with rms value $(\overline{v^2})^{1/2}$ as well as with v_e only up to an accuracy of a constant multiplier. Different experiments deal with different averages: $|\overline{v_x}|$, \bar{v} , $\overline{v^2}$, and so on. Of course, the order of magnitude of any quantity being measured may be evaluated by replacing v by one assumed value (i.e., the root-mean-square one), but a correct calculation always calls for actual averaging of the required quantity.

For example, let us calculate a number of particles striking a unit area of the wall per unit time. According to Eq. (1.1.4) the elementary flux is

$$dj = dN/S = v_x dn(v_x), \quad (1.4.10)$$

while the total flux is an integral over positive values of v_x :

$$j = \int_0^\infty v_x dn(v_x) = \frac{1}{2} n |\overline{v_x}|. \quad (1.4.10a)$$

If all molecules were moving with the same velocity to and fro, then the velocity would be chosen to be $|\overline{v_x}|$, giving exactly the same flux as in the Maxwellian gas. It is obvious that

$$|\overline{v_x}| = 2 \int_0^\infty v_x dW(v_x) = \frac{1}{\sqrt{\pi\alpha}} = \sqrt{\frac{2kT}{\pi m}} \quad (1.4.11)$$

coincides neither with the root-mean-square nor with the average modulus of the velocity, given by

$$\bar{v} = \int_0^\infty v dW(v) = \frac{2}{\sqrt{\pi\alpha}} = \sqrt{\frac{8kT}{\pi m}}. \quad (1.4.11a)$$

Using this mean value the expression (1.4.10) can be recast in the form

$$j = \frac{1}{4} n \bar{v}. \quad (1.4.12)$$

This result coincides with that for a flux of particles moving in all directions but with a single speed \bar{v} .

Stern Experiment

The concept of chaotic thermal motion and the shape of Maxwell's distribution were experimentally verified by Otto Stern in 1920. In this experiment, a hollow rotating cylinder, called the vacuum analyzer, is placed in the path of a molecular jet. During the short time interval when the vertical slot of the analyzer is aligned with the jet, molecules can enter the cylinder (Fig. 1.7). These inertially

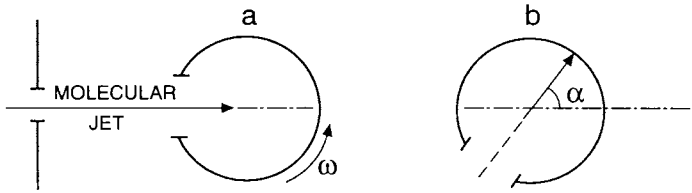


Figure 1.7 Configuration of the analyzer (a) at the time when molecules enter it and (b) at the moment of their adsorption.

moving molecules reach the screen on the opposite side of the analyzer at different times $\Delta t = D/v$, depending on their velocity (D is the cylinder diameter). Due to the fact that during the time Δt the cylinder rotates by a certain angle, the molecules encounter the screen not along the line opposite the slot but at a position which depends on their velocity: the lower their velocity the farther from this line (Fig. 1.7b). At a rather low analyzer temperature almost all the particles are deposited on the screen at the points of collision. Atoms of silver form a stratum on the screen, the thickness of which allows one to determine the number of deposited particles. Knowing the rotation angle of the analyzer $\alpha = \omega\Delta t$ provides a means to judge the velocity of particles which are deflected through this angle: $v = D/\Delta t = D\omega/\alpha$. Therefore one is able to reconstruct the distribution of absolute velocities of atoms which pass through the slot. The experimental determination and study of this distribution were a strong argument in favor of the existence of atoms and verified the validity of the *a priori* assumptions which were of fundamental importance in the derivation of the Maxwell distribution.

Structure of the Flux

However, we have not yet been given sufficient evidence to believe that the distribution thus obtained coincides with the Maxwell one. In the Stern experiment the distribution was reconstructed not for particles in the container but in the jet. The number of rapid molecules leaving the container is greater than the number of slow molecules escaping in the same time. For this reason alone, the distribution obtained by Stern must differ from the Maxwell distribution. The distribution of speeds in a jet is different from that in the volume, which is Maxwellian.

As follows from Eqs. (1.4.10), (1.4.3) and (1.4.5), the flux of particles with a given velocity is

$$dj = v_x n dW(\mathbf{v}) = v \cos \vartheta dW(v) \cdot n \frac{d\Omega}{4\pi}. \quad (1.4.13)$$

To obtain the normalized velocity distribution of particles in a jet we have only to divide (1.4.13) by its integral value (1.4.12):

$$\frac{dj}{j} = \frac{v}{\bar{v}} dW(v) \frac{\cos \vartheta d\Omega}{\pi} = dW_j(v) dW_j(\Omega). \quad (1.4.14)$$

Here the distribution of the speeds of the particles is

$$dW_j(v) = \frac{v}{\bar{v}} dW(v) = \frac{1}{2} \left(\frac{m}{kT} \right)^2 \exp \left(-\frac{mv^2}{2kT} \right) v^3 dv \quad (1.4.15)$$

and

$$dW_j(\Omega) = I(\vartheta) \frac{d\Omega}{2\pi}, \quad I(\vartheta) = 2 \cos \vartheta \quad (1.4.16)$$

is the distribution of the directions of motion within a semisphere.

In Stern's experiment the velocity distribution of particles moving along the bunch axis ($\vartheta = 0$) in a finite but small spherical angle $\Delta\Omega$ is measured. It was shown to coincide with Eq. (1.4.15). Apart from an unimportant constant this distribution differs from the Maxwell one by the extra factor v . As is clear from Eq. (1.4.13), its origin is associated with the advantage which rapid molecules have over slow molecules in escaping from the container in a given time. That is why both the average velocity and the average energy of particles in the bunch are greater than the Maxwell ones:

$$\bar{v}_j = \int v dW_j = \frac{\bar{v}^2}{\bar{v}} = \frac{3\pi}{8} \bar{v}, \quad \bar{\epsilon}_j = \frac{m}{2} \int v^2 dW_j = \frac{m\bar{v}^3}{2\bar{v}} = 2kT = \frac{4}{3} \bar{\epsilon}.$$

1.5 BAROMETRIC FORMULA

In the absence of an external field, it is natural to consider all points of the space filled by gas to be equivalent. Then the probability of entering any element of equal volume is identical:

$$dW(x, y, z) = \frac{dx dy dz}{V}. \quad (1.5.1)$$

However, this is not true if the gas in the vessel is under the influence of a gravitational field. In this case, different volume elements differ in the value of the potential energy of molecules contained in them. Generally speaking, one should take

$$dW = f(x, y, z) dx dy dz, \quad (1.5.2)$$

and special considerations are necessary for the determination of $f(x, y, z) \neq \text{const}$. If the gravitational force acts in the z direction, then the variation of $f(z)$ has the result that the gas density $n = n(z)$ is different at different heights. Due to Eq. (1.3.6) this must also affect the pressure.

The variation of pressure with the height is inevitable, at least because the gas confined in the vessel has weight only when the pressure on the bottom exceeds that on the lid. Assuming that the vessel is a weightless box in the form of a parallelepiped with a bottom area S the weight of the gas is

$$\mathcal{P} = S[p(0) - p(H)] = SkT[n(0) - n(H)]. \quad (1.5.3)$$

On the other hand, the gas weight is the product of the total number of molecules in the vessel and the molecular weight which is mg at reasonably small heights H :

$$\mathcal{P} = mgN = mgS \int_0^H n(z) dz. \quad (1.5.4)$$

Since the identity

$$mg \int_0^H n(z) dz = kT [n(0) - n(H)]$$

is valid at any H , $n(z)$ must satisfy the equation

$$\frac{dn}{dz} = -\frac{mg}{kT} n. \quad (1.5.5)$$

The solution of this equation

$$n(z) = n(0) \exp \left[-\frac{mgz}{kT} \right] \quad (1.5.6)$$

contains the integration constant $n(0)$ which is the gas density at the bottom of the vessel. Substituting (1.5.6) into the normalization condition $\int_0^H n(z) dz = N/S$ determines $n(0)$ to be

$$n(0) = \frac{N}{S} \frac{mg}{kT} \left[1 - \exp \left(-\frac{mgH}{kT} \right) \right]^{-1}. \quad (1.5.7)$$

With $mgH \ll kT$ (not very tall container or rather high temperatures) the gas density $n(z) \approx n(0)$, that is, it is practically uniform over the whole vessel, just

as in our everyday experience. However, when $mgH \gg kT$, the decrease in density with height becomes noticeable.

Conditions of the type

$$\alpha = \frac{mgH}{kT} = \frac{T_c}{T} > 1 \quad (1.5.8)$$

are typical for statistical physics. They represent a competition between deterministic mechanical action (in the given case, the gravitational force) and chaotic thermal motion. The gravitational force tries to make all molecules fall to the bottom of the vessel, while the thermal kinetic energy enables them to overcome the gravitation and move upwards. The dimensionless exponent (1.5.8) defines the relative magnitude of the two effects which is determined by the ratio of the corresponding energies: mgH and kT . Concentration of a gas at the bottom of the vessel may take place only when $T \ll T_c$. At $H = 1$ m the characteristic temperature $T_c = mgH/k \approx 5 \cdot 10^{-23} \times 10^3 \times 10^2 / 1.4 \times 10^{-16} \approx 3 \times 10^{-2}$ K. As a rule, the gaseous phase cannot exist at such low temperatures. Therefore the space inhomogeneity of a gas in a vessel of real size at a usual temperature $T \gg T_c$ is insignificant and should be taken into account just for the correct definition of the gas weight. One may hope to detect the gas inhomogeneity in a taller vessel, but from the same formula it follows that at room temperature a noticeable decrease in density (by a factor of e) is observed at $H = kT/mg = 1.4 \times 10^{-16} \times 300/5 \times 10^{-23} \times 10^3 = 10^6$ cm = 10 km. Obviously, it is impossible to imagine such a vessel but this suggests another possibility: comparison with the Earth's atmosphere.

The decrease in atmospheric density with height is a well-known fact. If it could be described by Eq. (1.5.6), then the corresponding pressure fall would be defined by the "barometric" formula

$$p(z) = p(0) \cdot \exp\left[-\frac{mgz}{kT}\right]. \quad (1.5.9)$$

It is also seen from Eq. (1.5.6) that the separation of gases with height, which actually happens, is due to different molecular weights

$$\frac{n'}{n''} = \frac{n'(0)}{n''(0)} \exp\left[\frac{(m'' - m')gz}{kT}\right]. \quad (1.5.10)$$

Good qualitative agreement between these conclusions and well-known facts suggests an attractive idea: to use the above formula for the quantitative description of the composition and density of the atmosphere at different altitudes. However, such an extrapolation is not quite adequate. The approximate law $F = -mg$ used to describe the action of the gravitational force is not valid at high altitudes. It should be replaced by Newton's law of gravitation. According to this law

$$U = f \int_{R_0}^R \frac{mM}{r^2} dr = fmM \left(\frac{1}{R_0} - \frac{1}{R} \right). \quad (1.5.11)$$

It has not yet been made clear, however, how this can be realized. The distribution of particles far from the Earth's surface is not one-dimensional, but has a spherical symmetry. Thus before employing (1.5.11), it is necessary to generalize the results obtained.

1.6 THE BOLTZMANN DISTRIBUTION

As the gas density at small height z is

$$n(z) = dN(z)Sdz = (N/S) \frac{dW}{dz},$$

the one-dimensional distribution of particles may be obtained from Eq. (1.5.6):

$$dW(z) = \frac{n(0)S}{N} \exp \left[-\frac{mgz}{kT} \right] dz = \frac{1}{Z} \exp \left[-\frac{mgz}{kT} \right] dz, \quad (1.6.1)$$

where $Z = N/n(0)S$. This is the probability to find a molecule in a layer of thickness dz . Though this distribution is obtained for the particular potential energy $u(z) = mgz$ the form of the distribution density

$$f(z) = \frac{1}{Z} \exp \left[-\frac{u(z)}{kT} \right] \quad (1.6.2)$$

indicates how to generalize this for other forms of $u(z)$. In particular, it is clear that even in the case considered, the reference system does not necessarily coincide with the most convenient one where the z axis is parallel to the force of gravity. Thus in the general case, the distribution (1.6.1) takes the form

$$dW(x, y, z) = \frac{1}{Z} \exp \left[-\frac{u(x, y, z)}{kT} \right] dx dy dz = \frac{1}{Z} \exp \left[-\frac{u(\mathbf{r})}{kT} \right] d\mathbf{r}. \quad (1.6.3)$$

It differs from the Maxwell distribution only in that the potential energy plays the role of the kinetic energy and $d\mathbf{r}$ is the element of volume in ordinary coordinate space, not in the space of velocities. This is the Boltzmann distribution.

By analogy with Eq. (1.4.3), for a spherically symmetrical field it may be represented as

$$dW(R, \theta, \varphi) = \frac{1}{Z} \exp \left[-\frac{u(r)}{kT} \right] R^2 dR \sin \theta d\theta d\varphi, \quad (1.6.4)$$

where $Z = \int \exp[-u(R)/kT] dR$. If we are interested in the composition of gas in the near-Earth layer of thickness ΔR , it is natural to employ (1.6.4). If the variation of density or pressure is of interest, we pass from the probability distribution to the density distribution and get the analog of the barometric formula

$$\begin{aligned} n(R) &= \frac{NdW(R)}{4\pi R^2 dR} = \frac{N}{Z} \exp\left(-\frac{u}{kT}\right) = \\ &= n(0) \exp\left[-\frac{fmM}{kT} \left(\frac{1}{R_0} - \frac{1}{R}\right)\right]. \end{aligned} \quad (1.6.5)$$

Thus knowing the density near the Earth's surface, we could, in principle, estimate its variation with height. Unfortunately, any conclusions on the Earth's atmosphere density following from (1.6.5) are substantiated only qualitatively. Quantitative agreement is impossible, at least, for the reason that Z diverges. Besides, the atmosphere is not in thermodynamic equilibrium. Its temperature near the Earth's surface differs from that at different altitudes, while in equilibrium it must be the same at all points of space. The difference in temperature is responsible for convectional gas flows (winds), heat exchange among neighboring layers and other phenomena incompatible with equilibrium. So this example is not perfect for a quantitative verification of the theory.

However, nature has indeed provided systems which are, on one hand, much more convenient from the experimental standpoint, and, on the other hand, are adequately modeled by the ideal gas. These are so-called suspensions or emulsions: solutions of noninteracting solid or liquid macroscopic particles, suspended in a transparent solvent. The fact that small particles of this kind perpetually move around in a random manner was first observed by Brown, a botanist, in the nineteenth century. Brownian motion is caused by random collisions of the small particles with molecules of the solvent. They alternately gain or lose momentum due to unbalanced collisions with molecules from all sides. As a result the Brownian particles participate in thermal motion along with the solvent molecules themselves in spite of the difference in size. In studies of such properties as distribution with height this difference is not essential; only the mass of dissolved particles is of importance. The mass may be chosen such that the distribution inhomogeneity can be easily observed in a vessel of moderate size.

Since a particle with mass m and density ρ suspended in a liquid of density ρ_0 experiences a buoyant force its weight in solution is $mg - mg\rho_0/\rho$. Therefore the analog of the barometric formula for Brownian particles is

$$n(z) = n(0) \exp\left[-\frac{mgz}{kT} \left(1 - \frac{\rho_0}{\rho}\right)\right] \quad (1.6.6)$$

Random motion of Brownian particles and their distribution with height has defied any explanation other than that given above. Thus the quantitative study of such systems performed by Perrin, in particular, the experimental verification of barometric formula (1.6.6), were a real triumph of both atomic and statistical theory, and finally led to their acknowledgment as the valid theories. Moreover, owing to Perrin's measurements the Avogadro number $N_0 = R/k$ was first determined to high accuracy using

$$k = \frac{mg}{T} \left(1 - \frac{\rho_0}{\rho}\right) \frac{z_2 - z_1}{\ln [n(z_1)] - \ln [n(z_2)]}. \quad (1.6.7)$$

The Boltzmann constant was found from Eq. (1.6.7) by calculating the particle density at different heights, then measuring the particles' mass by several methods to obtain the exact value.

As soon as k is known, the inverted problem may be solved with the same formula (1.6.7). This is the problem of the determination of small masses, which is of practical interest. The smaller the masses, the greater the distances that are required to reveal the difference between them at a given accuracy of density measurements. Since the height of the vessel is restricted, essential progress can only be achieved by enhancing the potential field. This aim is achieved by replacing the gravitational field by that of centrifugal force $F = m\omega^2 r$, which can be extremely strong in modern centrifuges. With this replacement, Perrin's method has become a technique which is extensively employed in chemistry and biology as an effective way of separating substances similar in molecular weight.

With the centrifugal potential

$$u = - \int_0^R m\omega^2 r dr = - \frac{m\omega^2 R^2}{2}, \quad (1.6.8)$$

the Boltzmann distribution is of the form

$$dW(\mathbf{R}) = \frac{1}{Z} \exp \left[\frac{m\omega^2}{2kT} R^2 \right] d\mathbf{R}, \quad (1.6.9)$$

or, in cylindrical coordinates,

$$dW(R, \varphi, z) = \frac{1}{Z} \exp [BR^2] R dR d\varphi dz, \quad (1.6.10)$$

where $B = m\omega^2/2kT$. For example, we centrifuge milk and wish to determine the number of oil particles in a layer of the thickness ΔR . The best way is to integrate the distribution (1.6.10) with respect to φ and z . However, if one is

interested in the density of particles it is better to proceed from Eq. (1.6.9) bringing this distribution into a “barometric form”

$$n = \frac{NdW}{d\mathbf{R}} = \frac{N}{Z} \exp[BR^2] = n(0) \exp[BR^2]. \quad (1.6.11)$$

The greater the angular frequency of rotation ω , the more inhomogeneous is the distribution of particles along the radius: the density at the periphery increases and that near the rotation axis decreases.

1.7 CANONICAL DISTRIBUTION

If one wishes to know the velocity of the molecule and at the same time its position, the answer is given by the product of corresponding probabilities—(1.4.1) and (1.6.3):

$$dW(\mathbf{r}, \mathbf{v}) = dW(\mathbf{r})dW(\mathbf{v}) = \frac{1}{Z} \exp\left(-\frac{\mathcal{E}}{kT}\right) dx dy dz dv_x dv_y dv_z, \quad (1.7.1)$$

where $\mathcal{E} = \epsilon + u = mv^2/2 + u(x, y, z)$ and

$$Z = Z_M Z_B = \int e^{-mv^2/2kT} d\mathbf{v} \int e^{-u/kT} d\mathbf{r} = \left(\frac{m}{2\pi kT}\right)^{3/2} \int e^{-u(x,y,z)/kT} dx dy dz. \quad (1.7.1a)$$

This is the Maxwell–Boltzmann distribution defined in so-called μ -space, the six-dimensional *configurational space* parametrized by the six coordinates x, y, z, v_x, v_y, v_z . The Maxwell and Boltzmann distributions are obtained from this distribution as particular cases by the familiar summation procedure

$$dW(\mathbf{v}) = \iiint dW(\mathbf{r}, \mathbf{v}) d\mathbf{r}, \quad dW(\mathbf{r}) = \iiint dW(\mathbf{r}, \mathbf{v}) d\mathbf{v}. \quad (1.7.2)$$

The Maxwell–Boltzmann distribution (1.7.1) gives a complete description of the translational degrees of freedom, which is quite sufficient in the case of monoatomic gas. However, for molecules, it is desirable also to know the probability of their rotation and orientation, energy of vibration, and so on. Hence, many other distributions may be required.

Generalizing Eq. (1.7.1) by induction, one can expect that the distribution applicable to various motions of the molecular system is similar in form to (1.7.1):

$$dW = \frac{1}{Z} \exp\left(-\frac{\mathcal{E}}{kT}\right) d\Gamma, \quad (1.7.3)$$

where \mathcal{E} is the total energy. It is necessary only to adjust the space element $d\Gamma$ to the product of the coordinate increments associated with a definite type of motion. However, as we have already seen, the element $d\Gamma$ has different statistical weights depending on the coordinates chosen to describe the motion. In order to determine its value, it is sufficient to calculate the statistical weight in some particular coordinate system. Then, by changing variables, we shall automatically obtain it in other coordinates. For example, one may find a coordinate frame in which the statistical weight is equal to unity, that is, indicate the *phase space* where the probability of entering isoenergy elements of equal size is identical. In other words, one should determine coordinates in which increments constitute equivalent "rooms," but not "stories" of different capacity. Formerly, this problem seemed obvious. Equal elements of Cartesian space $dx dy dz$ were naturally considered equivalent, while the similar elements in spherical coordinates $dr d\theta d\varphi$, were weighed correspondingly. Nevertheless, this was just a hypothesis; generally speaking it might be quite the reverse. This is our belief that only equal elements of real physical space are indistinguishable and therefore equiprobable.

Unfortunately, obvious things hide misunderstanding and confusion, particularly when they serve as a basis for generalization. What seems unquestionable in the case of ordinary coordinate space is not so evident even in the space of velocities, to say nothing of rotational or vibrational motion. Thus relation (1.7.3) becomes a law only after the element $d\Gamma$ is exactly defined.

For reasons to be clarified in Section 1.10, the probability of entering equal elements is considered to be identical only in the *phase space* of canonical variables q_i and p_i , which are generalized coordinates and momenta. It is known from mechanics that when the generalized coordinates q_i and the corresponding velocities $\dot{q}_i = dq_i/dt$ are chosen, the generalized momenta may be found by the formula

$$p_i = \frac{\partial L(q_i, \dot{q}_i)}{\partial \dot{q}_i} = \frac{\partial[\epsilon(q_i, \dot{q}_i) - u(q_i, \dot{q}_i)]}{\partial \dot{q}_i}. \quad (1.7.4)$$

Here ϵ is the kinetic energy, u is the potential energy, and $L = \epsilon - u$ is the Lagrange function.

The value $d\Gamma$ in the canonical Gibbs distribution (1.7.3) is

$$d\Gamma = d\mathbf{p}d\mathbf{q} = \prod_i dq_i dp_i, \quad (1.7.5)$$

so the statistical weight is equal to unity only in coordinate-momenta space. Hence, for a system of noninteracting point masses the Gibbs distribution is of the form

$$dW = \frac{1}{Z} \exp\left[-\frac{\epsilon + u}{kT}\right] d\mathbf{q}d\mathbf{p}, \quad (1.7.6)$$

where $\int dW = 1$, so

$$Z = \int q p e^{-\epsilon+u/kT} d\mathbf{q} d\mathbf{p}. \quad (1.7.7)$$

Substitution of $p_i = m\dot{q}_i = mv_i$ reveals the identity of this distribution and the Maxwell-Boltzmann one. The constant statistical weight m^3 is not essential, because it may be excluded by renormalization of the partition function Z .

The formula

$$d\Gamma = dpdq = |I| da db. \quad (1.7.8)$$

enables one to transform the canonical variables used in the Gibbs distribution to any other system. The Jacobian I of this transformation defines the statistical weight in the new variables. Should we need a more specific form of the distribution free of unnecessary variables, the particular expression for the statistical weight is obtained by integration with respect to “unwanted” variables.

1.8 DIELECTRIC PROPERTIES OF GASES

Generalized Coordinates and Momenta

To illustrate the application of the canonical distribution to some system, we consider a linear rotator—a rigid diatomic molecule whose atoms carry alternative charges $\pm e$. Such a molecular dumb-bell (Fig. 1.8) is characterized (apart from the mass $M = m_1 + m_2$) by two more constants—the moment of inertia in the center-of-mass system $I = m_1 r_1^2 + m_2 r_2^2$ and the permanent dipole moment $\mathbf{q} = e(\mathbf{r}_2 - \mathbf{r}_1) = e(r_2 + r_1) \mathbf{a}$ where $\mathbf{a} = \mathbf{r}_2/r_2 = -\mathbf{r}_1/r_1$. Accordingly, its kinetic energy along with the energy of translational motion involves the kinetic energy of rotation

$$\epsilon_{rot} = \frac{m_1 \dot{\mathbf{r}}_1^2}{2} + \frac{m_2 \dot{\mathbf{r}}_2^2}{2} = \frac{I}{2} \dot{\mathbf{a}}^2 \quad (1.8.1)$$

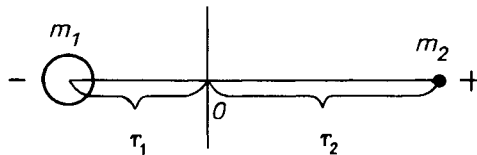


Figure 1.8 Configuration of masses and charges in a diatomic molecule relative to the center of mass.

and potential energy depending on the orientation of the dipole in an external electric field \mathbf{E} ,

$$u = -\mathbf{qE} = -q_z E = -qE \cos \theta . \quad (1.8.2)$$

Since the potential energy is easily expressed via the angle θ between the dipole and the field, it is natural to choose as generalized coordinates the two spherical coordinates θ and φ with respect to the molecular axis. In this case the kinetic energy should be expressed as a function of the generalized velocities $\dot{\theta}$ and $\dot{\varphi}$. The coordinate space of the linear rotator and the space of its generalized velocities are two-dimensional.

Let us bring the origin of coordinates into coincidence with the molecular center-of-mass. In this frame the translational motion vanishes. The radius-vector

$$\mathbf{a} = (a \sin \theta \cos \varphi, \quad a \sin \theta \sin \varphi, \quad a \cos \theta) \quad (1.8.3)$$

completely represents a molecule in this reference system. It circumscribes a sphere about the center-of-mass, each point of which is a possible state of the system. To be more exact, this is a set of states coincident in position but differing in the rotational velocity

$$\dot{\mathbf{a}} = a(\dot{\theta} \cos \theta \cos \varphi - \dot{\varphi} \sin \theta \sin \varphi, \quad \dot{\theta} \cos \theta \sin \varphi + \dot{\varphi} \sin \theta \cos \varphi, \quad -\dot{\theta} \sin \theta)$$

Squaring this expression and substituting it into (1.8.1), we have

$$\epsilon_{rot} = \frac{I}{2} [\dot{\theta}^2 + \sin^2 \theta \dot{\varphi}^2] . \quad (1.8.4)$$

Using this result in (1.7.4) and bearing in mind that the potential energy does not depend on $\dot{\theta}$ and $\dot{\varphi}$, we derive

$$p_\varphi = I \sin^2 \theta \dot{\varphi}, \quad p_\theta = I \dot{\theta} . \quad (1.8.5)$$

The generalized momentum p_φ corresponds to rotation about the z axis, and p_θ to rotation about the axis perpendicular to the plane passing through the z axis and the instantaneous position of the molecular axis. As is seen from Eq. (1.8.5) and Fig. 1.9, at a given velocity $\dot{\varphi}$ the angular momentum p_φ is the function of θ , and at $\theta = 0$ it is equal to zero. Thus, unlike p_θ and $\dot{\theta}$, the ratio between generalized momentum p_φ and generalized velocity $\dot{\varphi}$ is not a constant.

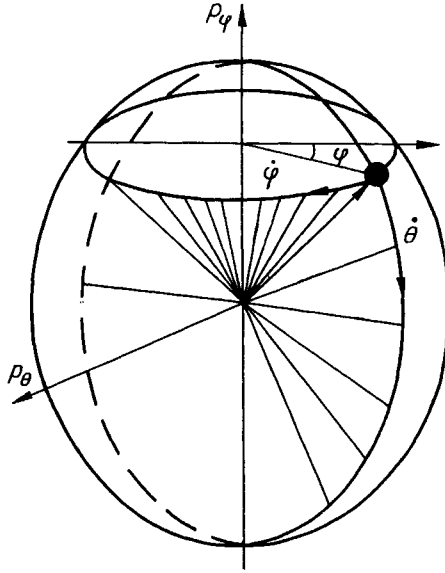


Figure 1.9 Components of angular velocity and momentum in spherical coordinates.

Probability Distribution

According to the Gibbs canonical distribution it is essential that

$$d\Gamma = d\theta d\varphi dp_\theta dp_\varphi, \quad (1.8.6)$$

but not $d\theta d\varphi d\dot{\theta} d\dot{\varphi}$. In view of (1.8.2), (1.8.4) and (1.8.5), the total energy in canonical variables is as follows

$$\mathcal{E}(\theta, \varphi, p_\theta, p_\varphi) = \frac{p_\theta^2}{2I} + \frac{p_\varphi^2}{2I \sin^2 \theta} - qE \cos \theta. \quad (1.8.7)$$

Now the distribution (1.7.3) can easily be made more specific. Using (1.8.6) and (1.8.7), we put it into the form

$$dW(\theta, \varphi, p_\varphi, p_\theta) = \frac{1}{Z} \exp \left[-\frac{p_\theta^2}{2IkT} - \frac{p_\varphi^2}{2IkT \sin^2 \theta} + \frac{qE}{kT} \cos \theta \right] dp_\theta dp_\varphi d\theta d\varphi. \quad (1.8.8)$$

The partition function is

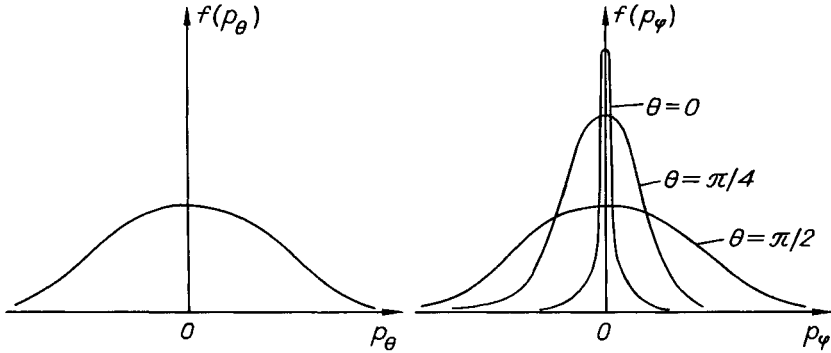


Figure 1.10 Distribution of angular momentum components at different orientations of the molecular axis given by θ .

$$Z = \frac{8\pi^2 I(kT)^2}{qE} \sinh\left(\frac{qE}{kT}\right).$$

According to (1.8.8), the probability of finding a certain value p_φ depends on θ . This is quite natural: the smaller the angle θ , the less probable are large values of p_φ . At $\theta = 0$, all p_φ are improbable, except zero (Fig. 1.10).

Now we express the distribution of molecules in terms of generalized coordinates and velocities. In view of (1.8.5)

$$dW(\theta, \varphi, \dot{\theta}, \dot{\varphi}) = \frac{1}{Z} \exp\left[-\frac{I\dot{\theta}^2}{2kT} - \frac{I\sin^2\theta\dot{\varphi}^2}{2kT} + \frac{qE}{kT} \cos\theta\right] I^2 \sin^2\theta d\theta d\varphi d\dot{\theta} d\dot{\varphi}, \quad (1.8.9)$$

where $\rho(\theta, \varphi, \dot{\theta}, \dot{\varphi}) = I^2 \sin^2\theta$ is the statistical weight, which is not equal to unity in these variables (in contrast to canonical ones) and could not be inferred beforehand.

If we are interested in the dipole orientation rather than in the rotation rate, then, following the routine procedure, we have

$$dW(\theta, \varphi) = \int_{p_\theta} \int_{p_\varphi} dW(\theta, \varphi, p_\theta, p_\varphi) = \frac{\alpha}{4\pi \operatorname{sh} \alpha} e^{\alpha \cos \theta} \sin \theta d\theta d\varphi, \quad (1.8.10)$$

where $\alpha = qE/kT$. For $\alpha \gg 1$, significant deflections of the molecular axis from the z axis are highly improbable, while at $\alpha \ll 1$, all directions are almost equiprobable (Fig. 1.11).

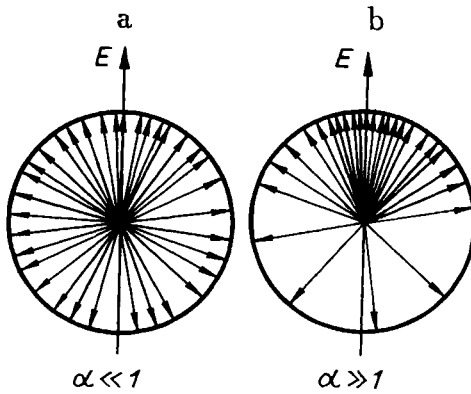


Figure 1.11 Distribution of dipole moments related to the external field E at (a) high and (b) low temperatures.

Electric Polarization

Let us calculate the equilibrium polarization of a gas in an electric field, which is the average dipole moment per unit volume

$$\mathbf{Q} = \int \mathbf{q} dn(\mathbf{q}). \quad (1.8.11)$$

The average number of molecules with a given orientation of the dipole moment \mathbf{q} contained in the unit volume is

$$dn(\mathbf{q}) = ndW(\theta, \varphi). \quad (1.8.12)$$

Due to the axial symmetry of the dipole moment distribution (1.8.10), the mean values of the transversal components of the dipole moment are equal to zero, and the problem reduces to the averaging of the longitudinal component

$$Q = nq \int_{\theta} \int_{\varphi} \cos \theta dW(\theta, \varphi) = nqL(\alpha), \quad (1.8.13)$$

where $L(\alpha)$ is the so-called Langevin function

$$L(\alpha) = \frac{ch\alpha}{sh\alpha} - \frac{1}{\alpha} = \frac{e^{\alpha} + e^{-\alpha}}{e^{\alpha} - e^{-\alpha}} - \frac{1}{\alpha} \begin{cases} 1 & \alpha \gg 1 \\ \frac{\alpha}{3} & \alpha \ll 1 \end{cases}. \quad (1.8.14)$$

Thus the equilibrium polarization of the gas is parallel to the applied field, and its absolute value is a function of the field and temperature. So the two limiting cases may be distinguished

$$Q = qn \frac{\alpha}{3} = \frac{1}{3} \frac{q^2 n}{kT} E = \chi \cdot E \quad \text{at } \alpha \ll 1; \quad (1.8.15a)$$

$$Q = qn \quad \text{at } \alpha \gg 1. \quad (1.8.15b)$$

At rather high temperatures, or, correspondingly, low fields, the polarization is linear in the field and the quantity

$$\chi = \frac{q^2}{3kT} n \quad (1.8.16)$$

is called the electric susceptibility per unit volume. At low fields the excess of dipoles lined up with the field is fairly insignificant, but increases in direct proportion to E . In this case, the linear field theory, or linear optics, is said to be valid, if we deal with alternating fields. Retaining the components quadratic in E in a power expansion of the Langevin function gives rise to the effects of nonlinear optics. Finally, at very strong fields ($\alpha \gg 1$), almost all molecules become orientated with the field, and further increase of E has practically no effect on the polarization ("saturation effect"). In ordinary fields and at room temperatures this case is realized only rarely. As a rule, $\theta = \chi E$, where χ , according to (1.8.16), increases in inverse proportion to the absolute temperature (the Curie law).

1.9 REAL GAS

With the advent of the Gibbs distribution, the problem with the ideal statement may be considered to be solved. All properties of a gas consisting of noninteracting particles are rigorously described by it, however complicated the structure of an isolated molecule.

Intermolecular Interaction

However, as soon as intermolecular interaction is taken into account, the situation becomes different. The ideal gas equation of state $pV = RT$ is not observed to be a universal law. Even real gases do not strictly obey it. In fact, there are as many equations of state as there are gases, since the interaction is specific for each particular kind of molecule. Any general regularity can be inferred only from a rough, idealized model of actual intermolecular interaction. The simplest and most general model of an angle-independent interaction

is that involving only two parameters: one for mutual attraction, and the other, for repulsion of molecules.

The mere existence of condensed phases of a substance—liquids and solids—suggests that at low temperature molecules are bound together by attraction forces. However, mutual attraction prevailing at remote distances gives way to repulsion at very close proximity. The origin of repulsion is even easier to understand than that of attraction. When molecules approach one another up to their “eigenvolume,” further approach encounters stiff resistance, since it can result in the deformation of the molecules’ structure or atomic shells. A quantitative measure of this resistance is the potential energy of interaction $u(r)$. It abruptly increases after passing through the minimum at $r = a_0$ where attraction and repulsion forces balance, then changes sign at $r = d$ and tends to infinity (Fig. 1.12). The approach of one molecule towards the other becomes energy-consuming as soon as their centers come closer than d . Thus the interaction law can be simplified assuming that at the distance d a molecule encounters a potential wall. This is equivalent to assuming that the molecules can be modeled as rigid impenetrable sphere of radius $d/2$. The only advantage of such a simplification is that we can easily allow for the “eigenvolume” (or excluded volume) of molecules $v_d = \frac{4}{3}(d/2)^3$, neglecting

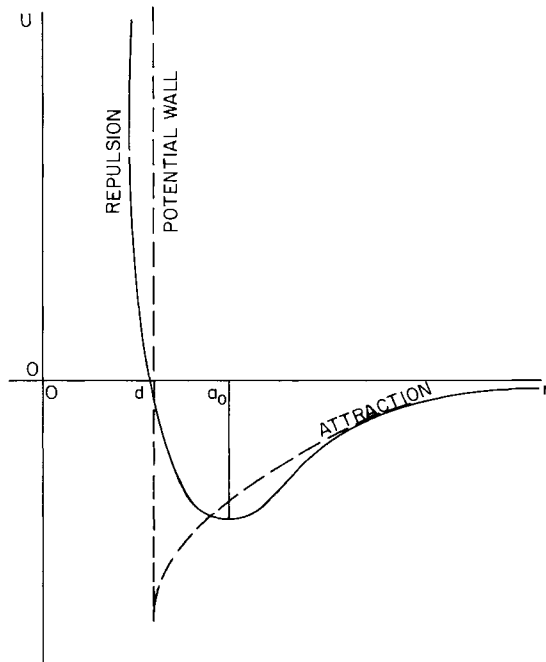


Figure 1.12 Actual intermolecular potential (solid line) and its approximation within the model of attracting hard spheres (dashed line).

the details. This is just the acknowledgment of the fact that the molecules are particles of finite size rather than point masses. The derivation of the van der Waals equation is based exactly on this idealization of molecules as hard spheres attracting one another.

Repulsion

First let us see what we obtain by making allowance for the molecules' eigen-volume. Consider one molecule as a point mass, and all the other molecules as hard spheres of radius d (Fig. 1.13). In our previous discussion, a point mass could be found at any point in space, while now a part of the space is excluded, equivalent to a total volume of spheres of doubled radius. Since the volume of such a sphere is $8v_d$, then in any cubic centimeter very remote from the vessel walls the fraction of excluded volume is $8v_d n$, while that of accessible volume is $1 - 8v_d n$. Thus in the vessel of a volume V , the total free volume is $V_f = V(1 - 8v_d n)$. In the elementary volume dV the free part is $dV_f = dV(1 - 8v_d n)$.

Since penetration into the occupied part of the space is impossible, only equal elements of the free part are occupied equiprobably. In other words, the probability of finding a molecule in any space element free of other molecules is dV_f/V_f . So far, this makes no difference, since the total volume and its unoccupied part are related in the same way: $dW = dV_f/V_f = dV/V$. However, for elements in the immediate vicinity of the walls the relationship between dV_f and dV is somewhat different. Since the molecules are actually hard spheres with the radius $d/2$, none of them including the chosen one can approach the wall closer than $d/2$. Therefore only semispheres presented inside the vessel constitute the excluded volume inaccessible near the wall while the opposite semispheres are of no importance. Each molecule in contact with the wall reduces the free part of the space by half as much as the molecule inside the volume (Fig. 1.14), namely, $4v_d$. If the corpuscular density in the neighborhood of the wall is n_s , in each near-surface unit volume just $4n_s v_d$ is filled by the matter, while the remaining part is a free volume $dV_s = dV(1 - 4v_d n)$.

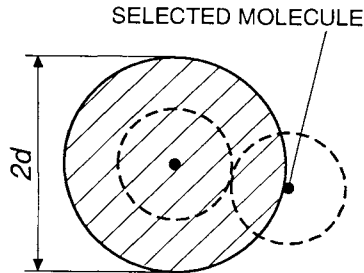


Figure 1.13 Excluded volume in a collision of hard spheres (shaded).

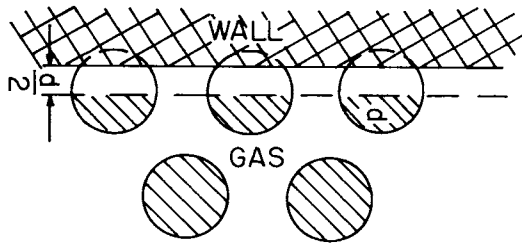


Figure 1.14 Excluded volume near the wall and in the interior of a gas container. The layer of width $d/2$ is unavailable to the center of any molecule.

Accordingly, the probability of finding a molecule near the surface is somewhat greater than that away from it.

$$dW_s = \frac{dV_s}{V_f} = \frac{1 - 4v_d n_s}{1 - 8v_d n} \frac{dV}{V}.$$

For this reason we have to distinguish between the near-surface density n_s and the average density $n = N/V$. Obviously,

$$n_s = \frac{NdW_s}{dV} = \frac{1 - 4v_d n_s}{1 - 8v_d n} n,$$

so

$$n_s = \frac{n}{1 - 4v_d n}. \quad (1.9.1)$$

The near-wall increase in the particles density also affects the pressure applied to the wall

$$p = n_s kT = \frac{nkT}{1 - 4v_d n}. \quad (1.9.2)$$

This is essentially the simplest estimate of *thermal* pressure of hard-sphere gas $p_t = \Gamma nkT$. Since $\Gamma = 1/(1 - 4v_d n) > 1$ at $v_d \neq 0$ the real gas pressure is greater than that in the ideal gas (point mass) model.

Attraction

If one takes into account now the mutual attraction of molecules, the opposite results are obtained. Consider a molecule far from the wall that is being attracted by each molecule nearby. Such a molecule is thrown from side to side, since the resultant of the attractive forces varies randomly in magnitude

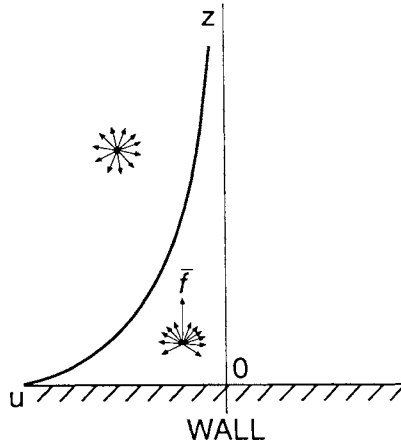


Figure 1.15 The resultant attractive force (near the wall and inside the gas container) and its potential $u(z)$.

and direction. However, the time-averaged force is equal to zero, because the molecule is pulled in different directions and none of them is preferred (Fig. 1.15).

However, a molecule near the surface experiences attraction only from the inside of the vessel, because the wall is still considered as ideal. Thus, despite fluctuations, the time-average resultant of attractive forces differs from zero. Due to symmetry, this average force must be perpendicular to the wall and directed inward. As a molecule moves away from the wall, the direction of the force remains the same, while its magnitude decreases and, eventually, goes to zero. At any point the average force is the increasing function of the density of molecules whose collective efforts draw a periphery molecule inside the vessel:

$$\bar{f} = \gamma(z)n . \quad (1.9.3)$$

The coefficient $\gamma(z)$ must be equal to zero deep inside the vessel (with $z \rightarrow \infty$), but increases monotonically when the wall is approached, reaching its maximum at $z = 0$. As with any other field, this field of average force may be associated with a certain potential going to zero away from the walls

$$u(z) = n \int_z^{\infty} \gamma(z) dz . \quad (1.9.4)$$

The distribution of molecules in such a field is described by the barometric formula:

$$n(z) = n \exp \left(-\frac{n}{kT} \int_z^\infty \gamma(z) dz \right). \quad (1.9.5)$$

Naturally, the gas density decreases approaching the wall, though the precise dependence is unknown due to the lack of knowledge of $\gamma(z)$. Fortunately, this is of minor importance. To find the pressure, we need only know the density in the vicinity of the wall

$$n(0) = n \exp \left(-\frac{n\bar{\gamma}}{kT} \right), \quad (1.9.6)$$

which is expressed in terms of the single unknown parameter $\bar{\gamma} = \int_0^\infty \gamma(z) dz$. The quantity $\bar{\gamma}n$ has the meaning of the “work expended on escaping from the gas,” that is, the energy spent by a “surface molecule” in overcoming the coupling forces that bind it to other molecules inside the gas. The parameter $\bar{\gamma}$ describes the attraction of molecules, just as ν_d determines the repulsion effect. It is seen from Eq. (1.9.6) that the pressure on the wall is

$$p = n(0)kT = nkT \exp \left(-\frac{n\bar{\gamma}}{kT} \right). \quad (1.9.7)$$

It is not surprising that the pressure is less than that of the ideal gas: attraction forces acting from inside partly prevent the boundary molecules from striking the walls.

Equation of State

Equation (1.9.2) is valid for noninteracting hard spheres and Eq. (1.9.7) for point particles attracting each other. These models can be synthesized so that both repulsion and attraction will be taken into account. For this purpose it is sufficient to generalize Eq. (1.9.6) by considering the near-border gas compression, as was done before for Eq. (1.9.1). Finally, we arrive at

$$n_s = \frac{n(0)}{1 - 4\nu_d n} = \frac{n}{1 - 4\nu_d n} \exp \left(-\frac{n\bar{\gamma}}{kT} \right) \quad (1.9.8)$$

and, consequently:

$$p = \frac{nkT}{1 - 4\nu_d n} \exp \left(-\frac{n\bar{\gamma}}{kT} \right). \quad (1.9.9)$$

This is the so-called Dieterici equation of state. When the exponent is much less than unity, one can easily derive, by power expansion of Eq. (1.9.9), the following equation for one mole of gas:

loop, including its inner region. Instead, a homogeneous phase decomposes into liquid and vapor and, thus, transforms into a binary system. When the pressure exerted on a dense homogeneous fluid tends to decrease at constant temperature, both phases and an interface appear simultaneously at $p = p_V$. The pressure of the saturated vapor p_V remains constant until all liquid is evaporated. Only after the liquid–vapor transition is complete does the system again become homogeneous and the gas pressure starts to fall upon expansion.

The homogeneous systems may not be distinguished if they are disordered. One can distinguish between the gas and liquid if only they are the integral parts of the binary system. The criterion is the density, which makes a “jump” at the interface. In Fig. 1.16 this jump is characterized by the difference between molar volumes, V_L and V_V . This difference decreases with rising temperature and goes to zero once the critical temperature T_c is achieved. For all $T > T_c$ (overcritical region) the existence of a binary system is impossible and, consequently, liquid and gas are indistinguishable.

For any temperature below critical the liquid is in equilibrium with its vapor at a distinct pressure p_V , kept constant on a horizontal “Maxwell shelf,” that joins the corresponding states on Fig. 1.16. The vapor pressure may be estimated on the basis of the so-called Maxwell rule (see Eq. (5.6.24) in Chapter 5):

$$p_V(V_V - V_L) = \int_{V_L}^{V_V} p(V, T) dV. \quad (1.9.11)$$

Thus, p_V is determined from the equality of the areas below the Maxwell shelf and the van der Waals loop joining the same states.

The extent to which the van der Waals theory represents the qualitative features of the behavior of real gases can be judged from Fig. 1.17, which depicts a family of nitrogen isotherms. They are plotted according to an empirical equation of state, which is far more complex than the van der Waals equation but approximates experimental data within the error. Parameters of the equation are adjusted using data related to stable isotherm branches (liquid and gas). In the unstable region, one can only extrapolate these data to it, relying on analytical continuation of well established isotherms $p(V)$. If the extrapolation is reliable, both branches are linked within the unstable region, thus demonstrating a behavior typical for the van der Waals loop. This was shown to be the case at a few different temperatures below critical one. Moreover, when estimating the vapor pressure using the Maxwell rule applied to the restored loops it was verified that p_v so obtained coincides with the experimental one. This is evidence that the van der Waals loop is something real.

Points connected by the Maxwell shelves lie on curve a (Fig. 1.17), called a binodal. An ascending branch of the binodal is called a liquid line and a descending branch a gas line. By carefully expanding a very pure liquid, it is

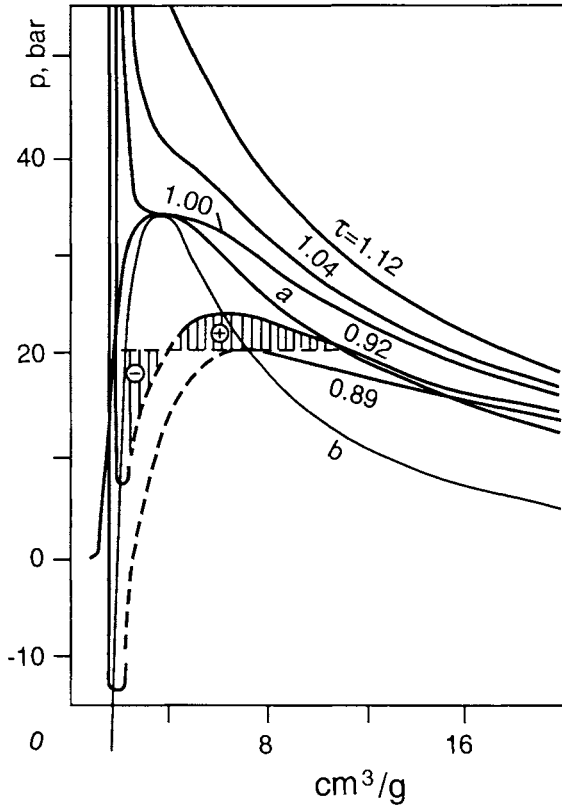


Figure 1.17 Nitrogen isotherms at corresponding temperatures $\tau = T/T_c$: (a) binodal (coexistence line), (b) spinodal. The loop for $\tau = 0.92$ is hatched. (From A. A. Vasserman *Russ. J. Phys. Chem.* **38**, 1289 (1964).)

possible to cross the binodal and move down along the isotherm to approach its minimum, unless it lands in the negative pressure region. Similarly, it is possible to advance upwards along the gas branch of the isotherm to its maximum. In these cases the homogeneous metastable states of the *overexpanded* liquid or *supersaturated* vapor are attained. Although unstable with respect to division into two phases they are still realizable. Totally unstable are the inner parts of the isotherms between the extrema situated on curve *b*, which is called spinodal (see Fig. 1.17). While its ascending branch corresponds to a maximally expanded condensed state, its descending branch corresponds to a maximally condensed gas state. Metastable states located between the binodal and spinodal may be also related either to an *overheated* liquid or to an *overcooled* vapor, provided they are compared with stable phases at the same pressure. The binodal and spinodal have a common apex at the critical point. The critical isotherm is bent at this point, and at higher temperatures $(\partial p/\partial V)_T < 0$ all along the isotherms.

The whole picture is described semiquantitatively by the van der Waals equation. Positions of isotherm extrema that constitute the van der Waals spinodal are located by the conventional condition:

$$\left(\frac{\partial p}{\partial V}\right)_T = -\frac{RT}{(V-B)^2} + \frac{2A}{V^3} = 0. \quad (1.9.12a)$$

As the temperature increases, the extrema come closer to each other and eventually merge at $T = T_c$ creating an inflection point, which is determined by an additional condition:

$$\left(\frac{\partial^2 p}{\partial V^2}\right)_T = \frac{2RT}{(V-B)^3} - \frac{6A}{V^4} = 0. \quad (1.9.12b)$$

Using both equations (1.9.12) one can find, within the van der Waals theory, the coordinates of the critical state:

$$V_c = 3B, \quad T_c = \frac{8}{27} \frac{A}{RB}, \quad p_c = \frac{A}{27B^2}. \quad (1.9.13)$$

The last coordinate was determined by substituting V_c and T_c into Eq. (1.9.10). All the parameters taken together determine the van der Waals gas compressibility factor at the critical point: $p_c V_c / RT_c = F_c = 3/8 = 0.375$. It turns out to be much higher than the experimental value. For example, for a series of saturated hydrocarbons $F_c = 0.267$. This value is in much better agreement with the value found by the Dieterici equation ($F_c = 0.2706$). However, any equations that use only two parameters can hardly claim to provide good quantitative agreement with experiment over wide ranges of p and V . Still, from the heuristic viewpoint these equations are very valuable owing to their simplicity and transparency as regards the physical sense.

The difference in size of molecules and in the cohesive force between them has quite a strong effect on the van der Waals parameters and, eventually, on critical characteristics of real gases (1.9.13). To facilitate and unify comparison of different molecular media, van der Waals put forward the idea of their "corresponding states," which are determined by the following reduced variables:

$$\pi = \frac{p}{p_c}, \quad \omega = \frac{V_c}{V}, \quad \tau = \frac{T}{T_c}. \quad (1.9.14)$$

With these variables, the van der Waals equation (1.9.10) acquires universality, independent of the nature of the gas:

$$\pi + 3\omega^2 = \frac{8\omega\tau}{3 - \omega} . \quad (1.9.15)$$

This universality is a useful guide for estimating the behavior of dense gases and liquids. It was formulated as a “principle of corresponding states”: all substances taken at the corresponding temperatures and pressures also have the same corresponding density.

As found, the principle of corresponding states is in good agreement with experimental data despite the fact that the van der Waals equation itself is not very accurate. In other words, the principle has far wider applications than the equation it is based on. Isotherms of various gases plotted as functions of the reduced variables (1.9.14) are, in fact, very close to each other and are nearly the same for gases having intermolecular interactions of the same type.

Compressibility Factor

The Hougen and Watson chart shown in Fig. 1.18 was prepared by averaging data for seven gases (H_2 , N_2 , CO , NH_3 , CH_4 , C_3H_8 and C_5H_{12}). It depicts the isothermal pressure dependence of the gas compressibility factor, $F = pV/RT$. A modern analog of this chart for N_2 is shown in Fig. 1.19. The latter gives an idea of isothermal behavior of $F(p)$ over much wider ranges and, in addition, for both gas and liquid states.

On these charts the ideal gas is presented by a single point: $p = 0$, $F = 1$. All isotherms begin from this point corresponding to an infinitely rarefied state, but behave differently as the pressure increases. For high-temperature isotherms the compressibility factor increases from the beginning. For low-temperature isotherms it first decreases and undergoes a sharp jump downwards upon gas liquefaction and only then tends upwards, returns to its starting value $F = 1$ and eventually exceeds it. This is because attraction makes compressibility smaller, while repulsion enhances it. With increasing temperature or pressure the role of repulsion increases and finally becomes dominating even if initially it was relatively low.

To make these arguments more concrete let us present the van der Waals compressibility factor as density expansion in the vicinity of the ideal gas state:

$$F = \frac{1}{1 - B/V} - \frac{A}{RTV} = 1 + \frac{B - A/RT}{V} + \left(\frac{B}{V}\right)^2 + \left(\frac{B}{V}\right)^3 + \dots \quad (1.9.16)$$

This form of the van der Waals equation can be regarded as a particular case of the virial expansion:

$$F = 1 + \frac{B_0}{V} + \frac{C_0}{V^2} + \frac{D_0}{V^3} + \dots, \quad (1.9.17)$$

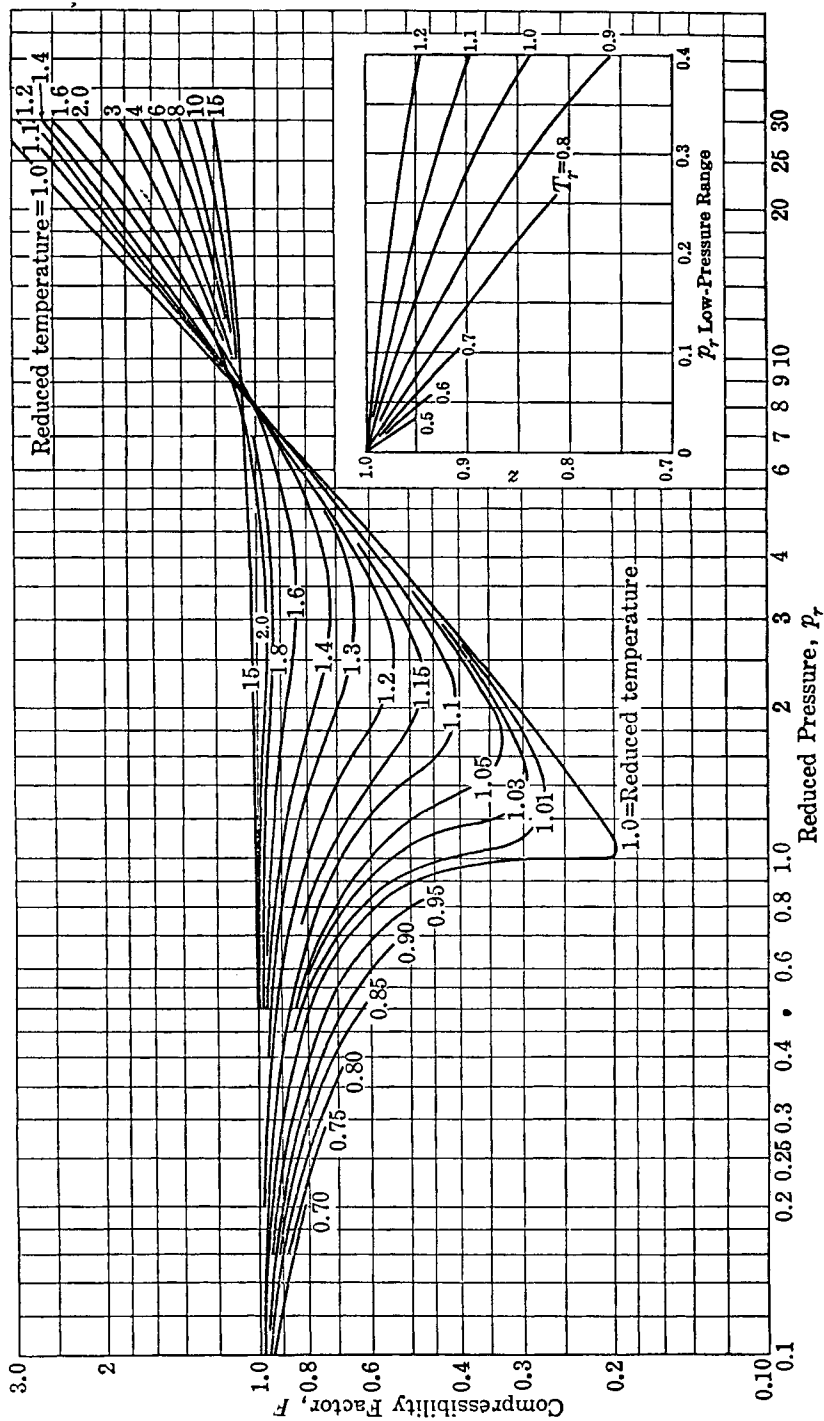


Figure 1.18 The compressibility factor as a function of the reduced pressure and the reduced temperature. (From O. A. Hougen and K. M. Watson, *Chemical Process Principles*, John Wiley (1947), Part II; see also Fig. 4.1-2 in *Molecular Theory of Gases and Liquids* by J. O. Hirschfelder, C. F. Curtiss, and B. R. Bird.)

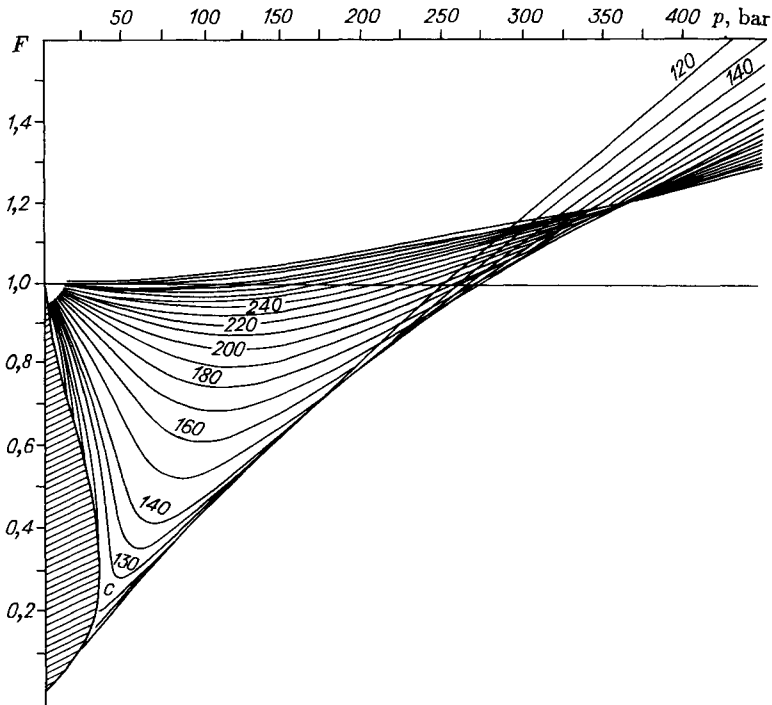


Figure 1.19 The contemporary Hougen–Watson chart for nitrogen.

whose coefficients are expressed in terms of intermolecular forces (Latin *vires*). Generally speaking, each of the coefficients depend on the forces of attraction and repulsion. However, within the approximate van der Waals model it is the second virial coefficient alone that takes care of both forces. This coefficient is defined as:

$$B_0 = B - \frac{A}{RT} . \quad (1.9.18)$$

The competition between attraction and repulsion affects not only the value, but also the sign of the coefficient, which determines the isotherm slope at $p = 0$:

$$F \approx 1 + \frac{B_0}{V} \approx 1 + \frac{B_0}{RT} p \quad \text{at} \quad |1 - F| \ll 1 . \quad (1.9.19)$$

The second virial coefficient is equal to zero at the so-called Boyle's temperature. Within the van der Waals theory this is:

$$T_B = \frac{A}{BR}. \quad (1.9.20)$$

Below Boyle's temperature, upon isothermal compression of a real gas the compressibility factor first falls. Above Boyle's temperature the compressibility factor increases from the very beginning to the very end.

On inspecting Figs. 1.18 and 1.19 one can easily see that below Boyle's temperature the compressibility factor equals unity at two points of any isotherm. One of the points, which is common for all isotherms, corresponds to the true ideal gas state at $p = RT/V \rightarrow 0$, when both van der Waals corrections are equal to zero. The second point corresponds to a "pseudoideal" state. In this state both corrections are significant, but are equal and opposite in sign and so cancel one another. As a result, one obtains again $pV = RT$. Pseudoideal states correspond to the points where isotherms cut the line $F = 1$. Their abscissae depend on the temperatures (both on pressure and density scales).

The locus where gas becomes pseudoideal is the "ideal gas curve," or the "orthometric curve." The latter notion was originally introduced by Batschinski. Assuming $F = 1$ and taking into account the definition of Boyle's temperature one can readily derive from the van der Waals equation the corresponding equation of the orthometric curve:

$$1 - B/V = T_B/T.$$

From this it follows that density on the gas orthometric line falls linearly with increasing temperature:

$$n = \frac{N_0}{B} \left(1 - \frac{T}{T_B}\right) = \frac{1}{4\nu_d} \left(1 - \frac{T}{T_B}\right). \quad (1.9.21)$$

This surprising and impressive linearity (see Fig. 4.16) discovered by Batschinski in 1906 was a subject of intensive studies made in the last century's sixties and seventies by Vasserman, Nedostup, Burshtein and Shokhirev. Quite recently this phenomenon was subjected to a new investigation by Ferschbach et al. who gave it a new name: "Zeno line".

Along this line the pressure changes parabolically:

$$p = nkT = \frac{RT}{B} \left(1 - \frac{T}{T_B}\right)^2. \quad (1.9.22)$$

It is seen that the orthometric curve $p(T)$ is a parabola with an apex at the point $T_B/2$. The maximum orthometric pressure is

$$p_0 = \frac{RT_B}{4B} = \frac{A}{4B^2}. \quad (1.9.23)$$

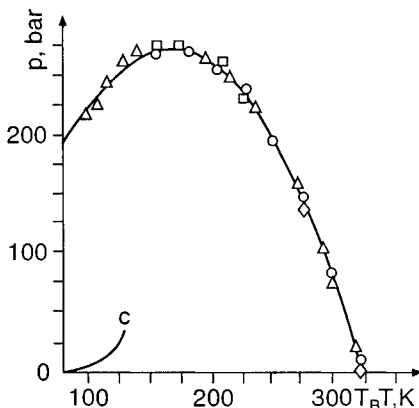


Figure 1.20 Nitrogen orthometric (“ideal gas”) curve. The coexistence line (binodal) shown in the lower part of the graph comes to an end at the critical point C.

These conclusions of the van der Waals theory are in excellent agreement with experimental studies of orthometric curves of noble and molecular gases, which condense in “simple liquids” (see Chapter 4). Fig. 1.20 shows a nitrogen orthometric curve, plotted using the most reliable experimental data of different authors. The curve is, indeed, parabolic along the whole length. Everywhere under this curve attraction forces dominate over repulsion, while above the situation is opposite. The liquid–vapor coexistence curve that ends with a critical point is deep inside the region where attraction plays a governing role.

The fact that the pressure, where pseudoidealization occurs, first increases with temperature and then falls is seen on close inspection of Fig. 1.19. Taking into account that near the orthometric maximum the pressure changes only slightly, one can expect that a few isotherms having temperatures close to $T_B/2$ will pass through pseudoideal states under nearly the same pressure. Due to the selection of exactly such isotherms for the Hougen–Watson chart (Fig. 1.18), it appears that they cross in at a common point. Apparently, the abscissa of the intersection point is nothing else but p_0 —the maximum orthometric pressure.

With relation (1.9.13) it is possible to obtain the following estimates of typical orthometric curve parameters:

$$T_B = \frac{27}{8} T_c, \quad p_0 = \frac{27}{4} p_c. \quad (1.9.24)$$

However, empirically, the actual T_B/T_c ratio is close to 2.64 rather than to 3.37 as follows from (1.9.24). It is exactly for this reason that the temperature of the orthometric maximum is very close to the critical temperature: $T_B/2 = 1.3 T_c$. Similarly, the maximum pressure, which according to the Hougen–Watson chart is equal to $8p_c$, is notably higher than the value obtained from (1.9.24): $p_0 = 6.8p_c$. However, one should not expect better from the van der Waals

equation, which uses only two parameters and is quantitatively valid for only low pressures.

1.10 BASIC IDEAS OF STATISTICAL THERMODYNAMICS

The above derivation of the van der Waals equation is possible due to the essential simplifications of the intermolecular potential. In any attempt to do it more rigorously and accurately we have to deal with actual interactions of particles, in which it is difficult or even impossible to separate attraction and repulsion. Fortunately, there is an alternative method which leads to a standard recipe for the calculation of thermodynamic properties of macroscopic systems with arbitrary interparticle interactions. This method was advanced by Gibbs.

The Gibbs Ensemble

The main idea was to consider N interacting particles as a unit rather than separately. To define the “gas state” as a whole, we need now to specify the positions and momenta of all N molecules. Formerly, the “state” was defined by the six variables (coordinates and velocities or coordinates and momenta) of a single molecule; now we need the $6N$ variables of all molecules in the given volume. To specify $6N$ numbers means to indicate the point in the $6N$ -dimensional configurational space (“ Γ -space”) that defines the state of the entire gas, while the point in the ordinary 6-dimensional “ μ -space” specifies that of one particle only.

In fact, in moving to the Γ -space terminology we can define by one point in Γ -space the distribution of N points in μ -space. This distribution is not, however, the Maxwell–Boltzmann distribution. For an arbitrarily chosen point in Γ -space, the distribution of particles corresponds to an instantaneously “photographed” gas state. Some time later, the state is changed and is therefore associated with another point in Γ -space or with another distribution of particles in μ -space. The gas as a mechanical system develops in time: the particles move, change their position, and, upon collisions, their velocity. The system passes through a series of states lying on a trajectory in Γ -space (Fig. 1.21a). In μ -space distributions permanently change from one to another. To illustrate this, consider, for example, the energy distribution in μ -space (Fig. 1.21b). A given point in Γ -space corresponds to one distribution, another point to another distribution, and thus Maxwell’s \bar{f} may be found only by exhausting all trajectory points, that is, by averaging over all possible distributions. It is easily seen that this procedure is similar to the determination of the average pressure (see Section 1.1). Each state of the system is associated with a certain pressure $F(t)/S$ that oscillates randomly in time about its mean value (Fig. 1.21c). Similarly, the instantaneous distribution of molecules in a gas differs

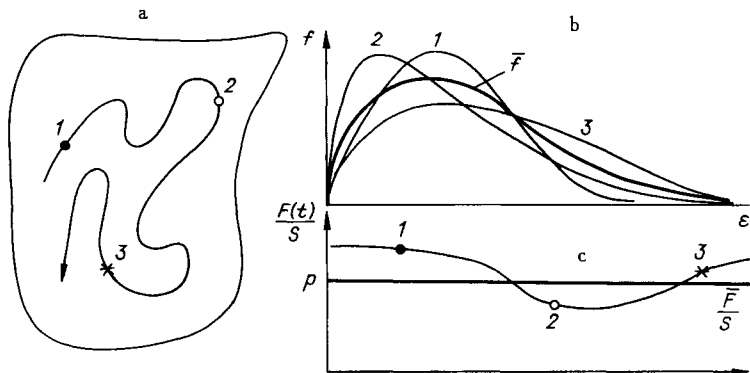


Figure 1.21 (a) The points of the trajectory in Γ -space, (b) the corresponding energy distributions, and (c) pressure acting on the wall at successive moments of time 1, 2, and 3.

from the time-averaged distribution which is the only appropriate one for a description of the system's equilibrium properties.

How can we find the time-averaged distribution? Before averaging the distributions, it is necessary to know the frequency of their realization, that is, the probability that the system will find itself at one or another point in Γ -space. This is the statement of the main problem of statistical mechanics. To clarify, let us imagine, as suggested by Gibbs, a collection of identical systems—an “ensemble” of identical boxes containing the same number of identical particles. Obviously, while the macroscopic gas state is the same in each of them, the microscopic states of the ensemble's systems do not necessarily coincide: each is associated with a different point in Γ -space. How can one find the equilibrium distribution of these points in Γ -space?

Microcanonical Distribution

Some information on the form of this distribution may be obtained from the fact that all points representing these systems in Γ -space move along the corresponding phase trajectories. We want the result of any averaging over the ensemble to be time-independent, as this is just what happens under equilibrium conditions. Therefore, we should require that the density of points in any Γ -space element be constant, despite motion. In other words, the probability of any microstate realization must be time-invariant. If all systems of the ensemble are isolated from heat and mass exchange with the environment, their internal motion conserves energy and they are described by ordinary mechanical laws. By these laws, when in motion, the points in the Γ -space of *canonical variables* (coordinates and momenta) behave as marked points of incompressible liquid: their density in a flow does not vary with time (“Liouville's theorem”). For everything to be time-invariant, the points must be distributed uniformly along the trajectory. Then the number of points enter-

ing any Γ -space volume element will coincide with the number of points leaving it in the same period of time. Thus it is the Liouville theorem that distinguishes the *phase space* of canonical variables as unique (between other configurational spaces). In this space and this space only the distribution over equal isoenergetic elements is assumed to be equiprobable (see Section 1.7). However, the Liouville theorem does not define the distribution of points in the phase space in a unique fashion. To meet the condition of equilibrium, we need only distribute the points uniformly along each trajectory. However, many trajectories have the same energy, and it is unknown how the point density will vary from one trajectory to another.

However, all trajectories are indistinguishable from any point of view. If isolated, the system has the same energy for any accessible point of Γ -space, that is, all points of Γ -space lie on a hypersurface of equal energy. Thus the only possible distinguishing feature disappears and the only way out is to assume that all trajectories are equivalent. Therefore, the equal volume elements of different trajectories must also be equivalent and consequently equally populated. In other words, the distribution of systems in Γ -space may be reasonably assumed to be completely uniform. Of course, such an extension of the conclusion following from the Liouville theorem should be considered as a principle. Its final statement is known as Gibbs' microcanonical distribution: an isolated system may be found equiprobably at any accessible state of the prescribed energy \mathcal{E} (between E and $E + \Delta E$), while the probability of finding it outside this energy layer is equal to zero. As usual, the probability is proportional to the volume of the element $d\Gamma$ where the system is sought:

$$dW = \begin{cases} \frac{d\Gamma}{\Delta\Gamma} = \Phi d\Gamma & E \leq \mathcal{E} \leq E + \Delta E, \\ 0 & \mathcal{E} < E \quad \mathcal{E} > E + \Delta E. \end{cases} \quad (1.10.1)$$

Here $\Delta\Gamma$ is the complete volume of the Γ -space accessible to the system at the given energy.

Gibbs' Canonical Distribution

The Gibbs canonical ensemble may be thought of as an ensemble of systems which are "Gibbs' boxes" disposed in a heat reservoir. Such systems are no longer isolated, but have a heat contact with the environment. In each system the temperature is held constant (equal to that of the reservoir), while the energy may vary. Due to the energy exchange with the reservoir, the system is able either to gain or to lose energy, thus moving from one isoenergy surface to another. As for a microcanonical ensemble, each system always remains on a single defined surface (within the layer of the thickness ΔE).

Therefore the microcanonical and canonical distributions differ in that the former has no exponential multiplier, while the latter includes this factor:

$$dW = \frac{1}{Z} \exp\left(-\frac{\mathcal{E}}{kT}\right) d\Gamma = \Phi(\mathcal{E})d\Gamma, \quad 0 \leq \mathcal{E} < \infty \quad (1.10.2)$$

This has nothing to do with the system's size. The canonical distribution is applicable both to an isolated molecule and to the gas on the whole.

In fact the availability of different energies leads to the introduction of a probability density $\Phi(\mathcal{E})$ in (1.10.2), which is the exponentially decreasing function of energy. Even considering it unknown, we can write

$$dW = \Phi(\mathcal{E})d\Gamma.$$

However, if the system consisted of two weakly interacting parts, so that $\mathcal{E} = \mathcal{E}_1 + \mathcal{E}_2 + \mathcal{E}_{\text{int}}$, $N = N_1 + N_2$, then the same relation would obviously be valid for each of them. Assuming them to be independent by virtue of weak interaction: $\mathcal{E}_{\text{int}} \ll \mathcal{E}_1, \mathcal{E}_2$, it is possible to determine the probability of finding the entire system in a certain state by the multiplication theorem:

$$dW(\mathcal{E}) = dW(\mathcal{E}_1)dW(\mathcal{E}_2).$$

Therefore

$$\Phi(\mathcal{E})d\Gamma = \Phi(\mathcal{E}_1)\Phi(\mathcal{E}_2)d\Gamma_1d\Gamma_2.$$

As $d\Gamma = d\Gamma_1d\Gamma_2$ and \mathcal{E}_{int} is negligible, $\Phi(\mathcal{E}_1 + \mathcal{E}_2) = \Phi(\mathcal{E}_1)\Phi(\mathcal{E}_2)$. By analogy with (1.2.6), this equation immediately gives

$$\Phi(\mathcal{E}) = \frac{1}{Z} e^{-\alpha\mathcal{E}},$$

where $\alpha = 1/kT$ and

$$Z = \int \exp(-\mathcal{E}/kT) d\Gamma, \quad (1.10.2a)$$

where $d\Gamma = dq_1dp_1dq_2dp_2\dots dq_Ndp_N$. A similar distribution for an isolated molecule may be obtained only for an ideal classical gas when $\mathcal{E} = \sum_{i=1}^N \epsilon_i$. Only in this case $dW = \prod_{i=1}^N dW_i$, so simply summing probabilities we get from (1.10.2)

$$dW(q_1, p_1) = \int_2 \dots \int_N dW(1, 2, \dots, N) = \frac{e^{-\epsilon_1/kT} dq_1 dp_1}{Z^{1/N}}, \quad (1.10.3)$$

that is, the conventional Maxwell–Boltzmann distribution. This result seems quite natural, since any classical molecule is a subsystem that interacts with the gas as with a thermostat, and the Gibbs distribution is well applicable to it.

In the case of an ideal (but not classical!) gas, passing from Γ -space to μ -space requires much greater effort and leads to distributions differing from the Maxwell–Boltzmann one. The reason is that even noninteracting quantum particles cannot be considered as independent subsystems.

For a classical real gas, a reduction of the type (1.10.3) is impossible for a different reason. If in total energy

$$\mathcal{E} = \sum \epsilon_i + U(q_1, q_2, \dots, q_N) \quad (1.10.4)$$

U is not ignored, then $dW \neq \prod_i dW_i$, and it is impossible to describe a real gas by any distribution in μ -space.

Entropy

So we return to the problem posed at the very beginning. Now the distributions in Γ -space are known, but we still do not know how to use them. Even in the derivation of the ideal gas equation of state, the problem was divided into two parts: firstly to find the distribution $dW(\mathbf{v})$, and then to establish the relationship between this distribution and the observed quantity, for example, pressure: $p = nm \int v_x^2 dW(\mathbf{v})$. This second part until now has remained uncertain. For an isolated system, we know the volume and internal energy (V and \mathcal{E}) of the gas, along with (1.10.1). In the case of an open system, its volume V and temperature T as well as distribution (1.10.2) are known. To define the state of the gas completely, the two known variables must be complemented by a third one. This need not be the pressure as determined earlier from T and V . But, whatever the third parameter is, it should be calculated from distributions related to the gas as a whole: either (1.10.1) or (1.10.2) according to the situation.

Let us vary the gas volume V with either $\mathcal{E} = \text{const}$ (isolated system), or $T = \text{const}$ (open system). This will cause a change in the gas pressure and other characteristic quantities. However, in this process the distributions (1.10.1) and (1.10.2) will remain unchanged, except for the normalization constants $\Delta\Gamma$ and Z . This suggests that these quantities contain the required information.

For example, for the ideal gas $\Delta\Gamma = \int d\Gamma \propto V^N$. Consequently, a twofold increase in the vessel's volume will lead to an increase in accessible phase volume $\Delta\Gamma$ by a factor of 2^N and, correspondingly, to a decrease in the probability density Φ of the same factor. The greater the number of accessible states, the smaller the normalized probability of attaining any one. For an isolated system the quantity

$$\Delta\Gamma = \int d\Gamma = \left(\underbrace{\int \dots \int}_q \underbrace{\int \dots \int}_p dq_1 \dots dp_N \right)_{V, \mathcal{E}=\text{const}}$$

is a measure of the macroscopic state degeneration, that is, the number of ways N molecules with any velocity may be arranged within the vessel, provided that the total energy of the system is kept within the specified range ΔE .

If an ideal gas is constituted of molecules of two types, both may be considered as subsystems with particle number N_1 and N_2 ($N = N_1 + N_2$). Each subsystem may be in any one of the states of its phase volume $\Delta\Gamma_1$ or $\Delta\Gamma_2$, respectively. The total number of all possible states of the whole system is determined by the product of these volumes $\Delta\Gamma = \int d\Gamma_1 \int d\Gamma_2 = \Delta\Gamma_1 \Delta\Gamma_2$. Hence, the relation between $\Delta\Gamma$ and any additive macroscopic characteristic of the system must be only of the form

$$S = k \ln \Delta\Gamma. \quad (1.10.5)$$

Only a logarithmic relationship ensures the additivity of

$$S = k \ln \Delta\Gamma_1 + k \ln \Delta\Gamma_2 = S_1 + S_2$$

when $\Delta\Gamma = \Delta\Gamma_1 \Delta\Gamma_2$ is multiplicative. However, the realization that S in the relationship (1.10.5), is the *entropy* was reached first by Boltzmann. He recognized that entropy is the measure of the system's disorder. The greater the number of distinguishable microstates which are compatible with the particular value of V and \mathcal{E} , the greater the entropy.

Fluctuations

It should be noted that not all states of an isolated system can be identified with the macroscopic equilibrium. For example, if all ideal gas molecules are concentrated in a small portion of the vessel, with the equilibrium velocity distribution remaining unchanged, this state should be considered as a fluctuation although it is accessible (belongs to $\Delta\Gamma$). The state when all molecules are uniformly distributed over the vessel and move with the same velocity $v = (2\mathcal{E}/Nm)^{1/2}$ is also a fluctuation.

Fortunately, such states which differ drastically from the average one are very few in number. For the majority of states, the corresponding distributions of molecules in the space of coordinates and velocities differ little from the equilibrium, time-averaged distribution. Due to the huge number of particles in an isolated system, the number of states of the system which are actually distinguishable from the equilibrium is a minute fraction of all states contained in $\Delta\Gamma$. Thus it makes no difference how the entropy of an isolated system is

defined: as a logarithm of the number of equilibrium states, or as a logarithm of all states compatible with the specified V and \mathcal{E} , as in Eq. (1.10.5).

Free Energy

In the case of an open system (canonical ensemble) the situation is quite different. Such a system can find itself in a state with arbitrary energy, that is, the whole volume of Γ -space is accessible to it. Naturally, the entropy cannot be expressed in terms of the total volume $\Delta\Gamma$ which is infinite, but solely in terms of the finite part $\Delta\Gamma_e$ that actually corresponds to equilibrium. Despite the possibility of an energy exchange with the environment, the open system is much more frequently found in this part of space than in the rest of it.

The reason for this is that the statistical weight $\rho(\mathcal{E})$ increases sharply with energy. In the case of one particle it increases as $\mathcal{E}^{1/2}$, while in a system of N noninteracting particles the degeneration of states with the same total energy increases as $\mathcal{E}^{N/2}$. Such an abrupt rise of $\rho(\mathcal{E})$ competes with the equally dramatic decrease of the exponential factor $\exp(-\mathcal{E}/kT)$. Consequently, there is a sharp maximum near $\mathcal{E} = \bar{\mathcal{E}}$, and any significant deviations of energy from $\bar{\mathcal{E}}$ are improbable (Fig. 1.22). So, by order of magnitude

$$\int dW = \int \Phi(\mathcal{E}) d\Gamma \approx \Phi(\bar{\mathcal{E}}) \Delta\Gamma_e = 1,$$

where $\Delta\Gamma_e = \rho(\bar{\mathcal{E}})\Delta E = 1/\Phi(\bar{\mathcal{E}})$ is the volume of that part of phase space where $dW/d\mathcal{E} = \Phi(\mathcal{E})\rho(\mathcal{E})$ is essentially different from zero. The definition of

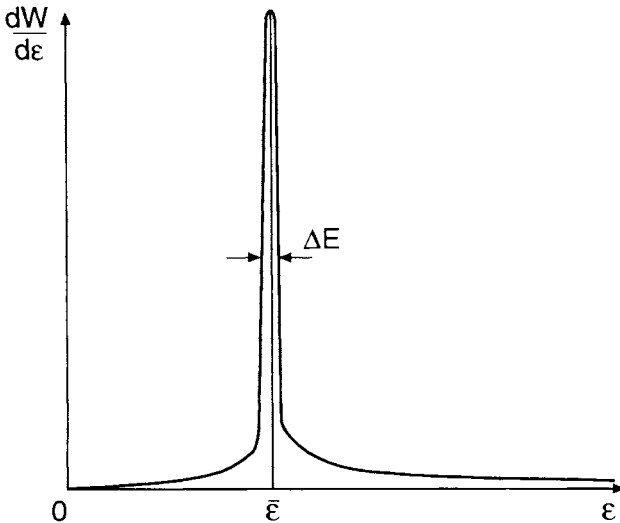


Figure 1.22 The canonical energy distribution for large system.

of entropy which remains the measure of equilibrium state degeneracy must be generalized as follows:

$$S = k \ln \Delta\Gamma_e = -k \ln \Phi(\bar{\mathcal{E}}), \quad (1.10.5a)$$

For isolated systems the definition of entropy thus generalized is identical to the previous one, since $\Phi(\bar{\mathcal{E}}) \equiv \Phi(\mathcal{E}) = 1/\Delta\Gamma$. As for the canonical ensemble (thermostated systems), substituting $\Phi(\bar{\mathcal{E}}) = \exp(-\bar{\mathcal{E}}/kT)/Z$ yields

$$\mathcal{F} = \bar{\mathcal{E}} - TS = -kT \ln Z. \quad (1.10.6)$$

Here \mathcal{F} is the Helmholtz free energy, and the average energy is exactly the internal energy of the system \mathcal{E} (the line above it is omitted here and below).

Computational Scheme

From Eqs. (1.10.5) and (1.10.6) we are able to calculate either the entropy or the free energy of the system, provided that the corresponding normalization constants $\Delta\Gamma$ or Z are known. With the above formulae we can calculate the macroscopic characteristics of the substance without determining the distributions in μ -space. That is why this procedure is applicable to both ideal and real gases as well as to condensed media. In outline it is as follows.

In the case of a microcanonical ensemble, the main problem is the calculation of the accessible phase volume $\Delta\Gamma(V, \mathcal{E})$ for a multiparticle mechanical system, provided the number and mass of molecules as well as their total energy \mathcal{E} and the vessel's volume V are known. If this problem is solved, formula (1.10.5) immediately gives the entropy as a function of the given variables: $S(V, \mathcal{E})$. Using equilibrium thermodynamics any other macroscopic parameters may be obtained from this relation which carries the full information about the system including the equation of state. In particular, from Eq. (5.2.36)

$$TdS = d\mathcal{E} + pdV \quad (1.10.7)$$

it follows that

$$p = -\left(\frac{\partial\mathcal{E}}{\partial V}\right)_S, \quad T = \left(\frac{\partial\mathcal{E}}{\partial S}\right)_V; \quad (1.10.7a)$$

thus both the pressure and the temperature are determined. As is customary in thermodynamics, the state parameters to be considered constant in differentiation are noted by indices to the right of the brackets.

If the ensemble is described by the canonical distribution, the main difficulties lie in the calculation of the statistical sum Z as a function of the volume V and the temperature T . This problem is usually a little easier than the previous

one. Once it is solved, Eq. (1.10.6) immediately yields the free energy $\mathcal{F}(V, T)$ which satisfies Eq. (5.5.8)

$$d\mathcal{F} = -pdV - SdT, \quad (1.10.8)$$

This then gives information about the rest of the parameters:

$$p = - \left(\frac{\partial \mathcal{F}}{\partial V} \right)_T \quad S = - \left(\frac{\partial \mathcal{F}}{\partial T} \right)_V. \quad (1.10.8a)$$

The results obtained from the microcanonical or canonical distributions are identical, because the equilibrium properties do not depend on whether the system is thermally isolated or not. However, mathematically, estimation of the statistical sum Z is often more convenient than that of $\Delta\Gamma$.

Ideal Gas

The validity of these general recipes may be easily verified using the simplest model of an ideal gas which is well known. For example, let us make use of the canonical distribution. As $\mathcal{E} = \sum_{i=1}^N p_i^2/2m$, all variables in (1.10.2a) separate, and upon integration we have

$$Z = V^N (2\pi mkT)^{3N/2}.$$

In view of (1.10.6), we find

$$\mathcal{F} = -NkT \ln \left[(2\pi mkT)^{3/2} V \right], \quad (1.10.9)$$

and (1.10.8a) gives

$$p = \frac{NkT}{V}, \quad S = kN \ln \left[V (2\pi mkT)^{3/2} \right] + \frac{3}{2} kN. \quad (1.10.10)$$

In particular, we have attained the aim of the derivation of the equation of state. The general method gives the required result: $p = RT/V$. However, neither free energy nor entropy are proportional to N as must be the case as when the system's volume increases with constant density. This is quite a surprise, because both \mathcal{F} and S are additive quantities. One can always run into difficulties in developing a new theory, but they are particularly undesirable at the end of a road which has appeared to be right! Naturally, it is tempting to overcome this impediment by making some minimal changes.

Identity of Microparticles

To get an idea of the required modifications, compare S from Eq. (1.10.10) with the Sackur–Tetrode formula (identical to Eq. (5.8.2) of Chapter 5) which is free of this problem:

$$S = kN \ln \left[\frac{V}{N} (2\pi mkT)^{3/2} \right] + \frac{5}{2} kN, \quad (1.10.11)$$

This differs from Eq. (1.10.10) only by the term $-kN \ln N/e$, that would appear in (1.10.10) if Z were divided by $N!$:

$$Z = \frac{1}{N!} (2\pi mkT)^{3N/2} V^N. \quad (1.10.11a)$$

Using the well-known Stirling formula $\ln N! \approx N \ln N/e$, the substitution of (1.10.11a) into (1.10.6) leads to the additive quantity

$$\mathcal{F} = -NkT \ln \left[(2\pi mkT)^{3/2} \frac{eV}{N} \right], \quad (1.10.12)$$

which in turn yields the correct result (1.10.11). The redefined \mathcal{F} as well as S depend on specific volume $v = V/N$, but not on the volume itself, so the paradox is resolved.

However, the multiplier $N!$ may enter Z solely from the canonical distribution which, therefore, must differ from (1.10.2):

$$dW = \frac{1}{Z} \exp \left(-\frac{\mathcal{E}}{kT} \right) \frac{d\Gamma}{N!}. \quad (1.10.13)$$

Similarly the microcanonical distribution should be modified

$$dW = \frac{d\Gamma}{\Delta\Gamma \cdot N!} \quad E \leq \mathcal{E} \leq E + \Delta E. \quad (1.10.14)$$

This innovation is well justified. The distributions themselves do not suffer any significant change; only the absolute weight of each state is redefined. Therefore if the problems are successfully remedied by this redefinition, the price is not too high. Moreover, innovations that are useful often prove to be necessary as well. Here the multiplier $N!$ in fact is a result of the fundamentally important property of microparticles, discussed in Chapter 5 (Section 5.8): their “identity” or indistinguishability. Due to this property, there is no meaning in discriminating between states of the system which differ only by permutation of the particles. These are all a single state, because identical particles cannot be numbered or marked.

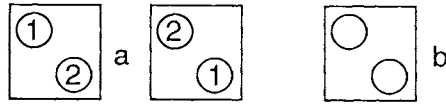


Figure 1.23 (a) Different states of distinguishable particles obtained by permutation and (b) a single state of indistinguishable particles.

This peculiarity manifests itself even in a system of two particles. If the particles were distinguishable (like billiard balls), then each configuration would be counted twice (owing to possible permutation), while if not, then only once (Fig. 1.23). Another example: after an exchange of apartments the tenants can always be identified, at least by fingerprints, if not by marked individuality. However, it is impossible to differentiate among electrons, protons, or identical atoms. We can say: there are two atoms occupying these two positions, but not: the first atom is here, and the second there. In calculating the number of states in Γ -space, this specific property of microparticles has so far been ignored: all states differing by the permutation of N particles (in all, $N!$) were considered in $d\Gamma$ as different. To correct this mistake, we now have to divide the result by $N!$ This is just what was done in (1.10.13) and (1.10.14).

Real Gas

Although in general the procedure is clear, the calculation of particular partition functions presents considerable problems once we pass to the real gas. The energy of any real system is composed of kinetic and potential energies. In the simplest case, the latter is additive with respect to the pair intermolecular interaction $u_{ik} = u(\mathbf{q}_i - \mathbf{q}_k)$:

$$U = \sum_{k>i} u_{ik} . \quad (1.10.15)$$

The partition function of distribution (1.10.13) is

$$Z = \frac{1}{N!} \int \dots \int \exp \left\{ - \sum_{i=1}^N p_i^2 / 2mkT - U/kT \right\} d\mathbf{q}_1 \dots d\mathbf{p}_N = Z_{id} \cdot Q^* . \quad (1.10.16)$$

This differs from its ideal analogue Z_{id} defined in (1.10.11a) in the presence of the extra multiplier, the dimensionless configurational integral

$$Q^* = \int_1 \dots \int_N e^{-U/kT} \frac{d\mathbf{q}_1}{V} \cdot \frac{d\mathbf{q}_2}{V} \dots \frac{d\mathbf{q}_N}{V} , \quad (1.10.17)$$

that is difficult to calculate. This may be considered as the result of averaging the integrand over a uniform distribution of N particles in the volume V .

Denoting the averaging by a bar and taking account of (1.10.15), we represent the configuration integral as

$$Q^* = \int_1 \dots \int_N \prod_{i=1}^{N-1} \Theta_i \frac{d\mathbf{q}_1}{V} \cdot \frac{d\mathbf{q}_2}{V} \dots \frac{d\mathbf{q}_N}{V} = \overline{\prod_{i=1}^{N-1} \Theta_i}, \quad (1.10.18)$$

where $\Theta_i = \exp[-\sum_{k=i+1}^N u(\mathbf{q}_k - \mathbf{q}_i)/kT]$ describes the interaction of the i th particle only with the $N-i$ particles with higher ordinal number. All Θ_i are of the same nature: they define the effect produced on the i th particle by its surroundings. As the arrangement of particles in the space changes, all Θ_i fluctuate over the entire range of possible values. At low gas densities the action of the surroundings on any particle is naturally assumed to be independent, that is, the mean of the product is equal to the product of means:

$$Q^* = \overline{\prod_{i=1}^{N-1} \Theta_i} = \prod_{i=1}^{N-1} \overline{\Theta_i}. \quad (1.10.19)$$

This assumption simplifies further calculations of the configurational integral, however, it restricts the region of applicability to relatively rarefied gases.

Changing variables to $\mathbf{r}_k = \mathbf{q}_k - \mathbf{q}_i$ we have

$$\begin{aligned} \overline{\Theta_i} &= \int_i \dots \int_N \exp\left[-\sum_{k=i+1}^N u(\mathbf{q}_k - \mathbf{q}_i)/kT\right] \frac{d\mathbf{q}_i}{V} \dots \frac{d\mathbf{q}_N}{V} \\ &= \int_{i+1} \dots \int_N \exp\left[-\sum_{k=i+1}^N u(\mathbf{r}_k)/kT\right] \frac{d\mathbf{r}_{i+1}}{V} \dots \frac{d\mathbf{r}_N}{V}. \end{aligned} \quad (1.10.20)$$

This expression may be presented as the product of equal multipliers:

$$\overline{\Theta_i} = \prod_{k=i+1}^N \int e^{-u(\mathbf{r}_k)/kT} \frac{d\mathbf{r}_k}{V} = \left[\int e^{-u(\mathbf{r}_k)/kT} \frac{d\mathbf{r}_k}{V} \right]^{N-i}.$$

For scalar interactions depending solely on the distance between particles, further simplifications are possible:

$$\overline{\Theta_i} = \left[\int_0^R e^{-u(r)/kT} \frac{4\pi r^2 dr}{V} \right]^{N-i} = \left[1 + \int_0^R \left(e^{-u(r)/kT} - 1 \right) \frac{4\pi r^2 dr}{V} \right]^{V(n-i)/V}. \quad (1.10.21)$$

Here R is the radius of the volume filled with gas. For simplicity, it is considered spherical. The last expression is given in a form convenient for passing to the limit $V \rightarrow \infty$ ($R \rightarrow \infty$) at constant gas density. This is quite justified, since the number of particles in the system is macroscopically large. The final

result must depend solely on the density as a universal parameter, and this is just what we have upon passing to the limit

$$\bar{\Theta}_i = \exp \left[\frac{N-i}{V} \int_0^\infty \left[\exp \left(-\frac{u(r)}{kT} \right) - 1 \right] 4\pi r^2 dr \right]. \quad (1.10.22)$$

Substituting this result into (1.10.19) yields

$$Q^* = \exp \left[\frac{N(N-1)}{2} \mu \right], \quad \mu = \int_0^\infty f(r) \frac{4\pi r^2 dr}{V}.$$

As N is large

$$Q^* \approx \exp \left(\frac{N^2}{2} \mu \right) = \exp \left[\frac{N^2}{2V} \int_0^\infty f(r) 4\pi r^2 dr \right], \quad (1.10.23)$$

where

$$f(r) = \exp \left(-\frac{u(r)}{kT} \right) - 1. \quad (1.10.24)$$

As the distance between molecules increases, the function $f(r)$ tends rapidly to zero (Fig. 1.24), thus providing the convergence of the integral in (1.10.23).

Substituting (1.10.23) in (1.10.16) and calculating the free energy by formula (1.10.6), we find

$$\mathcal{F} = \mathcal{F}_{id} - \frac{N_0^2 kT}{2V} \int_0^\infty f(r) 4\pi r^2 dr, \quad (1.10.25)$$

where \mathcal{F}_{id} is the free energy of an ideal gas (1.10.12). Therefore, the pressure

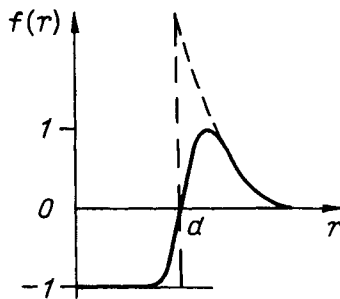


Figure 1.24 A qualitative view of the function $f(r)$ and its approximation in a model of attracting hard spheres (dashed line).

$$p = p_{id} - \frac{N_0^2 kT}{2V^2} \int_0^\infty f(r) 4\pi r^2 dr \quad (1.10.26)$$

proves to be different from $p_{id} = RT/V$. In virial form this equation of state appears as

$$F = 1 - n \frac{\int_0^\infty f(r) 4\pi r^2 dr}{2} = 1 + \frac{B_0}{V}. \quad (1.10.27)$$

Here we can easily recognize the reduced form of Eq. (1.9.19) with the second virial coefficient

$$B_0 = \frac{N_0}{2} \int_0^\infty [1 - e^{-u(r)/kT}] 4\pi r^2 dr, \quad (1.10.28)$$

expressed in terms of the intermolecular interaction potential.

In the van der Waals model of “hard spheres attracting one another,” the repulsive branch of the interaction is replaced by a potential wall at the distance of a molecular diameter: $u(d-0) = \infty$ (dashed line in Fig. 1.24). Taking this model and assuming that the average kinetic energy of particles exceeds the potential well depth, we get from (1.10.28) in the first approximation with respect to u/kT

$$B_0 \approx \frac{N_0}{2} \left[\frac{4}{3} \pi d^3 + \int_d^\infty \frac{u(r)}{kT} 4\pi r^2 dr \right] = B - \frac{A}{RT}. \quad (1.10.28a)$$

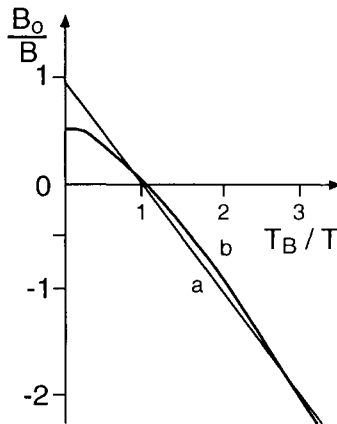


Figure 1.25 The second virial coefficient (a) in the van der Waals theory and (b) in the Lennard-Jones approximation of the interparticle potential.

From a formal standpoint, this result coincides with expression (1.9.18) obtained in the van der Waals theory, moreover, here the parameter $4N_0v_d = B$ is defined identically, and A is expressed in terms of the intermolecular interaction potential:

$$A = 2\pi N_0^2 \int_0^\infty |u(r)| r^2 dr. \quad (1.10.29)$$

Agreement with the van der Waals theory is achieved at the cost of considering the interaction potential in a rough approximation. Obviously, this introduces an error in the theoretical estimation of the second virial coefficient. It can be avoided by using the actual interaction potential in a rather rigorous and general formula (1.10.28). For noble and simple gases, the so-called “6–12 Lennard-Jones” potential

$$u(r) = 4\epsilon \left[\left(\frac{\sigma}{r}\right)^{12} - \left(\frac{\sigma}{r}\right)^6 \right], \quad (1.10.30)$$

is most often used. Here σ and ϵ are molecular constants

$$\sigma = 3 \div 6 \times 10^{-8} \text{ cm}, \quad \epsilon = 1 \div 30 \times 10^{-15} \text{ erg}.$$

The first term in (1.10.30) corresponds to repulsion, and the second to attraction of two particles separated by a distance r . The temperature-dependence of the second virial coefficient determined from (1.10.28) with this potential is given in Fig. 1.25. It is seen that in the high-temperature region it deviates essentially from the linear, van der Waals dependence. The reason is that for particles with high kinetic energy of particles, even a repulsive potential decreasing as abruptly as r^{-12} departs noticeably from a vertical wall.

On the other hand, the original van der Waals equation (1.9.16) describes the state of condensed media much better than Eqs. (1.10.27) and (1.9.19), however rigorous the definition of the second virial coefficient may be. Although using a rough potential model the van der Waals equation does allow for all orders of virial expansion, while here we have only succeeded in the correct determination of the first, linear in density term of the virial expansion (1.10.27). Although more sophisticated statistical methods allow one to express all virial coefficients in terms of $u(r)$ this does not improve the situation very much. It is impossible to sum up the series or reduce it to any expression similar to the van der Waals equation. As the density increases, the description of the substance requires not only linear but also quadratic and cubic corrections to be taken into account. For condensed matter the entire series is necessary, but even this is deficient, because the virial expansion diverges as the critical region is approached. Thus the virial expansion cannot in principle be applied to media of higher than critical densities.

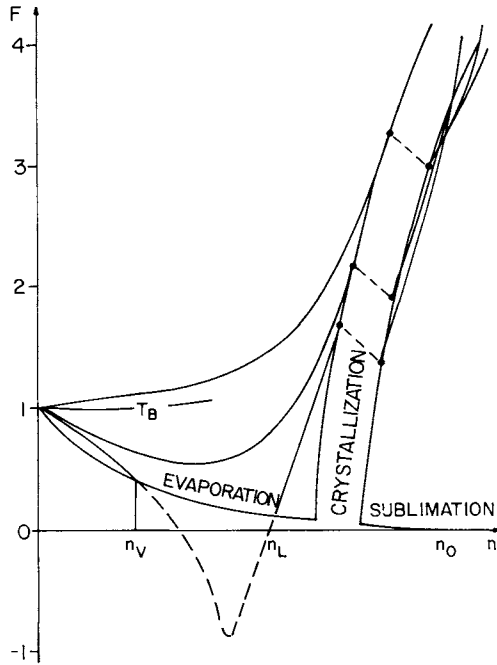


Figure 1.26 The dependence of the compressibility factor $F = pV/RT$ on the corpuscular density n . The dashed sections of the isotherms are their extrapolation to the density region intermediate between the vapor and the liquid or between the liquid and the crystal. n_V and n_L are the densities of the saturated vapor and liquid at boiling point while n_0 is the density of the tensionless state of the crystal.

To clear up this important point, consider the variation of the compressibility factor with density as schematically given in Fig. 1.26. In fact, the virial equation of state is equivalent to the Taylor series expansion about zero density. Its linear variant (1.10.27) is obviously inapplicable even to describe gas isotherms in the range $T_c < T < T_B$ to the right of the indicated minimum. For liquids, the entire series is not sufficient, because the curve has discontinuities associated with condensation, and the behavior of $F(n)$ is open to speculation (dashed line in Fig. 1.26). This is also valid for the solid phase. For this reason, it is useful to have an alternative to virial expansion, that is, an approximation intended for highly condensed media. This is the free volume theory of Lennard-Jones and Devonshire to be outlined below.

Free Volume Theory

The starting point in the calculation of configurational integral (1.10.17) of a condensed system is the model of dense packing of particles (Fig. 1.27a). Surrounded by neighbors on all sides, such particles move in a potential well

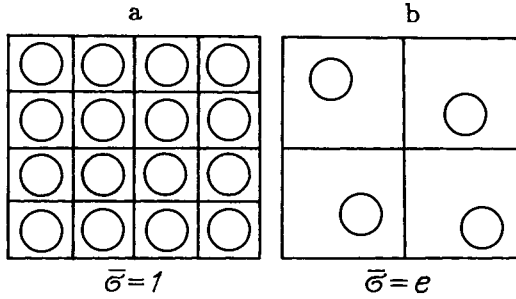


Figure 1.27 (a) A perfect simple lattice and (b) the expanded substance leaving room for a multiple occupation of cages.

with the effective potential $\Phi(\mathbf{q}_i)$. As a rule they do not leave the well, and the center-of-mass of each particle is always within the bounded *free volume*. Thus the molecules can be considered separately, with integration over spatial coordinates being restricted to a small cell, a region of order Δ . If the center of cell is placed at the origin of coordinates, its depth is $\Phi(0)$, and the total potential energy can be represented as

$$U = \frac{N}{2} \Phi(0) + \sum_{i=1}^N \Delta\Phi(\mathbf{q}_i). \quad (1.10.31)$$

Here $\Delta\Phi(\mathbf{q}) = \Phi(\mathbf{q}) - \Phi(0)$ is the cage potential delimiting the free volume, while the first term is the total potential energy of the substance when all particles are in the center of their cells. It is half as large as $N\Phi(0)$, because the interaction of a molecule with any other is counted twice in the sum $\sum_{i=1}^N \Phi_i(0) = N\Phi(0)$. This is taken into account by dividing the sum by 2.

Using the model (1.10.31), we can easily calculate the configuration integral (1.10.17) which is the product of the integrals over different cells summed over all possible permutations of particles:

$$\begin{aligned} V^N Q_N^* &= \exp\left(-\frac{N\Phi(0)}{2kT}\right) \int_V \dots \int_V e^{-\sum_i \Delta\Phi(\mathbf{q}_i)/kT} d\mathbf{q}_1 \dots d\mathbf{q}_N = \\ &= N! v_f^N \exp\left(-\frac{N\Phi(0)}{2kT}\right). \end{aligned} \quad (1.10.32)$$

Here

$$v_f = \int_{\Delta} \exp\left[-\frac{\Delta\Phi(\mathbf{q})}{kT}\right] d\mathbf{q} \quad (1.10.33)$$

is the free volume of the cell formed by summing the space elements accessible to a particle weighted by the probability of finding the particle in them.

Using Stirling's formula, substituting (1.10.32) into (1.10.16) and the result into (1.10.6) yields

$$\mathcal{F} = \mathcal{F}_{id} + NkT - NkT \ln \frac{v_f}{v} + N \frac{\Phi(0)}{2}, \quad (1.10.34)$$

where $v = V/N$ is the specific volume, and \mathcal{F}_{id} is defined in (1.10.12). This result is quite reliable for crystals, where the migration of particles between cells is very unlikely. However, in a liquid the neighborhood of the particle is not impenetrable, and under further rarefaction the notion of a cell becomes a mere conventionality. This limits the application of formula (1.10.34).

Its drawback is revealed in passing to the lowest densities. Although potential barriers are removed ($\Delta\Phi \rightarrow 0$ at $v \rightarrow \infty$) and almost the entire cage volume (see Fig. 1.27b) becomes accessible to the particle ($v_f \rightarrow v$), the sample free energy $\mathcal{F} \rightarrow \mathcal{F}_{id} + NkT$ still differs from the ideal gas value by NkT . The ideal gas pressure calculated by this formula proves to be correct, but the entropy differs from the ideal value: $S = S_{id} - Nk$. Obviously, this failing of (1.10.34) is due to the excessive order of the imposed cell structure, which underestimates the disorder arising in a real system under rarefaction. This drawback may be eliminated by introducing an additional parameter, the so-called "collective entropy" $\bar{\sigma}$ which varies from 1 to e with increasing v , thus correcting the asymptotic behavior of the free energy

$$\mathcal{F} = \mathcal{F}_{id} + NkT \ln \frac{e}{\bar{\sigma}} - NkT \ln \frac{v_f}{v} + N \frac{\Phi(0)}{2}. \quad (1.10.35)$$

Unfortunately, the explicit form of the $\bar{\sigma}(v)$ dependence remains unknown. This leads to some uncertainty in the equation of state

$$p = \frac{1}{N} \left(\frac{\partial \mathcal{F}}{\partial v} \right)_T = p_t - p_i, \quad (1.10.36)$$

where

$$p_i = \frac{1}{2} \frac{d\Phi(0)}{dv} \quad (1.10.37a)$$

is the so-called *internal* pressure, while

$$p_t = nkT \left(\frac{\partial \ln(\bar{\sigma}v_f)}{\partial \ln v} \right)_T = \frac{RT}{V} \left(\frac{\partial \ln(\bar{\sigma}v_f)}{\partial \ln v} \right)_T \quad (1.10.37b)$$

has the meaning of *motional* or thermal pressure. The former is analogous to the van der Waals term A/V^2 in Eq. (1.9.10) and depends on the volume only. However, the latter is created by particle motion, which is thermal in origin at real gas temperatures. From a phenomenological point of view the equation

$$p + p_i = p_t \quad (1.10.38)$$

is valid for all phases of the substance, although the particular form of the components is different.

The free-volume theory was first advanced by Lennard-Jones and Devonshire in 1937. It became immediately evident that despite all simplifications of the model, it was still too complicated for particular calculations. This is partly due to the fact that the potential of a cell resulting from an actual crystallographic arrangement of the neighboring molecules proved to be too cumbersome for analytical calculation of the free volume. Thus the authors of the theory and their adherents preferred to use the angle averaged potential

$$\Delta\Phi(q) = c \left[\frac{1}{4\pi} \int \int u \left(\sqrt{a^2 + q^2 - 2aq \cos \theta} \right) \sin \theta d\theta d\varphi - u(0) \right]. \quad (1.10.39)$$

This implies that particles of the first coordination sphere equally distant from the cell center are uniformly distributed over the sphere of radius a .

Even for hard spheres of diameter σ it is customary to employ a “smeared” or “sphericalized” free volume. The structures of the first shell in simple liquids and their crystals are similar. Each molecule in a cell of a face-centered cubic lattice has 12 nearest neighbors, a distance of a away. The volume per molecule is $v = a^3/\sqrt{2}$ and the cell corresponding to this volume is dodecahedron. If $v^* = v/\sigma^3 \gg 1$ ($a \gg \sigma$) the full volume of a cell is available for a center of molecule (“wanderer”) inside it, but the cell borders are just conditional, because they are transparent. At higher densities each face is partly protected from penetration of a wanderer by a spherical body of corresponding neighbor. The emigration is possible only through the chinks between them at the tops of dodecahedron (Fig. 1.28). At even higher densities ($v < 2\sigma^3$) the wanderer can not escape from the “cage” formed by its nearest neighbors. So the region of applicability of the free volume theory to hard sphere model is actually

$$2\sigma^3 > v > \sigma^3/\sqrt{2},$$

where the lowest limit corresponds to the tightest possible packing. At such densities the shape of a cage becomes rather whimsical and its volume, which is free for wanderer center, is hardly available for calculation. On the contrary, the smeared free volume is the largest sphere which can fit inside the exact cages shown in Fig. 1.28. This approximation is appropriate for untransparent

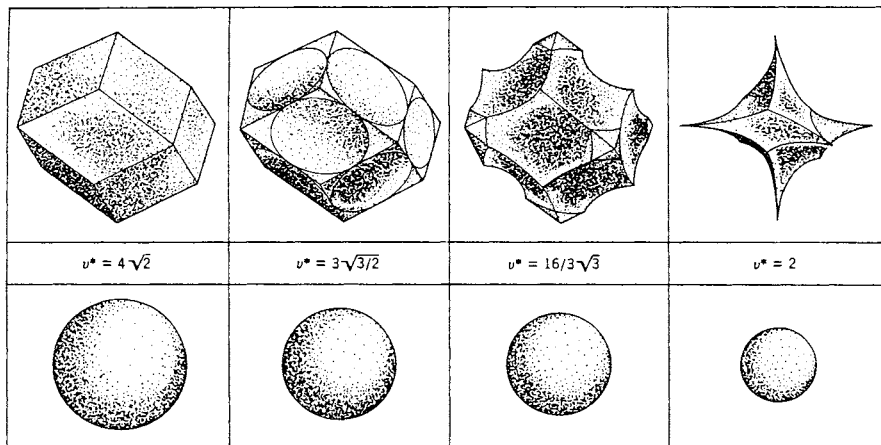


Figure 1.28 The figures in the top row show the shape of the exact free volumes at different densities for face-centered lattice ($v^* = v/\sigma^3$). The corresponding “smeared” free volumes are shown in the bottom row. (From R. J. Buehler, R. H. Wentorf, J. O. Hirschfelder, and C. F. Curtiss, *J. Chem. Phys.*, **19**, 61 (1951).)

cages but becomes questionable at lower densities when the wanderer is no longer confined to the cage formed by the nearest neighbors.

In (1.10.39) only the contribution from the nearest neighbors is taken into account but the contribution of remote particles has to be also averaged in a similar fashion. The best version of the theory took account of the three nearest spheres which turned out to be quite sufficient for the short-range Lennard-Jones potential. The results of the calculations are illustrated in the original diagram presented in Fig. 1.29. Qualitatively they reproduce the behavior of the isotherms given in Fig. 1.26, but the breaks due to evaporation and crystallization of the substance are absent. The reason is that the collective entropy was taken to be equal to unity because the recipe for its calculation had not yet been found. Within the framework of this theory, thermodynamic properties of solids may be described semiquantitatively, while those of liquids only qualitatively. In fact, the theory is applicable only in the neighborhood of the knot point shown in Figs. 1.26 and 1.29. Conversely the virial expansion is valid in the region of quasilinear variation of $F(n)$ near the ideal gas state which is also the knot point of the compressibility factor isotherms.

1.11 HEAT CAPACITY OF GASES

Sometimes it happens in science that the most radical innovations appear under most prosaic circumstances. One of the problems facing statistical physics was the calculation of the molecular heat capacity of ideal gases. No

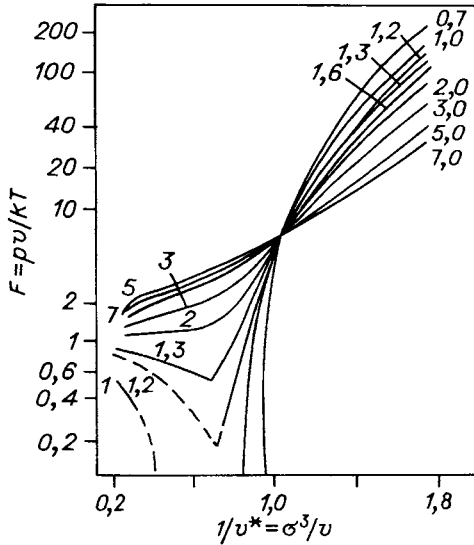


Figure 1.29 The compressibility factor F as a function of the reduced density $1/v^*$. The curves are isotherms labeled by the values of the reduced temperature $T^* = kT/\epsilon$. (From R. H. Wentorf, R. G. Buehler, J. O. Hirschfelder and C. F. Curtiss, *J. Chem. Phys.* **18**, 1484 (1950); see also Fig. 4.7–3 in *Molecular Theory of Gases and Liquids* by J. O. Hirschfelder, C. F. Curtiss, B. R. Bird.)

fundamental difficulties were expected. However, this problem proved to be one of the “hard nuts to crack” which served to verify the newly born physical theory.

According to the formal definition, the molar specific heat at constant volume is given by

$$C_V = \left(\frac{\partial \bar{E}}{\partial T} \right)_V = N_0 \frac{d\bar{E}}{dT}. \tag{1.11.1}$$

For an ideal gas it is expressed via the total heat energy per molecule \bar{E} including all possible types of intramolecular motion. In the simplest case of an atomic gas, the particles are capable of nothing but translational motion, that is, $\bar{E} \equiv \bar{\epsilon} = \frac{3}{2}kT$, and $C_V = \frac{3}{2}R \approx 3 \text{ cal/mole} \cdot \text{deg}$. The validity of this conclusion is verified experimentally: the heat capacity of single-atom molecules is temperature-independent and is equal to three. However, this is the only point of excellent agreement between the theory and experiment. Extension of the calculation to diatomic molecules capable not only of translation, but also of rotation and vibration leads to the conclusions which do not show even qualitative agreement with experiment.

To clarify the essence of the problem, let us note that in the most general case \bar{E} is uniquely expressed in terms of Z :

$$\bar{E} = \frac{1}{Z} \int E \exp\left(-\frac{E}{kT}\right) dpdq = -\frac{\partial(\ln Z)}{\partial\left(\frac{1}{kT}\right)}. \quad (1.11.2)$$

Thus the calculation of heat capacity is reduced to that of the partition function:

$$Z = \int_p \int_q \exp\left(-\frac{E}{kT}\right) dpdq. \quad (1.11.3)$$

For translational, rotational and vibrational motion (in the harmonic approximation) calculations are similar and give identical results. Let us see it for ourselves.

Translational Motion

In the absence of external fields $E = \sum_{i=x,y,z} (p_i^2/2m)$, and

$$Z = V(2\pi mkT)^{3/2}. \quad (1.11.4)$$

There is one translational degree of freedom per axis, each associated with the multiplier $(2\pi mkT)^{1/2}$ in Z . The average energy $kT/2$ accounts for any of them according to Eq. (1.11.2). Since there are three translational degrees of freedom, the total heat energy $\bar{E} = \frac{3}{2}kT$. It is remarkable that it does not depend on the molecular mass but is completely determined by the temperature. As has already been shown, the corresponding specific heat is $\frac{3}{2}R$.

Rotational Motion

In the absence of orienting fields the calculation is similar to the previous one. The Gibbs distribution obtained from (1.8.8) with $E = 0$ takes the form

$$dW(p_\theta, p_\varphi, \theta, \varphi) = \frac{1}{Z} \exp\left[-\frac{p_\theta^2}{2IkT} - \frac{p_\varphi^2}{2IkT \sin^2 \theta}\right] dp_\theta dp_\varphi d\theta d\varphi.$$

The substitution $p_1 = p_\theta$, $p_2 = p_\varphi/\sin \theta$ brings the distribution to a more conventional form:

$$dW(p_1, p_2, \theta, \varphi) = \frac{1}{Z} \exp\left[-\frac{p_1^2}{2IkT} - \frac{p_2^2}{2IkT}\right] dp_1 dp_2 \sin \theta d\theta d\varphi. \quad (1.11.5)$$

In these variables, the energy is a coordinate-independent quadratic function of momenta. Thus

$$Z = \int \exp\left(-\frac{p_1^2}{2IkT}\right) dp_1 \int \exp\left(-\frac{p_2^2}{2IkT}\right) dp_2 \int d\Omega = 8\pi^2 IkT, \quad (1.11.6)$$

which involves two equal multipliers $\sqrt{2\pi IkT}$ which yield $kT/2$ each, if substituted into (1.11.2). Therefore, $\bar{E} = kT/2 + kT/2$ and $C_V = R \approx 2$ cal/mole · deg. As in the previous case, the average energy does not depend on the parameters of the molecule itself such as the moment of inertia.

The presence of only two components $kT/2$ in the expression for average rotational energy is due to the specific geometry of linear molecules. Such molecules have only two rotational degrees of freedom. The molecule's rotation about its own axis is neglected for reasons which will be clarified later. Only nonlinear molecules have three rotational degrees of freedom. As before, each contributes one $kT/2$, whatever the magnitude of the corresponding moment of inertia. In this case, the total energy $\bar{E} = 3(kT/2)$, and $C_V = \frac{3}{2}R$.

Vibrational Motion

It is reasonable to choose the quantity $q = x_2 - x_1 - a$ as one of canonical variables describing the vibrational motion of diatomic molecules (a is the equilibrium distance between atoms located at the points x_1 and x_2). The greater the bond stretching q , the greater the effort required to return the atoms to their equilibrium position. In the harmonic approximation they are proportional and opposite in sign

$$F = -\beta q. \quad (1.11.7)$$

If linear dependence holds within the whole range of q , the oscillator is called harmonic. The corresponding equation of motion

$$m\ddot{q} = F = -\beta q \quad (1.11.8)$$

shows that the vibrational frequency $\omega_0 = \sqrt{\beta/m}$ is the basic characteristic of the oscillator. The total energy of harmonic vibrations

$$E = \frac{p^2}{2m} + \int \beta q dq = \frac{p^2}{2m} + \frac{m\omega_0^2 q^2}{2}, \quad (1.11.9)$$

where $p = m\dot{q}$. Thus

$$Z = \int \exp\left(-\frac{p^2}{2mkT}\right) dp \int \exp\left(-\frac{q^2 m\omega_0^2}{2kT}\right) dq = \frac{2\pi kT}{\omega_0}. \quad (1.11.10)$$

Although in this case the multipliers appearing on integration over different variables (coordinates and momenta) are not equal to each other, the difference is insignificant. On substitution into (1.11.2) and differentiation, all T -independent parameters disappear. Thus we arrive at the same result

$$\bar{E} = \frac{kT}{2} + \frac{kT}{2} \quad \text{and} \quad C_V = R.$$

Equipartition Law

It is seen that identity of all estimates of the mean heat energy and its invariance to the type of motion are due to similar dependence of mechanical energy on the corresponding coordinates. In all examples given above the energy proved to be a quadratic form of coordinates or momenta. Thus the following generalization is justified: if the energy takes the form

$$E = \sum_{\ell=1}^i \gamma_{\ell} \xi_{\ell}^2, \quad (1.11.11)$$

then its average equilibrium value at any γ_{ℓ} is

$$\bar{E} = \sum_{\ell=1}^i \gamma_{\ell} \overline{\xi_{\ell}^2} = \sum_{\ell=1}^i \frac{kT}{2} = i \frac{kT}{2}, \quad (1.11.12)$$

where i is the number of quadratic terms in Eq. (1.11.11).

Sometimes this statement is formulated as a law or *the principle of equipartition of energy* among the various degrees of freedom. It is implied that each quadratic term in (1.11.11) is associated with one or another degree of freedom of mechanical motion. Therefore the corresponding mean energy is equal to $kT/2$, whatever the value of γ_{ℓ} . Thus for translational motion there are always three degrees of freedom, for rotational motion, either two or three, depending on the molecule's shape. As for vibrational motion, note that, according to (1.11.9), the expression for energy involves two (not one) quadratic terms corresponding to vibrational motion: one term is related to the kinetic part of the energy, the other, to the potential part. For each of the terms there is one $kT/2$. Hence, the above formulation of the law will remain valid, provided that not one but two degrees of freedom are assigned to each vibrational mode of a molecule.

Unfortunately, an artificial "doubling" of vibrational degrees is not the only correction to the "equipartition" law that should be taken into account. In the presence of external fields translational and rotational degrees of freedom also have not only kinetic but potential energy as well. However, potential energy terms like mgz or $qE \cos \theta$ are not quadratic in the coordinates, so they do not

fall under the equipartition law at all. Leaving them for later consideration, let us concentrate on a gas free from external fields which is the best object for the verification of the equipartition law.

Temperature Anomalies

If the total number of the gas molecules' degrees of freedom is i , then, according to (1.11.12) and (1.11.1), $C_V = iR/2 = i \text{ cal/mole} \cdot \text{deg}$, that is, the absolute value of specific heat coincides numerically with i .

This consequence of the equipartition law, and, in fact, the Gibbs distribution itself, did not agree with experimental findings concerning polyatomic molecules. In particular, the experience shows that for diatomic molecules at ordinary temperatures $C_V = \frac{5}{2}R$, not $\frac{7}{2}R$, as follows from the equipartition law taking that there are three translational, two rotational and two vibrational degrees of freedom. Even if we assume that the molecule does not oscillate, the agreement is violated as soon as the temperature falls, because the heat capacity falls as well approaching the atomic value $\frac{3}{2}$ (Fig. 1.30). For molecular hydrogen, for example, this limit is reached at temperatures below 80°C . On the other hand, the specific heat of diatomic and polyatomic gases increases with rising temperature, and, eventually, becomes equal to $iR/2$ (unless dissociation takes place) in excellent agreement with the equipartition law, but in contrast with their room temperature values which are $5R/2$ and $3R$, respectively, as if vibrations were absent.

We run into a paradoxical situation: though the deductions of the theory do not completely agree with experiment, they are by no means senseless and

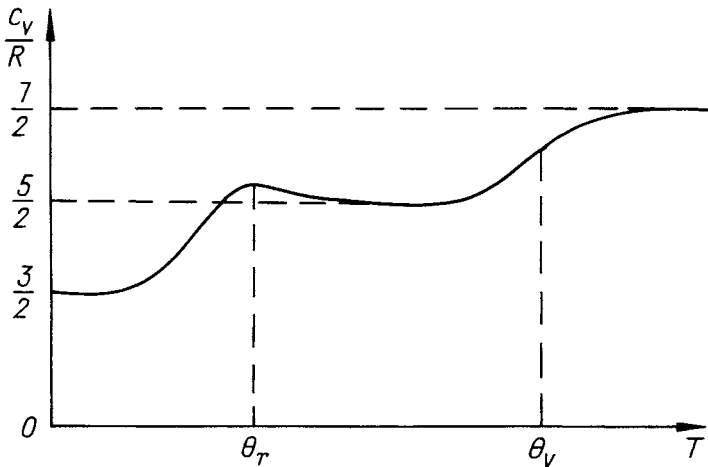


Figure 1.30 A schematic plot of the diatomic specific heat as a function of temperature. Characteristic temperatures for rotation and vibration are Θ_r and Θ_v correspondingly.

adequately represent physical reality in a restricted temperature range. Obviously, the theory should be not abandoned, but modified somehow so that we can predict which degrees of freedom and what temperature range should be taken into account, and which degree must be considered to be not involved in the heat motion. The problem is: can it happen that some type of motion contributing to the heat capacity under certain conditions will prove to be inessential in another circumstances? To see that this situation is quite possible, let us consider the potential part of translational and rotational motion energy in external field and its contribution to heat capacity.

(a) Assume that a vessel with a gas is in a uniform gravitational field. Then integrating over coordinates, we can see that the multiplier V in Eq. (1.11.4) is replaced by the following partition function

$$Z = \iint dx dy \int_0^H \exp\left(-\frac{mgz}{kT}\right) dz = \frac{SkT}{mg} \left[1 - \exp\left(-\frac{mgH}{kT}\right)\right]. \quad (1.11.13)$$

The corresponding part of the heat energy, naturally separated from other (kinetic) components, is

$$\bar{U} = mg\bar{z} = kT - \frac{mgH}{\exp\left(\frac{mgH}{kT}\right) - 1}. \quad (1.11.14)$$

With $mgH \ll kT$, the total center of gravity is approximately in the center of the vessel and $\bar{U} = \frac{1}{2}mgH - \frac{1}{12}[(mgH)^2/kT]$. Naturally, the heat capacity is close to zero, since the distribution of molecules in height, and, therefore, their total potential energy are essentially unaffected by the temperature variation: $C_V = N_0(d\bar{U}/dT) = (R/12)[(mgH)/kT]^2 \ll R$. As the temperature rises, $C_V \propto 1/T^2 \rightarrow 0$, because the distribution becomes more uniform.

On the contrary, at $mgH \gg kT$, $\bar{U} \approx kT$. Similarly to the equipartition law, the corresponding specific heat is constant although $C_V = R$, instead of $R/2$. The heat capacity is height-independent because the gas is at the bottom of the vessel and the position of the lid is of no importance. As the temperature increases, energy is expended in shifting the center of gravity of the gas upwards, R for each degree.

In general, the dependence of C_V on T may be inferred from Fig. 1.31: the boundary between the region of constant C_V and hyperbolic disappearance of the specific heat is governed by the characteristic temperature $T_c = mgH/k$.

(b) Now take the case that molecules with a dipole moment are placed in a uniform electric field. The potential energy related to a rotation by the angle θ may be determined by the procedure described above. However, this is quite unnecessary, as $\bar{U} = -\bar{q}_z E$, and $\bar{q}_z = qL(\alpha)$ has already been calculated in (1.8.13). So we immediately obtain

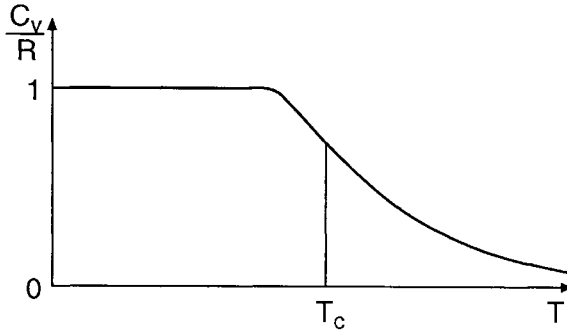


Figure 1.31 The ideal gas heat capacity in a homogeneous gravitational field.

$$C_V = N_0 \frac{d\bar{U}}{dT} = R \left(1 - \frac{\alpha^2}{\text{sh}^2 \alpha} \right),$$

where $\alpha = qE/kT$ as before. An analysis of this expression shows that under saturation conditions ($qE \gg kT$), the heat capacity is equal to R , while at high temperatures ($qE \ll kT$) it tends to zero by a hyperbolic law: $C_V = (R/3)(qE/kT)^2$, just as in the previous example (see Fig. 1.31).

The nature of the extra heat capacity of a dielectric in an external field is rather obvious. The increase in temperature turns some dipoles opposite to the field increasing their potential energy at the expense of the heat taken out of the thermostat. As soon as a uniform distribution of dipoles in all directions is attained, further rise of temperature is no longer of any importance, and the heat supply ceases.

In both examples the heat capacity goes to zero above a characteristic temperature. Of course, this cannot be attributed to the fact that the energy is nonlinear in the coordinate. The decrease in the heat capacity is due to a limited phase space. The first example demonstrates this most clearly: if the vessel were infinitely tall ($H = \infty$), that is, z varied from 0 to ∞ , then the specific heat would remain constant (equal to R) over the whole temperature range. In the second case, we have the same situation: the projection of the moment on the z axis affecting the energy $U = -q_z \cdot E$ is bounded from above ($|q_z| < q$). If one had $q = \infty$, the characteristic temperature $T_c = qE/k$ could also never be reached.

In the case of translational, rotational and vibrational motions, the corresponding canonical variables vary in an infinite range. Besides, a comparison of Figs. 1.30 and 1.31 shows that the anomalous behavior of $C_V(T)$ corresponding to these types of motion is opposite in character. At high temperatures excellent agreement with the equipartition law is observed, and only at fairly low temperatures does the heat capacity decrease, tending to zero. An explanation could be found if the phase space of these variables proved to be

bounded from below rather than from above. This important point will enable us to clear up the cause of the heat capacity paradox.

1.12 HARMONIC OSCILLATOR QUANTIZATION

Freezing out of Vibrations

The problems of the classical theory of heat capacity cannot be eliminated by perfecting the gas model. They are fundamental. The equipartition law is a direct consequence of the Gibbs distribution. Its failure means that either the distribution itself is invalid, or the use of classical mechanics is not justified; and at first glance one will tend to blame the former.

However, the reason proved to be different. It lies in the unjustified extension of Newton's mechanics to elementary particles. The mechanical properties of atoms and molecules could not be predicted *a priori*. This unsuccessful attempt to describe them classically brought about innovations in principle which helped to resolve the paradox of heat capacities and formed the basis for the first quantum postulates. The most revolutionary principle of quantum mechanics had been formulated long before direct experimental study of elementary particles became feasible.

This principle was established by Planck in order to eliminate the so-called "ultraviolet catastrophe"—another consequence of the equipartition law (see Chapter 2, Section 2.3). In outline, it is as follows: a radiation field may be treated as an ensemble of harmonic oscillators which are described in the same fashion as harmonic vibrations of molecules. If the field is in equilibrium with the substance, then, according to the equipartition law, the thermal energy per oscillator is equal to kT . However, as the number of field oscillators is infinitely large (with frequencies between 0 and ∞), their total energy is to be ∞ ! Of course, this is not the case. By analyzing the experimental energy spectrum of equilibrium radiation Planck discovered that the mean thermal energy per oscillator is

$$\bar{E} = \frac{h\nu}{\exp(h\nu/kT) - 1}, \quad (1.12.1)$$

where $h = 6.6 \cdot 10^{-27}$ erg \cdot s is the Planck constant. At low frequencies ($\nu \ll kT/h$) this expression reduces to the classical result $\bar{E} = kT$, while at high frequencies it goes to zero. The absence (freezing out) of high frequency vibrations resolves the ultraviolet paradox, but is completely inconsistent with the equipartition law, according to which the mean energy of vibrations does not depend on their frequency.

The experimentally obtained formula (1.12.1) also eliminates the difficulties in the theory of heat capacities related to the vibrational energy of molecules. It is seen that for each oscillator with vibration frequency ν there is a character-

istic temperature $\Theta = h\nu/k$. At higher temperatures $\bar{E} = kT$, $C_V = R$, and at lower ones $\bar{E} = h\nu \exp(-h\nu/kT)$ and $C_V \rightarrow 0$ with $T \rightarrow 0$ (vibrations are frozen out). However, we still do not know what drawback in the previous calculations must be rectified to derive this formula theoretically.

Energy Quantization

With a contradiction of this kind, it is useful to examine it from different viewpoints. Sometimes this helps to reveal the cause of the difficulty. In the case under discussion, it is profitable to reconsider the problem in energy space. To this end, it is necessary to carry out the change of variables from p and q to $E = p^2/2m + (m\omega^2 q^2/2)$ and $\varphi = \arctg(p/q)$ (energy and phase of vibration) with the subsequent integration over phases (from 0 to 2π). As usual, the first step is to calculate the Jacobian

$$I = \frac{\partial(E, \varphi)}{\partial(p, q)} = \frac{m^2\omega^2 + tg^2\varphi}{m(1 + tg^2\varphi)}.$$

The element of the phase space in the new variables is as follows

$$d\Gamma = dpdq = \frac{dEd\varphi}{I} = \frac{m}{m^2\omega^2 + tg^2\varphi} \frac{dEd\varphi}{\cos^2\varphi}. \tag{1.12.2}$$

The isoenergy states constitute an ellipsoid-shaped strip (Fig. 1.32), the area of which is found by direct integration over φ :

$$d\Gamma = \oint_{\varphi} d\Gamma = dE \oint \frac{md\varphi}{(m^2\omega^2 + tg^2\varphi) \cos^2\varphi} = \frac{2\pi}{\omega} dE = \frac{dE}{\nu}. \tag{1.12.3}$$

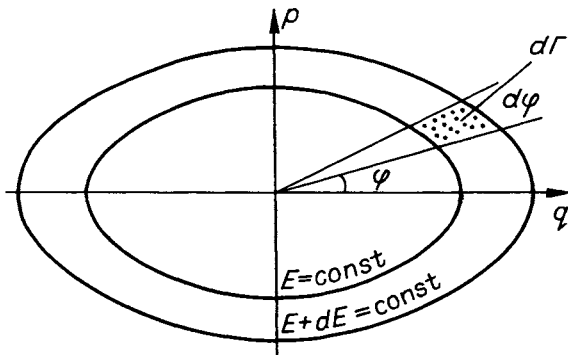


Figure 1.32 An isoenergy strip of the phase space of the harmonic oscillator.

With this in mind, we can write two equivalent definitions for Z

$$Z = \iint e^{-E/kT} dpdq = \int_0^\infty e^{-E/kT} \frac{dE}{\nu}. \quad (1.12.4)$$

Either of them yields the same result: (1.11.10). However, the second expression has an advantage: its structure gives a clue to a possible way to modify the theory.

Let us state the question in the following way: what value of Z , if substituted into (1.11.2), will lead to the correct result (1.12.1)? Accordingly, we equate (1.11.2) to (1.12.1). Then the desired value of Z is defined by a simple differential equation

$$-\frac{d \ln Z}{d\alpha} = \frac{1}{\exp \alpha - 1},$$

where $\alpha = h\nu/kT$. Its solution is

$$Z = \frac{C}{1 - \exp(-\alpha)} = \frac{C}{1 - \exp(-h\nu/kT)}. \quad (1.12.5)$$

Now the problem is laid bare and brought to the point where making the next step requires outstanding shrewdness. The question arises: is there any analogy between the expression (1.12.5) obtained from experimental data and its theoretical analog (1.12.4)? It is not so easy to reveal the analogy, but to use it for a radical modification of the theory is even more difficult. Making such generalizations calls for extraordinary courage. However, this is just what enabled Planck to derive his famous quantum principle.

Planck has noted that expression (1.12.5) may be rewritten using the familiar geometric progression formula

$$\frac{Z}{C} = \sum_{N=0}^{\infty} e^{-\alpha N} = \sum_{N=0}^{\infty} e^{-E_N/kT}. \quad (1.12.6)$$

This result resembles the last version of expression (1.12.4), if we assume (without proof!) that integration should be replaced by summation, taking

$$E_N = N h\nu, \quad N = 0, 1, 2, \dots, \infty. \quad (1.12.7)$$

However, in this case we have to hold that the system's energy cannot take any values, but only those rigorously specified, that the energy changes discretely rather than continuously, and that one allowed value is separated from the next by an energy interval, or *quantum*, of magnitude $h\nu$. Thus the oscillator cannot be found in any state as before, but only in some definite states of motion with energies as specified by Eq. (1.12.7).

So the introduction of formula (1.12.7) is not simply an ordinary working hypothesis, or an improved model of the phenomenon: the quantization of energy reveals the qualitative inadequacy of classical mechanics in its failure to describe the mechanical behavior of atoms and molecules.

High Temperature Limit

The new physical concept does not exclude the previous one, but just reveals its narrowness. This is a brief formulation of the “correspondence principle,” according to which a general physical theory must reduce to a particular one in a region where the latter is applicable. To verify the results of the classical theory, we need to show that at high temperatures the sum over states (1.12.6) reduces to the partition function (1.12.4). The procedure is rather simple. For

$$\frac{h\nu}{kT} \ll 1 \quad (1.12.8)$$

the summation in (1.12.6) may be replaced by integration

$$Z = C \sum_{N=0}^{\infty} e^{-Nh\nu/kT} \rightarrow C \int_0^{\infty} e^{-Nh\nu/kT} dN = C \int_0^{\infty} e^{-E/kT} \frac{dE}{h\nu}. \quad (1.12.9)$$

It can be easily seen that this asymptotic formula is similar or even identical to the estimate of Z given by expression (1.12.4). The only difference, the constant multiplier, is eliminated by an appropriate choice of C .

Quantum Cells

However, this should be done without haste. The simplest choice is to put $C = h$, but the requirements of the correspondence principle can also be met in another way. In fact, previously any distribution was determined to be accurate up to a constant multiplier G

$$dW = \frac{1}{Z} \exp\left(-\frac{E}{kT}\right) G d\Gamma, \quad Z = G \int \exp\left(-\frac{E}{kT}\right) d\Gamma.$$

Nothing depended on this constant, except the setting of a zero for the thermodynamic functions (1.10.5) and (1.10.6). So we have always considered $G = 1$. However, now it is time to make another choice: we put $G = 1/h$ and $C = 1$, thus making (1.12.9) correspond to (1.12.4). With this correction, the classical canonical distribution appears as

$$dW = \frac{1}{Z} \exp\left(-\frac{E}{kT}\right) \frac{d\Gamma}{h}, \quad Z = \frac{1}{h} \int \exp\left(-\frac{E}{kT}\right) d\Gamma. \quad (1.12.10)$$

On the other hand, the quantum distribution takes the conventional form

$$W_N = \frac{1}{Z} \exp\left(-\frac{E_N}{kT}\right), \quad Z = \sum_{N=0}^{\infty} \exp\left(-\frac{E_N}{kT}\right), \quad (1.12.11)$$

where W_N is the dimensionless probability of a state N .

The question of the definition of the constants C and G , that is, whether the Planck constant should appear in the classical distribution or in the quantum one, may seem pointless: at first sight, nothing depends on the answer. However, there are reasons to prefer the solution which leads to (1.12.10) and (1.12.11). If the phase space volume is measured in units of h , as in (1.12.10), then

$$\frac{d\Gamma(E)}{h} = \frac{dE}{h\nu} = dN. \quad (1.12.12)$$

This equality following from (1.12.3) and (1.12.7) establishes a common terminology, that is, a correspondence between the classical “phase volume” and the quantum “number of states.” Now the statement that the probability of finding an oscillator with energy E is proportional to the volume $d\Gamma(E)$ is not quite correct. It is better to say that this probability is measured by the number dN of possible quantum states falling within this interval (it is implied that $dE \gg h\nu$).

In fact, when one has a discrete set of states, the question of how they can be counted does not arise. Nonetheless, if calculations are done in the space of continuously varying variables p and q , the same result may be obtained by dividing it into cells of volume h , with each cell containing one real state. In the case of the harmonic oscillator, the cells are concentric ellipsoidal strips separated by permitted phase trajectories.

Bohr’s Postulate

So far the above reasoning has referred to the harmonic oscillator only. Now let us generalize. Rewriting (1.12.12) in integral form, and bearing in mind that the area bounded by the phase trajectory of the system is to be found, we get

$$\Gamma(E) = \oint pdq = Nh. \quad (1.12.13)$$

This relation carries double information: the classical oscillator property (1.12.3) which can be represented as $\Gamma(E) = \int_0^E d\Gamma = E/\nu$ and the quantization condition (1.12.7) selecting solely allowed values $E = Nh\nu$. Remarkable that the frequency of vibration ν , which is the special parameter of the oscillator, is absent in the final expression (1.12.13) although it appears in both premises. When applied to the oscillator, Eqs. (1.12.7) and (1.12.13) serve equally well for energy quantization. However, from the viewpoint of generalization, Eq.

(1.12.13) is preferable, because this expression does not depend on specific features of the system. The idea of applying it to the quantization of translational and rotational motion, as well as the motion of an electron inside an atom, is very attractive. This idea belonged to Bohr who applied Eq. (1.12.13) to find permitted orbits, and, therefore, energies of electrons in hydrogen-like atoms. The great success of the Bohr theory in the explanation of atomic spectra has verified the general character of this quantization rule. Without going into detail (otherwise, we will find ourselves deep inside the field of atomic physics), we shall simply note that before the emergence of rigorous quantum mechanics, Bohr's quasiclassical quantization rule (1.12.13) was the only reliable basis for interpreting and calculating line spectra of elements—the stumbling block of classical prequantum physics.

1.13 FREEZING OUT OF HEAT MOTIONS

Though in principle any type of motion is subjected to quantization, it is not always necessary. At temperatures $T \gg \Theta = h\nu/k$, even an oscillator may be described classically. Each type of motion has its own characteristic temperature $\Theta = \Delta E_1/k$ where ΔE_1 is the energy difference between the lowest (ground state) and the first excited state of the discrete energy spectrum. The effect of quantization is significant only in the range $0 \leq T \leq \Theta$, but Θ takes different values for different types of motion. For molecular vibrations with a typical frequency $\nu \approx 10^{13}$ Hz, the characteristic temperature

$$\Theta = \frac{h\nu}{k} = \frac{6.6 \cdot 10^{-27} \cdot 10^{13}}{1.4 \cdot 10^{-16}} = 471 \text{ K} \approx 200^\circ\text{C}$$

is so high that at room temperatures vibrations are frozen out (most molecules do not vibrate). On the other hand, the characteristic temperature for translation is so close to absolute zero that the classical approximation is applicable at practically all temperatures.

An example will be illuminating. Placing a particle into a cubic box with the edge \mathcal{L} , we see that the phase trajectory of translational motion between the opposite walls is a rectangle (Fig. 1.33) of the area

$$\oint pdq = 2 \int_{-\mathcal{L}/2}^{\mathcal{L}/2} pdq = 2p\mathcal{L}.$$

According to the quantization rule (1.12.13), the momentum along any axis is strictly specified:

$$p = N \frac{h}{2\mathcal{L}}, \quad N = 0, 1, 2, \dots \quad (1.13.1)$$

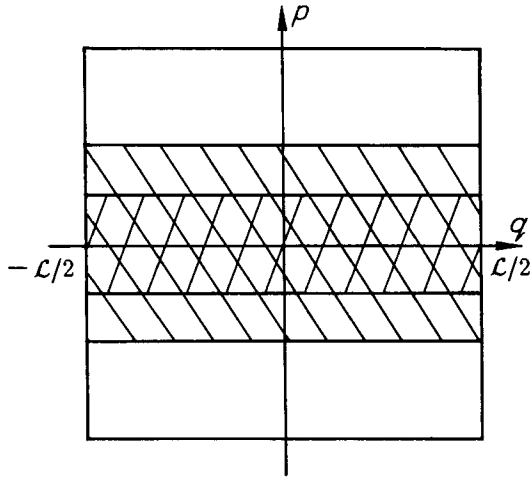


Figure 1.33 Quantum cages of a particle freely moving between the walls of potential well. Hatched regions are onefold and twofold areas of a cage.

Here q is any of x, y, z , and p is any of p_x, p_y, p_z , so

$$p_x = N_x \frac{h}{2\mathcal{L}}, \quad p_y = N_y \frac{h}{2\mathcal{L}}, \quad p_z = N_z \frac{h}{2\mathcal{L}},$$

and

$$p^2 = \frac{h^2}{4\mathcal{L}^2} N^2, \quad N^2 = N_x^2 + N_y^2 + N_z^2 = 0, 1, \dots \quad (1.13.2)$$

Thus $\Delta E_1 = h^2/8m\mathcal{L}^2$. In a vessel of the size 1 cm

$$\Theta = \frac{h^2}{8m\mathcal{L}^2k} = \frac{43 \cdot 10^{-54}}{8 \cdot 4 \cdot 10^{-23} \cdot 1.4 \cdot 10^{-16}} = 10^{-15} \text{ K}. \quad (1.13.2a)$$

This is an extremely low, unattainable temperature. Nearly all gases condense long before they are cooled to such temperatures. Therefore, in the gaseous phase (at $T \gg \Theta$) translation is of classical character. This explains the successful interpretation of gas properties on the basis of the Maxwell and Boltzmann distributions.

However, the determination of Θ by comparing kT with the first quantum from below may seem questionable. Unlike a harmonic oscillator, the quantized spectrum of translational energy $\epsilon = p^2/2m$ is not equidistant. The energy difference between the neighboring levels $\Delta\epsilon_N = \epsilon_N - \epsilon_{N-1} = h^2(2N-1)/8\mathcal{L}^2m$ increases with increasing N . Even if kT is

large as compared with $\Delta\epsilon_1$, we may be quite sure that it is less than some rather large $\Delta\epsilon_N$. However, this is not important. In the classical limit $\bar{\epsilon} = \frac{3}{2}kT = \frac{p^2}{2m}$, so the quantum number of the corresponding energy level is $\bar{N} \approx \sqrt{3kTm}(2\mathcal{L}/h) = \sqrt{3T/2\Theta}$. As the temperature rises, this number increases along with the distance between neighboring levels $\Delta\epsilon_{\bar{N}} \approx h^2\bar{N}/4\mathcal{L}^2m$. However, the ratio $\Delta\epsilon_{\bar{N}}/\epsilon_{\bar{N}} = 2\bar{N}/\bar{N}^2 = 2/\bar{N} \ll 1$ decreases monotonically with temperature. It can exceed unity at $\bar{N} \ll 1$ only, that is, at $T \ll \Theta$. This is just the case where the first quantum may be compared with kT , since all higher levels are already empty.

Hence, vibrational motion at room temperatures is practically frozen out, while translational motion is classical. Rotational motion occupies an intermediate position. Applying the same quantization rule (1.12.13) to angular momentum projections, we get for each

$$\oint p_\varphi d\varphi = 2\pi p_\varphi = Nh; \quad p_\varphi = N\hbar. \quad (1.13.3)$$

Thus angular momentum takes values of integer multiples of $\hbar = h/2\pi$. Similarly, for a molecule rotating about all three axes, we obtain

$$\epsilon = \frac{N_1^2\hbar^2}{2I_1} + \frac{N_2^2\hbar^2}{2I_2} + \frac{N_3^2\hbar^2}{2I_3}. \quad (1.13.4)$$

In general, the moments of inertia I_i are different for different axes. At $I_i = 10^{-40}$ g cm², the characteristic temperature is

$$\Theta_i = \frac{\hbar^2}{2I_i k} \sim \frac{10^{-54}}{2 \cdot 10^{-40} \cdot 1.4 \cdot 10^{-16}} \approx 30 \text{ K}. \quad (1.13.5)$$

Rotational motion of molecular hydrogen is frozen out at a temperature near 80 K, because it has the lowest moment of inertia, and correspondingly the largest Θ . The larger a molecule, the lower the freezing temperature of rotational motion.

If we have a linear molecule, the moment of inertia for rotation around the molecular axis is obviously equal to zero, and the characteristic temperature corresponding to this degree of freedom is infinitely high. That is why the mean energy of such a rotation is equal to zero, and it makes no contribution to the heat capacity. Thus the fact that linear molecules have two instead of three rotational degrees of freedom is exclusively of quantum origin. Consider a planar triatomic molecule of H₂O type. This is an isosceles triangle rotating in all three directions (Fig. 1.34). The minimum moment of inertia is associated with the axis parallel to the base $H - H$ of the triangle, since the vertex angle is obtuse. Now imagine that this angle increases: the inertia moment under discussion will decrease to become zero at the angle 180°, that is, when the

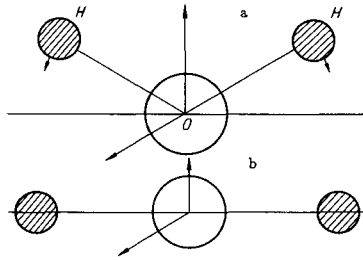


Figure 1.34 The geometrical structure of (a) a water molecule and (b) a linear molecule like CO_2 .

molecule is linear. The corresponding Θ will increase gradually and become infinite in a linear molecule. In this limit the related degree of freedom may be excluded from consideration when calculating the heat capacity.

Summing up, we can say that at extremely low temperatures gas molecules execute only translational heat motion, at room temperatures, translational and rotational motions, and only if heated considerably will there be all three types including vibrational motion. This explains the general pattern of the variation of heat capacity with temperature as shown in Fig. 1.30. However, the mechanisms of the unfreezing of rotational and vibrational motions are quite different. When vibrational degrees of freedom appear, the heat capacity increases monotonically with rising temperature, gradually approaching the classical limit. In the case of rotational motion the specific heat of linear molecules passes through the maximum before the classical limit is reached (see Fig. 1.30). These subtle details of the behavior of $C_V(T)$ behavior near characteristic temperatures cannot be understood in the context of Bohr's quasiclassical theory. Although effective in estimating the magnitude of quanta, it does not allow one to correctly determine the positions of levels in the energy spectrum.

To deal with this difficulty, let us take proper account of the results of a consistent quantum theory. According to (1.13.4), the rotational energy of a diatomic molecule is $\epsilon = (\hbar^2/2I) N^2$ where $N = (N_x^2 + N_y^2)^{1/2}$. However, actually

$$\epsilon = \frac{\hbar^2}{2I} N(N+1). \quad (1.13.6)$$

Each energy level, except the lowest one, is degenerate, that is, consists of $2N+1$ sublevels differing only in the spatial orientation of the angular momentum (Fig. 1.35a). As for the harmonic oscillator, its spectrum, if rigorously calculated, proves to be similar to the quasiclassical spectrum (1.12.7), but differs from it in that all levels are shifted upward along the energy axis by a half quantum:

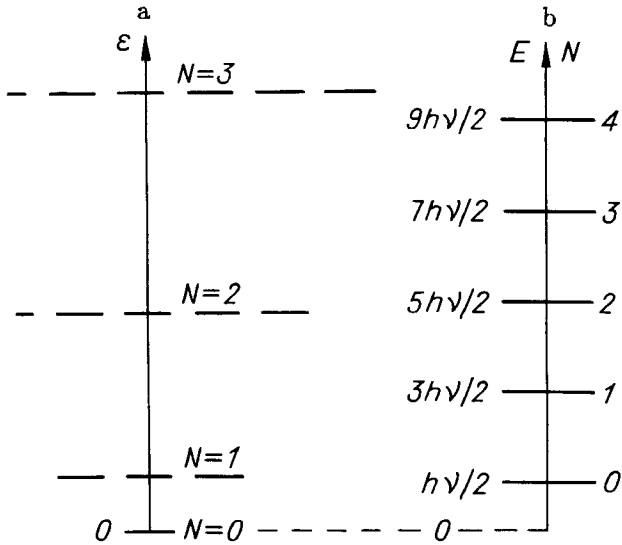


Figure 1.35 The energy spectra of (a) a linear rotator and (b) an oscillator.

$$E = (N + \frac{1}{2}) h\nu . \quad (1.13.7)$$

This difference implies that even at $T = 0$, when thermal motion is completely frozen out, the energy of vibrations is not zero. In the lowest state, the oscillator is not at rest, but executes purely quantum motion (*zero vibrations*) with energy equal to $h\nu/2$ (Fig. 1.35b).

Taking this into consideration let us calculate the real state sums of the quantum rotator and oscillator to disclose the origin of the abovementioned difference in the temperature dependence of their heat capacities. For rotator with spectrum (1.13.6), the state sum

$$Z = \sum_{N=0}^{\infty} (2N + 1) e^{-(\Theta/T)N(N+1)} \quad (1.13.8)$$

may be transformed using the Euler-Macloren formula

$$\sum_{N=0}^{\infty} f(N) = \int_0^{\infty} f(x) dx + \frac{f(0)}{2} - \frac{1}{12} f'(0) + \frac{1}{720} f'''(0)$$

into the following series in Θ/T :

$$Z = \frac{T}{\Theta} \left[1 + \frac{1}{3} \frac{\Theta}{T} + \frac{1}{15} \left(\frac{\Theta}{T} \right)^2 + \dots \right]. \quad (1.13.9)$$

Thus the mean rotational energy of the molecule in the high temperature limit may be estimated as follows:

$$\frac{\bar{\epsilon}}{k\Theta} = - \frac{\partial \ln Z}{\partial (\Theta/T)} = \frac{T}{\Theta} - \frac{1}{3} - \frac{1}{45} \frac{\Theta}{T}, \quad \Theta \ll T \quad (1.13.10)$$

It differs from its classical limit $\bar{\epsilon} = kT$. As the temperature rises, this deviation decreases to a constant value equal to $k\Theta/3$, but does not disappear completely (Fig. 1.36a). Besides, there is a point of inflection on the curve $\bar{\epsilon}(T)$ at which the specific heat $C_V = N_0 d\bar{\epsilon}/dT$ is at its maximum shown in Fig. 1.30. This follows from the fact that the specific heat calculated from Eq. (1.13.10) approaches its limit from above

$$C_V = R \left[1 + \frac{1}{45} \left(\frac{\Theta}{T} \right)^2 \right], \quad \Theta \ll T.$$

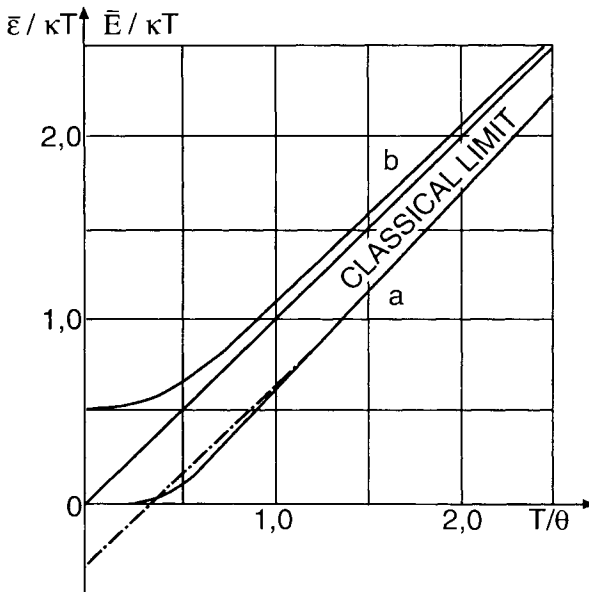


Figure 1.36 Average thermal energies of (a) the linear rotator and (b) the oscillator as a function of temperature.

A different situation arises with the harmonic oscillator. Its mean energy differs from the quasiclassical value found earlier only by a constant $h\nu/2$:

$$\bar{E} = \left(\bar{N} + \frac{1}{2}\right) h\nu = k\Theta \left[\frac{1}{\exp\left(\frac{\Theta}{T}\right) - 1} + \frac{1}{2} \right]. \quad (1.13.11)$$

In the high temperature limit the energy approaches its asymptotic value from above (see Fig. 1.36b):

$$\bar{E} \approx kT \left[1 + \frac{1}{12} \left(\frac{\Theta}{T}\right)^2 \right], \quad \Theta \ll T. \quad (1.13.12)$$

Thus, the heat capacity increases monotonically as shown in Fig. 1.30.

In a real theory of heat capacities it is necessary to allow for the fact that actually molecular vibrations are never purely harmonic: the vibrational levels are equidistant only deep in the potential well where it has a near-parabolic shape. In reality, as the energy increases, the difference between levels decreases. However, more importantly, at high energies the molecules become unstable and dissociate. This leads to an increase in the total number of particles and a qualitative change in their degrees of freedom.

At significantly high temperatures one must also take account of the excitation of electrons in molecules and atoms to higher energy levels. These excitations are associated with quanta of the order of electronvolts, so the electrons motion remains frozen out up to $10^3 \div 10^4$ K. However, with enough heating, the electrons become involved in thermal motion; first they are excited to higher levels, and then leave the particles ("heat ionization").

Finally, at temperatures of millions, in fact dozens of millions of degrees, when all molecules have already dissociated and all atoms have been ionized, it is time for atomic nuclei excitation and fission will occur. This is just what takes place deep inside the Sun and other stars (thermonuclear reactions).

1.14 GAS PARAMAGNETISM

The angular momentum of a molecule or an atom is due to the rotation of their constituents, ions and/or electrons. As they are charged particles, simultaneously, there arises a magnetic moment. Due to their common origin, the two moments are directly proportional with coefficient γ called the gyromagnetic ratio. The potential energy of a magnetic moment in a constant magnetic field H ,

$$U = -\vec{\mu} \cdot \vec{H} = -\mu_z H, \quad (1.14.1)$$

depends on the angle between the moment and the field, just as the energy of a dipole in an electric field. One might then infer that the picture of magnetic polarization must be similar to the electric one described in detail in Section 1.8.

Actually, this is not true. According to the quantum interpretation of charge rotation, the magnetic moment is quantized in the same way as the corresponding angular momentum (1.13.3)

$$\mu_z = \gamma p_\varphi = \gamma \hbar N, \quad (1.14.2)$$

where N is the quantum number, and $\gamma \hbar \approx 10^{-20}$ erg/G. The quantization of magnetic moment brings about the quantization of the potential energy

$$U_N = -\mu_z H = -\gamma \hbar H N. \quad (1.14.3)$$

As the z -projection of magnetic dipole cannot exceed its magnitude ($|\mu_z| \leq \mu = \gamma H J$), N varies within the finite limits

$$N = -J, -J+1, \dots, J-1, J. \quad (1.14.4)$$

All in all, there are $2J+1$ values of the moment projection (Fig. 1.37). Thus paramagnetic polarization is a purely quantum phenomenon disappearing in

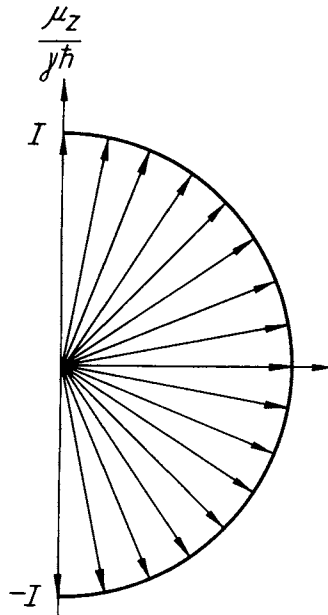


Figure 1.37 The quantized states of a magnetic moment in an external field.

the classical limit attained at $\hbar \rightarrow 0$. The quantum number J defining the absolute value of the moment can be either integer or semiinteger. If the magnetic moment is created solely by the orbital movement of electrons in atoms, J is an integer. At the same time, the electrons themselves have a moment—"spin"—different from zero and equal to $\frac{1}{2}$. As a result, the total moment of the atom, composed of the orbital and the spin moments, is integer if the number of electrons is even, and semiinteger if it is odd.

This brief excursus into quantum mechanics is quite sufficient for the statistical calculation of paramagnetic polarization. From (1.14.3) we see that for fields of attainable strength $\sim 10^4 \cdot \text{G}$,

$$\Delta U = U_N - U_{N-1} = \gamma \hbar H \sim 10^{-16} \text{ erg}; \quad (1.14.5)$$

that is at room temperatures, ΔU is considerably less than kT . Although magnetic quanta take an intermediate position between rotational and translational quanta, they are not as small as the latter and may not be ignored. Like dielectric polarization, paramagnetic polarization saturates at rather low temperatures: $\Theta = \Delta E/k \sim 1\text{K}$.

Spin $\frac{1}{2}$

To be specific, first consider pure spin magnetism with $J = \frac{1}{2}$. In this case, the calculation of magnetization is even more simple than in the classical situation. According to (1.14.14), now we have $N = \pm \frac{1}{2}$, that is, only two states instead of a continuous set. The spins are aligned either with the field or against it. Correspondingly, they have the energy of either the lower or the upper level (Fig. 1.38):

$$U_1 = -\gamma \frac{\hbar}{2} H \quad \text{or} \quad U_2 = \gamma \frac{\hbar}{2} H. \quad (1.14.6)$$

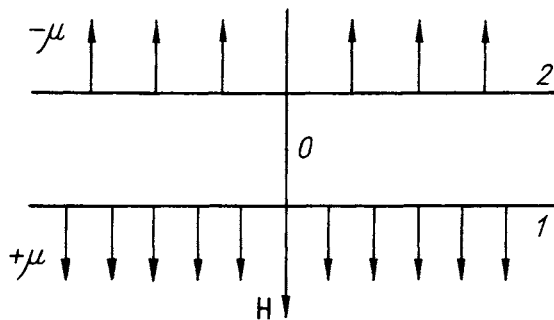


Figure 1.38 Distribution in a two-level system of projections of spin $1/2$ in a magnetic field H .

As there are only two states the whole distribution (1.12.11) reduces to two probabilities

$$W_1 = \frac{\exp(\alpha/2)}{\exp(\alpha/2) + \exp(-\alpha/2)}, \quad W_2 = \frac{\exp(-\alpha/2)}{\exp(\alpha/2) + \exp(-\alpha/2)}, \quad (1.14.7)$$

where $\alpha = \gamma\hbar H/kT$. These are also the probabilities of the corresponding orientation of magnetic moment. Under equilibrium conditions, the spins are distributed over projections in accordance with these probabilities

$$N_1 = nW_1, \quad N_2 = nW_2, \quad (1.14.8)$$

where n is the total number of paramagnetic particles in unit volume. Naturally, their average magnetic moment

$$\overline{M} = \mu N_1 - \mu N_2 = \mu n(W_1 - W_2), \quad (1.14.9)$$

where $\mu = \gamma\hbar/2$. It is determined merely by the excess of spins parallel to the field over those aligned against it. According to (1.14.9) and (1.14.7), the mean magnetic moment of a unit volume is

$$\overline{M} = \mu n \frac{1 - e^{-\alpha}}{1 + e^{-\alpha}}. \quad (1.14.10)$$

In the high temperature limit, with $\alpha = 2\mu H/kT \ll 1$, we can obtain the Curie law simply by expanding the exponents in Eq. (1.14.10)

$$\overline{M} = \frac{\mu^2 n}{kT} H = \frac{\gamma^2 \hbar^2 n}{4kT} H = \chi H. \quad (1.14.11a)$$

When the magnetization is proportional to the applied field, the paramagnetic susceptibility decreases in inverse proportion to temperature. The close similarity between magnetic and dielectric polarization in the linear region is emphasized by the formal resemblance of (1.14.11a) to (1.8.15a). In the low temperature range where $\alpha \gg 1$ the situation is quite different. In this case, as in (1.8.15b), the saturation effect is observed:

$$\overline{M} = \mu \cdot n. \quad (1.14.11b)$$

Under intense cooling, almost all spins are orientated parallel to the field, and at absolute zero those aligned against it disappear as completely as dissidents in a totalitarian system. However, the ordering in paramagnetics and dielectrics proceeds variously.

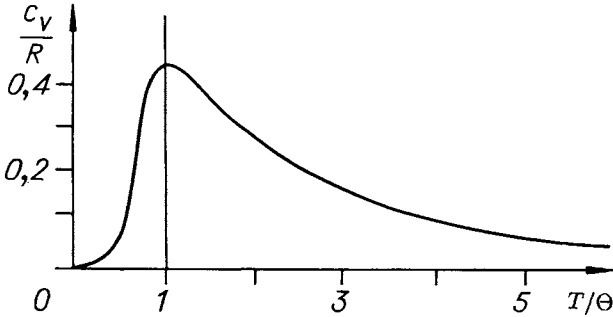


Figure 1.39 Temperature-dependence of two-level system heat capacity.

This difference is particularly pronounced in the temperature dependence of the heat capacity related to the polarization effect. Obviously, the polarization energy of a unit volume is $n\bar{U} = -\bar{M}H$, while the molar specific heat is

$$C_V = -N_0 \frac{d\bar{U}}{dT} = -\frac{d\bar{M}}{dT} N_0 H / n. \quad (1.14.12)$$

As is seen from this formula and Eq. (1.14.10), the heat capacity associated with magnetic polarization is nowhere constant (Fig. 1.39). In the high temperature (classical) limit it is not equal to “ R ” for the same reason as the specific heat of polarized dielectric is not: the phase space is bounded above. Comparison of Fig. 1.31 and Fig. 1.39 shows that in this region the heat capacities vary according to the hyperbolic law $C_V = R(\mu H/kT)^2$. However, in the opposite case, where saturation takes place, the dielectric specific heat was found to be constant in qualitative agreement with the classical equipartition law. On the contrary, the specific heat of paramagnetics departs from classical result $C_V = R$ and goes to zero.

This is due to the fact that the spin phase space is bounded both from above *and* from below. All intermediate energies between U_2 and U_1 are forbidden by quantization; thus $C_V \rightarrow 0$ as soon as kT becomes less than $\Delta U = U_2 - U_1$. So, if there is a continuous set of orientations (as in the dielectric), the system’s ordering by cooling requires that R calories be removed for each degree bringing the gas closer to absolute zero. In the case of two orientations, the closer to zero, the less energy is needed.

General Case

The difference between magnetic and dielectric polarization is particularly pronounced in the case of the spin equal to $\frac{1}{2}$ because only two possible orientations are compared with the continuous set. In fact, the electric dipole orientations are also quantized, but this fact was neglected because of the great

number and small value of the corresponding energy quanta. The difference between discretely and continuously oriented dipoles must disappear with increasing absolute value of the moment J and the number of its orientations, provided that the energy interval which is being divided into the increasing number of quanta remains constant.

According to (1.14.2), (1.14.3), (1.14.4), and (1.12.11), the magnetic polarization of unit volume containing molecules with moment J is the following mean value:

$$\bar{M} = n \sum_{N=-J}^J \gamma \hbar N W_N = n \gamma \hbar \frac{d \ln Z}{d \alpha}. \quad (1.14.13)$$

Direct calculation of the state sum, which is a finite geometric progression, yields

$$Z = \sum_{N=-J}^J e^{\alpha N} = \frac{e^{\alpha J} - e^{-\alpha(J+1)}}{1 - e^{-\alpha}}. \quad (1.14.14)$$

On substituting (1.14.14) into (1.14.13) and differentiating, we derive

$$\bar{M} = \gamma \hbar n \left[\frac{J e^{\alpha J} + (J+1) e^{-\alpha(J+1)}}{e^{\alpha J} - e^{-\alpha(J+1)}} - \frac{e^{-\alpha}}{1 - e^{-\alpha}} \right]. \quad (1.14.15)$$

This result is the most general estimate of magnetization suitable both for $J = 1/2$ when it reduces to (1.14.10) and for any other J , either integer or semiinteger. In this formula the purely quantum nature of paramagnetism manifests itself in the fact that at $\hbar \rightarrow 0$ \bar{M} becomes zero as well. However, it is also possible to pass to another limit:

$$J \rightarrow \infty, \quad \hbar \rightarrow 0 \quad \text{at} \quad \mu = \gamma \hbar J = \text{const}, \quad (1.14.16)$$

This results in an infinite increase in the number of quanta within the fixed energy range $(-\mu H, \mu H)$. In this case, Eq. (1.14.15) gives

$$\bar{M} = \mu n \left[\frac{e^{\mu H/kT} - e^{-\mu H/kT}}{e^{\mu H/kT} - e^{-\mu H/kT}} - \frac{kT}{\mu H} \right] = \mu n L \left(\frac{\mu H}{kT} \right). \quad (1.14.17)$$

This formula differs only in notations from Eqs. (1.8.13) and (1.8.14). Passing to the limit (1.14.16) makes the energy space so finely divided that it is practically continuous, so that the result of the classical theory of orientational polarization is again valid.

1.15 COLLISIONS

Though the equilibrium state of matter was studied and described without any connection with its origin, the reasoning thus far has assumed the ability of isolated macrosystems to return into equilibrium from any nonequilibrium state. Formally one can apply the microcanonical distribution either to a single particle in a box or to an ensemble of point masses isolated in it. However, neither of these systems is appropriate for thermodynamic treatment. Once in a state different from equilibrium, such a system will remain that state, because point particles do not collide with one another and their speeds are conserved in elastic collisions with the walls. Thus, an originally non-Maxwellian distribution will remain so in all future times.

However, in real systems the Maxwell distribution of velocities and the Boltzmann distribution of positions are always restored. Transformation of the initial distribution into an equilibrium one is called a *relaxation process*, and it may proceed in velocity and coordinate spaces with different *relaxation times*. Why and how does relaxation occur? The answer to this question is to be found in the context of physical kinetics.

Relaxation

The answer first came through Krylov's stirring hypothesis. In outline, this is as follows. It is supposed that an isolated macrosystem is able, in a fairly short time, to get from almost any state accessible to it to any other element of the phase volume. In physical kinetics this hypothesis is as fundamentally important as the microcanonical distribution in the equilibrium theory.

Let us consider as an example the rapid expansion of gas into a larger volume. The point representing the system in Γ -space starts from the region initially accessible to the system and, following an intricate trajectory, crosses the expanded phase space in all directions. At first it cuts it roughly into a few pieces, which are in their turn divided later into smaller fractions and so on. Owing to this, in a rather short time approximately equal shares of the trajectory are found in equal volumes of the phase space. Further, the system point continues to move in such a way as to effectively continue this partitioning process. So, the longer the time elapsed from the start, the more truly one can say that all equal elements of phase space contain the same fraction of the phase trajectory. The more uniform is the "stirring" of the trajectory in the accessible phase space, the less the deviation from equilibrium. If most trajectories emerging from the small fraction of the phase space specified by the initial conditions are well stirred, then systems starting from adjacent or nearby points may be found in quite different places. As the starting point is not known with certainty, after a lapse of the relaxation time, the expanded system can be found in any element of the new phase space with the same (microcanonical) probability.

Not all the systems are capable of “stirring.” Roughly speaking, the system has this property if it consists of a great number of particles bound to each other by a definite interaction. Obviously, neither a free particle in a box, nor an ensemble of point masses meet these requirements. When considering an ideal gas, the interparticle interaction ensuring stirring has not even been mentioned. However, this should be taken into account as soon as the question about the attainment of equilibrium arises. The efficiency of this interaction affects the relaxation time. In gases the interaction results in scattering of molecules during collisions. They makes the trajectory of each molecule extremely intricate, to say nothing of the gas on the whole. That is why the required property of stirring is inherent in real gases.

Not all interaction and not every system may result in sufficiently effective stirring. For gases, the existence of this property determined exactly by such a collisional mechanism was theoretically proved by Krylov and subsequently verified by computer simulations. By computer one can follow the trajectory of a many-particle system, on condition that it obeys Newton’s laws, and collisions are elastic. It turns out that two or three collisions of a particle are enough for the original distribution in velocities to go over the Maxwell one, and for the entropy to attain its equilibrium, that is, maximum, value.

However, there are systems which are not capable of stirring at all. In this case, equilibrium is attained exclusively by external action. The interaction with the environment, which is in equilibrium itself, gradually brings the system under discussion into equilibrium state with the same temperature. This is how, for example, the equilibrium distribution over vibrational and rotational states is attained in the gas phase. Translational degrees of freedom act as the environment. The relaxation of intramolecular motion proceeds at the expense of the kinetic energy of colliding particles. Also the equilibrium properties of extremely rarefied gases are established due to inelastic collisions with the vessel’s walls, provided that the walls are thermostated.

Velocity-Dependent Collision Rate

Is the rate of collisions in the gas phase high enough to ensure fairly rapid attainment of equilibrium? The answer is given by an elementary estimate of the number of collisions suffered by a rigid molecule of radius r_1 , moving through a gas of hard spheres of radius r_2 . The idea can easily be understood if we imagine that all particles are immobile except the molecule under consideration. It follows its own path, colliding from time to time with other particles. In a second the molecule covers a distance equal to its speed, and experiences as many collisions as there are hard spheres on the way.

The last statement needs clarification. In the case of a real, smooth interaction between particles, it is not so easy to determine which molecules collided, and which did not. The advantage of the hard sphere model is that here the problem is solved geometrically. Molecules collide, if they touch, otherwise, collision does not take place. Enclosing the center of the moving molecule in a

sphere of the radius $r_1 + r_2 = R$, we can consider other molecules as the point masses. Collision will occur only with those of them whose distance from the trajectory of the moving molecule's center is not larger than R . In other words, in one second of motion, only particles whose centers are confined within a cylinder of cross-section $\sigma = \pi R^2$ and length ν will collide with the moving molecule. The volume of the cylinder is $\sigma\nu$, the density of particles in the unit volume is n , therefore, the number of collisions per unit time

$$\nu = n\sigma\nu. \quad (1.15.1)$$

The above estimate would be satisfactory if the velocity of the moving particle were considerably greater than the velocities of particles which are targets. For example, such is the case for the electrons moving in a gas whose thermal velocity is greater than that of the molecules because of the difference in masses. When molecules of comparable masses collide, to say nothing of identical particles, the calculation must be adjusted.

It turns out that even in this case the calculation can be reduced to the previous one. We need only apply the procedure which is extensively used in kinetics: to divide the ensemble of colliding particles into subensembles. Moving to a coordinate system associated with the chosen molecule which moves with velocity \mathbf{v} , we can classify other molecules by their relative velocity \mathbf{w} . This classification is determined by the Maxwell distribution of the velocities \mathbf{v}' of the target molecules which may be represented as a distribution of the relative velocities $\mathbf{w} = \mathbf{v}' - \mathbf{v}$:

$$dW(\mathbf{v}') = \frac{1}{Z} e^{-m\mathbf{v}'^2/2kT} d\mathbf{v}' = \frac{1}{Z} e^{-m(\mathbf{v}+\mathbf{w})^2/2kT} d\mathbf{w} = dW_{\mathbf{v}}(\mathbf{w}). \quad (1.15.2)$$

Here m is the mass of target particles, different from M , which denotes the mass of the chosen particle.

Now if we select the subensemble of particles where all molecules have the given relative velocity \mathbf{w} (Fig. 1.40), all arguments leading to (1.15.1) may be repeated once again. Thus the rate of collisions with the given subensemble is

$$d\nu_{\mathbf{w}} = \sigma w n dW_{\mathbf{v}}(\mathbf{w}). \quad (1.15.3)$$

The total number of collisions that the molecule with the velocity ν experiences with all subensembles is as follows

$$\nu_{\mathbf{w}} = \int_{\mathbf{w}} d\nu_{\mathbf{w}}(\mathbf{w}) = \frac{n\sigma}{\alpha} \left[\frac{1}{2\nu} \Phi(\sqrt{\alpha\nu}) + \alpha\nu\Phi(\sqrt{\alpha\nu}) + \sqrt{\frac{\alpha}{\pi}} e^{-\alpha\nu^2} \right], \quad (1.15.4)$$

where the probability integral $\Phi(x) = (2/\sqrt{\pi}) \int_0^x e^{-z^2} dz$, and $\alpha = m/2kT$. With $\sqrt{\alpha\nu} \gg 1$, when the speed of the chosen particle is essentially greater than the mean speed of molecule-targets, $\Phi(\sqrt{\alpha\nu}) \approx 1$ and the rate of collisions

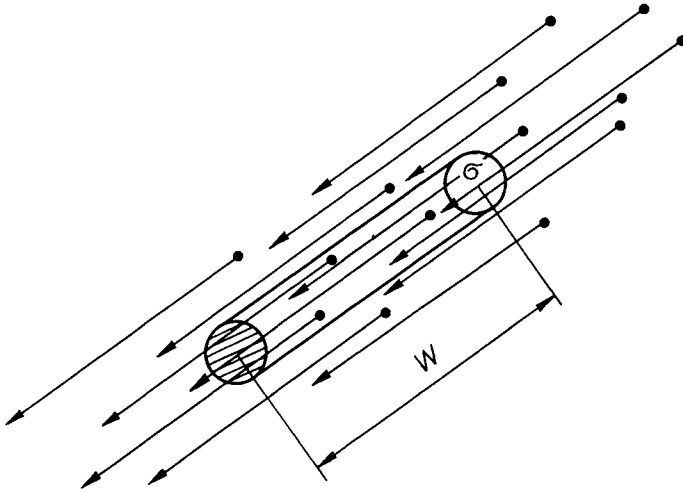


Figure 1.40 The target molecule (hatched) in a flux of particles moving with velocity w . Those of them contained in the cylinder with base σ and height w will collide within a second.

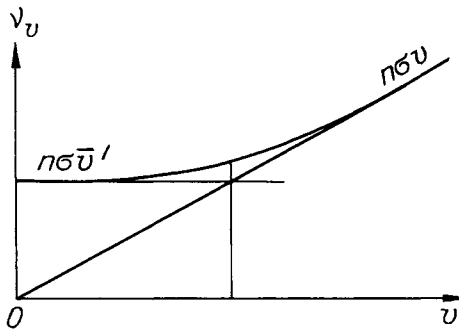


Figure 1.41 The increase of collision rate with velocity of a molecule moving through a gas.

$\nu_v \rightarrow n\sigma v$, just as in (1.15.1). However, unlike the case of immobile targets, at $v \rightarrow 0$ the number of collisions does not go to zero, but proves to be equal to $2\sigma n / \sqrt{\pi\alpha} = n\sigma \bar{v}'$. It is greater, the more intense the heat motion of surrounding molecules impacting the immobile particle (Fig. 1.41).

The Mean Collision Rate

Now let us make allowance for the fact that after each collision the velocity of the molecule changes. The fraction of time the molecule spends in the state with the given velocity v is determined by the Maxwell distribution $dW(\mathbf{v})$. The

average number of collisions it experiences moving from time to time with different velocities is

$$\nu = \int \nu_{\mathbf{v}} dW(\mathbf{v}) = \sigma n \int_{\mathbf{v}} \int_{\mathbf{v}'} w dW(\mathbf{v}') dW(\mathbf{v}). \quad (1.15.5)$$

Converting to the variables \mathbf{w} and $\mathbf{v}_0 = (M\mathbf{v} + m\mathbf{v}')/(M + m)$, we obtain

$$dW(\mathbf{v}) \cdot dW(\mathbf{v}') = dW(\mathbf{w}) \cdot dW(\mathbf{v}_0),$$

where $dW(\mathbf{w}) = (\mu/(2\pi kT))^{3/2} e^{-\mu w^2/2kT} d\mathbf{w}$ is the unconditional distribution of relative velocities, and $dW(\mathbf{v}_0)$ that of the velocity of the center of gravity of the colliding molecules ($\mu = mM/(m + M)$ is the reduced mass).

Upon integration over \mathbf{v}_0 in (1.15.5), we find

$$\nu = \sigma n \int w dW(\mathbf{w}) = \sigma n \bar{w} \quad (1.15.6)$$

or

$$\nu = n\sigma \sqrt{\frac{8kT}{\pi\mu}} = \sqrt{\frac{m+M}{M}} n\sigma \bar{v}' = \sqrt{\frac{m+M}{m}} n\sigma \bar{v}, \quad (1.15.7)$$

where $\bar{v} = \sqrt{8kT/\pi M}$, $\bar{v}' = \sqrt{8kT/\pi m}$.

Thus the total number of collisions is obtained from (1.15.1) by substituting w for ν , and the dependence $\nu(\bar{v})$ is qualitatively similar to the dependence $\nu_{\mathbf{v}}(v)$ given in Fig. 1.41, provided that \bar{v} is considered as a function of M at fixed temperature. When $M = m$, (1.15.7) yields

$$\nu = \sqrt{2} n\sigma \bar{v}. \quad (1.15.8)$$

As is seen the motion of similar partners increases the number of collisions by a factor of 1.4 compared to the case where they are immobile.

Now we can estimate the order of the molecules' free path time under normal conditions: $n = 10^{19} \text{ cm}^{-3}$, $\bar{v} = 10^5 \text{ cm/sec}$; $r_1 = r_2 = 2 \cdot 10^{-8} \text{ cm}$. In this case the cross-section of collisions is equal to $50 \cdot 10^{-16} \text{ cm}^2$, and

$$\nu = \sqrt{2} \cdot 50 \cdot 10^{-16} \cdot 10^{19} \cdot 10^5 \approx 7 \cdot 10^9 \text{ Hz}. \quad (1.15.9)$$

Consequently, if the Maxwell distribution of velocities is violated somehow, it is recovered within nanoseconds.

Experimental Verification

When a new physical idea or concept is advanced, it is always desirable to have direct experimental verification of its existence. In an experiment in which molecular beam was passed through a gas of rather low density, the collisions were visualized through the scattering of the beam molecules and the free path distribution was easily measured.

At some time each molecule experienced a first collision. As a result it changed its direction of motion, and left the beam. So the number of molecules in the beam decreased gradually with distance from the source (Fig. 1.42). This number could be measured by erecting a screen in the beam's path. It was established that the number of molecules which settled on the screen decreased exponentially depending on the distance between the screen and the source.

This exponential decrease was foreseen even by Clausius. The number of molecules involved in collisions and thrown out of the beam between x and $x + dx$ must be proportional to dx and to the number of molecules $N(x)$ which safely reached the borderline, that is, avoided collisions in the interval $(0, x)$. Therefore

$$-dN = a \cdot N(x)dx . \tag{1.15.10}$$

In the gas phase, the coefficient a cannot depend on x , for there is no reason to believe that in any interval dx collisions occur more often than in any other.

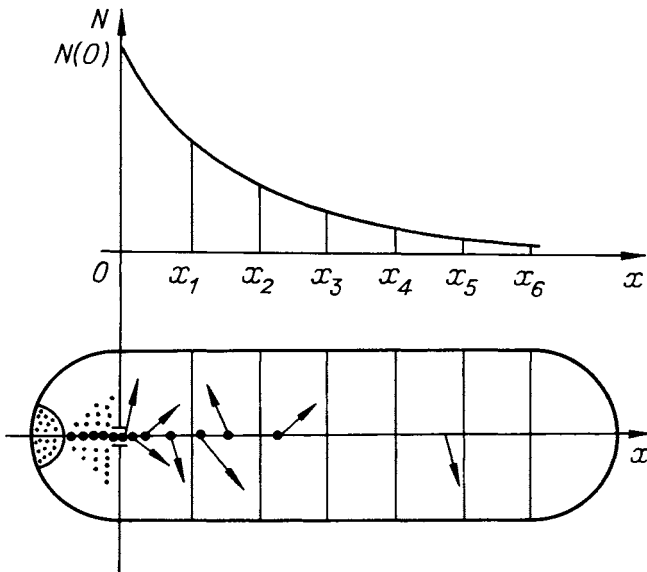


Figure 1.42 The scattering of a molecular jet in a gas, showing the resulting number density at section x .

This is a homogeneous flux of events, but their density in space a may depend on the velocity of the molecules in the beam, as in (1.15.4).

Solving (1.15.10), we obtain the number of particles which covered the distance x without a single collision

$$N(x) = N(0)e^{-ax}. \quad (1.15.11)$$

The thickness of the layer of molecules settled on the screen must be proportional to this value. This dependence was verified experimentally both qualitatively and quantitatively; moreover, plotting $\ln N$ against x , the value a was easily measured by the straight line slope.

Free Path

By definition the mean free path is

$$\ell = \int_0^{\infty} x dW(x)$$

where $dW(x)$ is the probability of colliding in the interval dx after passing the distance x without a collision. This probability is defined by the ratio of the number of molecules involved in the first collision in the interval dx to the total number of molecules $N(0)$ which “went to the starting line,” that is,

$$dW(x) = -\frac{dN}{N(0)} = a \frac{N(x)}{N(0)} dx = ae^{-ax} dx.$$

Thus, the mean length of the molecules' free path in the gas

$$\ell = a \int_0^{\infty} xe^{-ax} dx = \frac{1}{a}, \quad (1.15.12)$$

is equal to inverse a and the distribution of free paths may be represented as follows:

$$dW(x) = \exp(-x/\ell) \frac{dx}{\ell}. \quad (1.15.13)$$

The free path length ℓ is related to the free path time $\tau_0 = v_v^{-1}$:

$$\ell = v\tau_0. \quad (1.15.14)$$

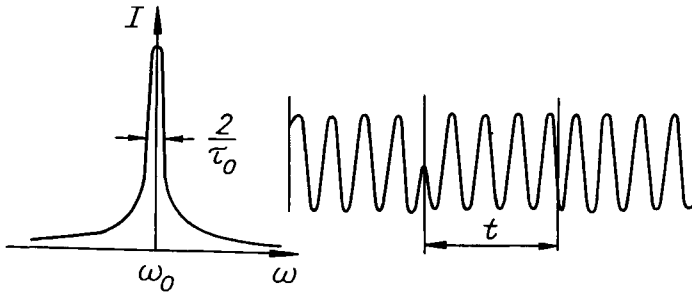


Figure 1.43 The spectrum of a Lorentzian wave: monochromatic radiation with its phase broken at each collision.

In view of $x = vt$, substitution of (1.15.14) into (1.15.13) yields the distribution in the free path times of

$$dW(t) = \frac{1}{\tau_0} e^{-t/\tau_0} dt. \quad (1.15.15)$$

This may be also subjected to experimental (spectroscopic) test. According to the Lorentz model, each collision results in an abrupt change in the phase of the electromagnetic wave frequency ω_0 radiated by the excited atom. The duration of a monochromatic piece of wave (Fig. 1.43) is determined by the probability of spending the time without collisions: $W_0 = \exp(-t/\tau_0)$. It can be shown that in this case the radiation spectrum shape is defined as

$$g(\omega) = \frac{Re}{\pi} \int_0^\infty \exp \left[-\frac{t}{\tau_0} + i(\omega_0 - \omega)t \right] dt = \frac{\tau_0/\pi}{(\omega - \omega_0)^2 \tau_0^2 + 1}. \quad (1.15.16)$$

Such a profile is called Lorentzian or impact. One can find the free path time of gas molecules from its width.

As τ_0 depends on v , the free path length $\ell(v) = v/\nu_v(v)$ increases monotonically with increasing velocity, tending to its upper limit $1/n\sigma$ which is reached at $v \gg \bar{v}'$. The average length of the free path may be defined as

$$\overline{\left(\frac{v}{\nu_v} \right)} \approx \frac{\bar{v}}{\nu} = \frac{1}{n\sigma} \sqrt{\frac{m}{m+M}} = \lambda. \quad (1.15.17)$$

It depends on the gas density only, and does not exceed the value $1/n\sigma$. Two mutually related parameters ν and λ are of fundamental importance in the construction of physical kinetics in the gas phase. At ordinary densities $n \sim 10^{19} \text{ cm}^{-3}$ and $\sigma = 5 \cdot 10^{-15} \text{ cm}^2$ $\lambda = 2 \cdot 10^{-5} \text{ cm}$. However, λ may be essentially extended by exhausting the gas from the vessel: at $p = 10^{-4} \text{ atm}$

$\lambda \sim 0.2$ cm, while at $p = 10^{-5}$ atm $\lambda \sim 2$ cm. Under more intense evacuation of the vessel, λ exceeds the vessel size, and the gas turns into the so-called physical vacuum or ultrararefied gas. We shall see further that the latter is distinctly different in all its properties from a dense, ordinary gas.

Poissonian Statistics

It is of interest to ask what is the probability that only one collision occurs in the interval $(0, t)$ at time $t_1 \leq t$. Evidently this is a coincidence of two independent events:

- that the molecule moving through the gas experiences its first (after $t = 0$) collision in time element dt_1 and
- that this collision will be the first and the last, i.e., there will be no more collisions between t_1 and t .

The probability of such a realization of molecule's trajectory is given by the product of the corresponding probabilities: to have a first collision at the given time

$$dW = \frac{1}{\tau_0} e^{-t_1/\tau_0} dt_1$$

and to have no collisions between t_1 and t

$$W_0 = e^{-(t-t_1)/\tau_0}. \quad (1.15.18)$$

The result does not depend on t_1 if we assume for simplicity that τ_0 is v -independent ($M \gg m$):

$$dW_1 = dW \cdot W_0 = e^{-t/\tau_0} \frac{dt_1}{\tau_0}. \quad (1.15.19)$$

The probability that only one collision happened anywhere between 0 and t is the following integral

$$W_1 = \int_0^t dW_1 = e^{-t/\tau_0} \frac{t}{\tau_0}. \quad (1.15.20)$$

A simple generalization shows that the probability for two successive collisions to happen at times t_1 and t_2 is

$$dW_2 = e^{-t/\tau_0} \frac{dt_1}{\tau_0} \frac{dt_2}{\tau_0}, \quad (1.15.21)$$

while the probability of having just two collisions anywhere in the interval $(0, t)$ is

$$W_2 = \frac{e^{-t/\tau_0}}{\tau_0^2} \int_0^t dt_2 \int_0^{t_2} dt_1 = e^{-t/\tau_0} \frac{t^2}{2\tau_0^2}. \quad (1.15.22)$$

For an arbitrary number of collisions n we obtain in the same way

$$W_n = \frac{1}{n!} \left(\frac{t}{\tau_0} \right)^n e^{-t/\tau_0}. \quad (1.15.23)$$

This is the normalized Poissonian distribution of collisions: $\sum_{n=0}^{\infty} W_n = 1$. The average number of collisions in time t is evidently

$$\bar{n} = \sum_{n=0}^{\infty} n W_n = t/\tau_0, \quad (1.15.24)$$

but the distribution about the mean is determined by the Poisson distribution (1.15.23).

Velocity Relaxation

Collisions of hard spheres are instantaneous, while those of real molecules are not. However, they are still considered as instantaneous in the so-called *impact approximation* as their duration in rare gases is much less than the free path time τ_0 . Temporal change of the velocity in the impact approximation is a so-called *purely discontinuous random process*. While constant between impacts, the velocity abruptly changes at the moments of collisions as is shown in Fig. 1.44 for an arbitrary projection of velocity. The successive values of the projection v_i form a Markovian chain because any subsequent value depends only on a previous one. This dependence is given by the probability $F(v, v') dv$ to obtain the value v after collision if the velocity before it was v' .

Many different realizations of a random process lead to the same value v at time t when initially (at time 0) it was v_0 . The chain between these values may be shorter or longer depending on how many collisions happen in the interval $(0, t)$. The conditional probability of the event $\varphi(v, t; v_0, 0)$ must sum up all possibilities as follows:

$$\begin{aligned} \varphi(v, t; v_0, 0) &= \delta(v - v_0) W_0 + F(v, v_0) W_1 + \int F(v, v_1) dv_1 F(v_1, v_0) W_2 + \dots \\ &= [\delta(v - v_0) + \Phi] e^{-t/\tau_0} \end{aligned} \quad (1.15.25)$$

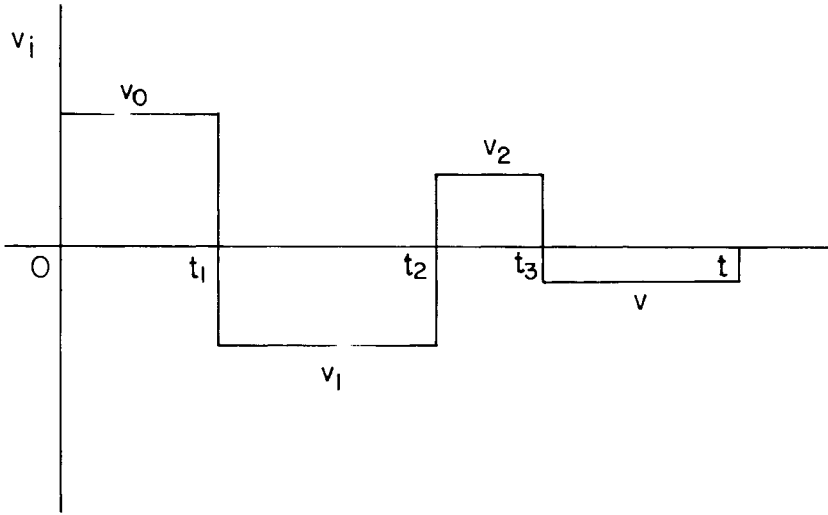


Figure 1.44 Time variation of a velocity component in three collisions: realization of a Poissonian process.

where

$$\begin{aligned} \Phi = & F(v, v_0) \frac{t}{\tau_0} + \int F(v, v') dv' F(v', v_0) \frac{t^2}{2! \tau_0^2} \\ & + \int F(v, v') dv' \int F(v', v_1) dv_1 F(v_1, v_0) \frac{t^3}{3! \tau_0^3} \dots \end{aligned} \quad (1.15.26)$$

satisfies the integral equation

$$\dot{\Phi}(v, t; v_0, 0) = \frac{1}{\tau_0} F(v, v_0) + \frac{1}{\tau_0} \int F(v, v') \Phi(v', t; v_0, 0) dv' \quad (1.15.27)$$

with initial condition $\Phi(0) = 0$. Differentiating (1.15.25) taking into account (1.15.27) we find the Kolmogorov–Feller equation for the conditional probability:

$$\dot{\varphi}(v, t; v_0, t) = -\frac{1}{\tau_0} \left[\varphi(v, t; v_0, 0) - \int F(v, v') \varphi(v', t; v_0, 0) dv' \right], \quad (1.15.28)$$

that must be solved with initial condition $\varphi(0) = \delta(v - v_0)$.

Starting from any initial value v_0 the velocity distribution must relax in time to the equilibrium Maxwellian distribution:

$$\varphi(v, \infty; v_0, 0) = f(v). \quad (1.15.29)$$

Therefore $\dot{\varphi} \rightarrow 0$ at $t \rightarrow \infty$ and we find from Eqs. (1.15.28) and (1.15.29) the condition of stationarity of the equilibrium velocity distribution:

$$f(v) = \int F(v, v') f(v') dv'. \quad (1.15.30)$$

This may be considered as a direct consequence of the principle of *detailed balance* ensuring the equality of the rates of forward and back transitions between any two elements of the phase space:

$$F(v', v) f(v) = F(v, v') f(v') \quad (1.15.31)$$

The identity of the two statements is proved by integration of the last, taking into account the normalization condition: $\int F(v', v) dv' = 1$. This puts a limitation on the choice of $F(v, v')$.

The most popular model for this kernel was proposed by Keilson and Storer:

$$F(v, v') = F(v - \gamma v'). \quad (1.15.32)$$

Its particular shape is uniquely determined by Eq. (1.15.30) if $f(v)$ is known. For the one-dimensional Maxwellian distribution (1.2.13) it is

$$F(v - \gamma v') = \sqrt{\frac{\alpha}{\pi(1 - \gamma^2)}} \exp\left(-\frac{\alpha(v - \gamma v')^2}{1 - \gamma^2}\right), \quad (1.15.33)$$

where γ is a real numerical parameter with $|\gamma| \leq 1$. Its physical sense becomes clear after an estimate of the average velocity after collision:

$$\langle v \rangle = \int v F(v - \gamma v') dv = \int_{-\infty}^{+\infty} z F(z) dz + \gamma v' \int_{-\infty}^{+\infty} F(z) dz = \gamma v'. \quad (1.15.34)$$

Collisions are *strong* at $\gamma = 0$ as each of them completely restores the equilibrium: after collision

$$F = f(v) \quad (1.15.35)$$

whatever is the velocity before it. Collisions are *weak* at $\gamma \rightarrow 1$ as the velocity decreases just a little (γ times) after a single collision and relaxes to 0 as a result of a long sequence of them (see Fig. 1.45).

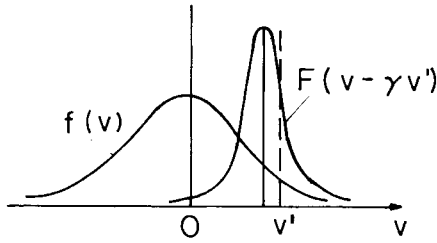


Figure 1.45 The Keilson–Storer kernel $F(v)$ for weak collisions in comparison with the one-dimensional Maxwellian distribution $f(v)$.

To find the relaxation law one has to multiply the Kolmogorov–Feller equation (1.15.28) by v and integrate, taking into account (1.15.34):

$$\dot{\bar{v}} = -\frac{\bar{v}}{\tau_0} + \frac{\gamma\bar{v}}{\tau_0} = -\Gamma\bar{v}, \quad (1.15.36)$$

where

$$\Gamma = \frac{1 - \gamma}{\tau_0} = n\sigma_v v \quad (1.15.37)$$

is the relaxation rate of velocity. The effective cross-section of the process σ_v may be less than geometrical σ . The solution of Eq. (1.15.36) leads to exponential velocity relaxation

$$\bar{v}/v_0 = \exp(-\Gamma t), \quad (1.15.38)$$

that is identical to $W_0 = \exp(-t/\tau_0)$ only in the limit of strong collisions.

Strong and Weak Collisions

The efficiency of hard sphere collisions depends on the masses of the colliding objects. If the target particle is so heavy that it may be considered as practically immobile, then the result of the collision is the elastic scattering of the light molecule center from a sphere of radius R . The scattering angle depends on the point of contact which is different for different molecules in a flux of point masses flying towards the sphere with the same initial velocity v' . Since the angle of incidence α is equal to the angle of reflection, the scattering angle $\Theta = 2\alpha$ (Fig. 1.46). This angle is the same for all points inside a differential cross-section $d\sigma$ which is an area increment of the circle of radius $R \sin \alpha$:

$$d\sigma = d(\pi R^2 \sin^2 \alpha) = 2\pi R^2 \sin \alpha \cos \alpha d\alpha. \quad (1.15.39)$$

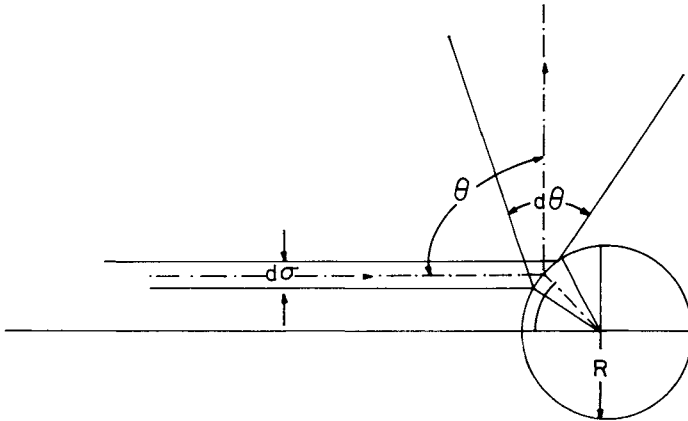


Figure 1.46 Elastic collision of a light molecule with a heavy one at an angle α with radius-vector of a contact point (the scattering angle $\Theta = 2\alpha$).

The solid angle of scattering is

$$d\Omega = 2\pi \sin \Theta d\Theta = 8\pi \sin \alpha \cos \alpha d\alpha. \quad (1.15.40)$$

Hence, the differential cross-section

$$d\sigma = \frac{R^2}{4} d\Omega \quad (1.15.41)$$

does not depend on α and the full cross-section $\sigma = (R^2/4) \int d\Omega = \pi R^2$ is purely geometrical.

The average projection of the velocity of the scattered molecule on the initial direction of motion is

$$\langle v \rangle = - \int v' \cos \Theta d\sigma / \sigma.$$

From this we obtain, taking into account (1.15.39),

$$\langle v \rangle = -v' \int_0^{\pi/2} \cos 2\alpha \sin 2\alpha d\alpha = 0. \quad (1.15.42)$$

Thus the light particle (for example, an electron) is scattered uniformly in all directions, unlike the energy which is conserved in this approximation because $|\mathbf{v}|$ remains the same after collision. Therefore the real cross-section of electron energy relaxation though nonzero is much less than σ .

On the other hand, the velocity of a heavy molecule moving in a light gas is not significantly changed in a single collision and it requires many collisions to relax. Since both the velocity and the energy are slowly changing, the collisions may be considered as weak. The limit $\gamma \rightarrow 1$, when

$$M \gg m \quad \text{and} \quad \Gamma \ll \frac{1}{\tau_0}, \quad (1.15.43)$$

is appropriate for Brownian particles.

To give a proof of the strong collision limit is more problematic. Simultaneous relaxation to equilibrium of both the direction and magnitude of the velocity are required in each collision. In order to meet these requirements the colliding particles must be of comparable or equal masses:

$$\text{if } M \approx m \quad \text{then} \quad \Gamma \approx \frac{1}{\tau_0}, \quad (1.15.44)$$

and hence $\gamma \approx 0$. Although approximate, the strong collision model is very useful for simple estimates and is widely used in kinetics.

Collisional relaxation of angular momentum is very similar to that of translational velocity and even the cross-sections are comparable. Vibrational relaxation, especially in diatomic molecules, is much slower and the rates of energy and phase relaxation are rather different. The slowest is spin relaxation in gases (governed by very weak magnetic interaction) whose cross-section may be many orders of magnitude less than σ .

1.16 TRANSFER PHENOMENA

Local Equilibrium

We can now proceed to the solution of the basic kinetic problem: the description of irreversible processes. Unfortunately, it is not so easy to apply general ideas of stirring to particular problems. These ideas serve to strengthen our belief that one or two strong collisions are quite sufficient for the complete recovery of the equilibrium velocity distribution at any point of the system. In practice, this assurance is embodied in the concept of *local equilibrium* which is of fundamental importance in considering the majority of irreversible, non-equilibrium processes. It is supposed that energy-momentum exchange between particles proceeds in such a way that after the first strong collision each molecule acquires equilibrium properties typical for the point of space where the collision occurred. The domain of validity of this hypothesis is bounded by slow irreversible processes, when the notion of local temperature, density, and so on, may be introduced at each point of the space. Primarily, these are

transfer phenomena—heat conduction, diffusion, viscosity—which, as is evident in everyday experience, are fairly slow.

For example, if heat flows from a hot glass to a cool one through a plane gas layer in the double window frame, the “local temperature” at any point between the glasses can be easily measured, but no temperature can be assigned to the gas on the whole, which is in a nonequilibrium state. Thus one can speak about “local equilibrium” at its own temperature in each microregion with linear extent of the order λ . The flux of particles from other regions continually disturbs this local equilibrium, but it is recovered again and again in a time of the order $\tau_c = 1/\nu$. The spatial size of the microregions is determined by the fact that molecules retain their properties solely during the free path, and change them abruptly upon collision. That is why, despite the large velocities of molecules $\bar{v} \sim 10^5$ cm/s, the energy transfer proceeds gradually, from microregion to microregion, rather than immediately from one wall to another. Moving from hot regions to cool ones, a molecule releases its excess energy upon collision after each free path. It retains just the energy typical for the microregion where the collision occurred. On the other hand, molecules moving in the opposite direction heat up progressively, so they are not treated as alien inclusions in any region, and equilibrate with the “natives” immediately after the first collision.

This qualitative picture—the gradual adaptation of molecules to the properties of those space points (and at that time) where (and when) they experience collisions—forms the basis of the kinetic theory of quasistatic transfer phenomena. However, the calculations may be more or less rigorous, from quite primitive to rather complicated, depending on how accurately the different details of a phenomenon are taken into account. In order to elucidate the essence of the method, let us begin from the most elementary approach.

Heat Conduction

Consider heat transfer through some section perpendicular to the energy flux. If diffusion is absent the fluxes of particles j_+ and j_- , passing through the section from the right and from the left are equal to one another: $j_+ = j_- = j_0$. However, the energy transferred by particles moving in opposite directions is not the same. The particles moving from the left are “more hot,” while those coming from the right are “more cool,” if $dT/dx < 0$ (Fig. 1.47).

What are their energies? Here some simplifications are necessary. Suppose that all particles suffer their last collision before reaching the section at point x exactly at the distance λ from it. Then the particles, moving through the section from the left, will transfer the mean heat energy $\bar{\epsilon}(x - \lambda)$ characteristic for the point $x - \lambda$, while those coming from the right will approach the same section with the energy $\bar{\epsilon}(x + \lambda)$. The dependence of mean energy on x is conditioned by the fact that $\bar{\epsilon} = C_V T/N_0$, while $T = T(x)$. The resultant heat (energy) flux through the section is expressed as the difference of the two opposite fluxes:

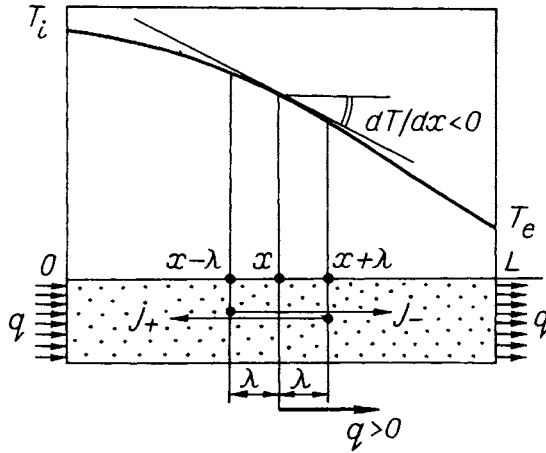


Figure 1.47 Heat transfer through a window with parallel glass panes at 0 and at L , one neighboring the high interior temperature T_i and the other the low exterior temperature T_e . The figure shows the variation of temperature in the intervening space, and denotes the flux of molecules in the direction of positive temperature gradient by j_+ and in the direction of negative gradient by j_- .

$$\begin{aligned}
 q &= \bar{\epsilon}(x-\lambda)j_- - \bar{\epsilon}(x+\lambda)j_+ \\
 &= \frac{C_V}{N_0} j_0 [T(x-\lambda) - T(x+\lambda)] = -\frac{2C_V j_0 \lambda}{N_0} \cdot \frac{dT}{dx}. \quad (1.16.1)
 \end{aligned}$$

The above expansion of $T(x-\lambda)$ and $T(x+\lambda)$ as a power series with an accuracy to the first-order terms is justified by the assumption that λ is small compared to the macroscopic scale of T variation.

Strictly speaking, it is incorrect to assign the same energy to all particles in the flux, since the kinetic energy depends on the velocity of motion and cannot be averaged independently of j_0 . However, this error is partly justified by the fact that the flux itself is estimated by the Joule method, wherein the same velocity \bar{v} is assigned to all particles. Besides, taking that all particles move solely in three perpendicular directions (along coordinate axes), with the same number of particles moving back and forth in each direction, one can easily see that $j_0 = \frac{1}{6}\bar{v}n$, so

$$q = -\frac{1}{3} \frac{C_V \bar{v} \lambda n}{N_0} \frac{dT}{dx} = -\kappa \frac{dT}{dx}. \quad (1.16.2)$$

This is the “Fourier law.” It claims that the heat flux is proportional to the temperature gradient and opposite to it in sign. Of course, the verification of this empirical dependence by direct kinetic calculation is important, but even

more essential is a disclosure of the microscopic sense of thermal conductivity κ and its dependence on different gas parameters:

$$\kappa = \frac{1}{3} \cdot \frac{C_V \bar{v} \lambda n}{N_0} = \frac{1}{3} \cdot \frac{C_V}{M} \cdot \frac{m \bar{v}}{\sigma}, \tag{1.16.3}$$

where M is a molar mass. In particular, though surprisingly at first sight, κ is independent of the gas density, as $\lambda \approx 1/n\sigma$.

Viscosity

Internal friction, or viscosity, is revealed when a gas is in motion: flows through a tube, or around some surface. Layers adjacent to solid surfaces are retarded by friction against the surface, while layers away from it rub against each other. As a result, the flow is gradually slowed down as it approaches the lower (immobile) surface (Fig. 1.48), and the relative velocity of the layer adjacent to an upper (moving surface) is also zero.

However, how does it happen that the gas layers experiencing internal friction though the molecules do not interact with each other most of time? Again, this is due to collisions. The heat velocity of molecules is much greater than the macroscopic speed of any gas layer $u(x)$. Being orientated in different directions, thermal motion freely carries a molecule from a slow layer to one moving more rapidly, and vice versa. Upon collision in the new layer, the molecule changes its macroscopic speed to become indistinguishable from its new neighbors, that is, the molecule is either accelerated or retarded, giving up the difference in momentum to an other. The total momentum carried by the “emigrants” from one layer to another per unit time is equal to the friction force acting in the section separating the layers (see Fig. 1.48).

Thus the calculation should proceed similarly to the previous one. The only difference is that in this case it is not energy which is transferred, but the macroscopic momentum $mu(x)$ where $u(x)$ is the velocity of the gas flux perpendicular to the x axis. Now C_V/N_0 is replaced by m , and $T(x)$ by $u(x)$; all the rest remains unchanged. So, by analogy with (1.16.2), we can immediately write

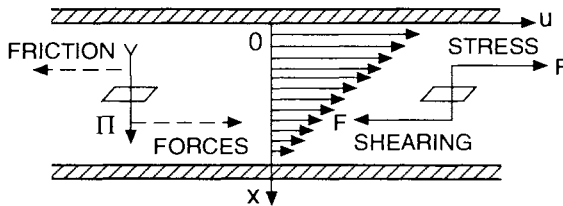


Figure 1.48 Velocity distribution in a laminar stream between two parallel plates the upper of which moves to the right.

$$F = -\frac{1}{3} m\bar{v}\lambda n \frac{du}{dx} = -\eta \frac{\partial u}{\partial x}. \quad (1.16.4)$$

The viscosity

$$\eta = \frac{1}{3} nm\bar{v}\lambda = \frac{1}{3} \frac{m\bar{v}}{\sigma} \quad (1.16.5)$$

is independent of the gas density as well as thermal conductivity (Maxwell's law).

Comparing formulae (1.16.5) and (1.16.3) gives an important relation between the kinetic coefficients, which is independent of the microscopic parameters:

$$\frac{\kappa M}{\eta C_V} = 1. \quad (1.16.6)$$

Experiments confirm that this ratio is really constant and universal. Such a relation between such apparently different phenomena could seem paradoxical, if they had not been considered from a common standpoint, which is a concept of local equilibrium.

In fact, the numerical value $\kappa M/\eta C_V$ varies from one gas to another, although it remains of order of magnitude unity. This is no surprise. In such rough calculations there is an inevitable error in estimating the numerical parameter. However, the information on the nature of the phenomena and semiquantitative estimates of the kinetic coefficients is so valuable that we have to reconcile ourselves to this inaccuracy of the method. Further we shall consider possible causes of the trouble and methods of eliminating them.

Diffusion

It is well known that diffusion is the penetration of one substance into another due to the thermal motion of molecules. If we deal with a gas, an example is the spread of perfume from a person who has just visited a hairdresser's or barber's shop. However, the gas mixing process may be accelerated by convectional flows due to wind or even breathing, that is, solely mechanical mixing which has nothing to do with diffusion. Thus pure diffusion can only be observed under experimental conditions, for example in the experiment carried out by Loschmidt.

In this experiment, two tubes filled with different gases at one and the same pressure are brought in contact. Then the partition separating them is taken away, and the gases begin mixing. Checking the gas composition some time later, one can see that the longer the time period since the start of the experiment, the more homogeneous the mixture. It is to be noted that this is a lengthy process (hours), so over a short time interval it may be treated as quasistationary, that is, with the concentration gradient approximately constant. Thus this process can be considered from the same standpoint as the above phenom-

ena. For simplicity, let us concentrate on self-diffusion, which is observable in the case when molecules are different isotopes of the same gas distinguishable by some appropriate technique.

How can we calculate the flux of particles through a perpendicular section, if the gas is nonuniform in density? In other words, what should we mean by n in the Joule estimate $\frac{1}{6}n\bar{v} = j_{\pm}$? At which point should $n(x)$ be taken? According to the hypothesis of local equilibrium, the density of particles moving in columns towards the section is specified by the points where they started. After each free path λ , the columns are rearranged, adjusting to the density of particles at the points where they experienced collision. The last path before the section begins a distance λ from it; therefore, the density of particles in the flux passing through the section is $n(x - \lambda)$, if they move from left to right, and $n(x + \lambda)$ in the opposite case.

Thus $j_- = (\bar{v}/6)n(x - \lambda)$, and $j_+ = (\bar{v}/6)n(x + \lambda)$. Because of the difference between j_- and j_+ the resulting diffusion flux is

$$j = j_- - j_+ = \frac{1}{6} \bar{v} [n(x - \lambda) - n(x + \lambda)] = -\frac{1}{3} \bar{v} \lambda \frac{dn}{dx} = -D \frac{dn}{dx}, \quad (1.16.7)$$

where

$$D = \frac{1}{3} \bar{v} \lambda \approx \frac{\bar{v}}{3n\sigma} \quad (1.16.8)$$

is the diffusion coefficient.

Comparing (1.16.8) with (1.16.6) and (1.16.3), we find two more relations connecting the transfer coefficients

$$\frac{\eta}{\rho D} = 1, \quad (1.16.9)$$

$$\frac{\rho DC_V}{\kappa M} = 1, \quad (1.16.10)$$

where $\rho = nm$. A more rigorous theory adjusts the above relations for a gas of hard spheres:

$$\frac{\kappa M}{\eta C_V} = \frac{5}{2}, \quad \frac{\eta}{\rho D} = \frac{5}{6}, \quad \frac{\rho DC_V}{\kappa M} = \frac{12}{25}. \quad (1.16.11)$$

In view of these numerical corrections, we obtain

$$\kappa = \frac{\alpha}{\sigma} \sqrt{\frac{T}{M}} \frac{\text{cal}}{\text{cm} \cdot \text{deg} \cdot \text{sec}}, \quad \eta = \frac{\beta}{\sigma} \sqrt{TM} \frac{\text{g}}{\text{cm} \cdot \text{sec}}, \quad D = \frac{\gamma}{nk\sigma} \sqrt{\frac{T}{M}} \frac{\text{cm}^2}{\text{sec}},$$

$$\text{where } \alpha = 6,2 \cdot 10^{-4}; \quad \beta = 8,4 \cdot 10^{-5}; \quad \gamma = 8,3 \cdot 10^{-3}.$$

Refinement of Calculations

The method employed above simplifies rather brutally the picture of the phenomenon for the sake of brevity and simplicity of description. Nevertheless, the dependence of the kinetic coefficients on any varying parameters seems to be reasonable. To be sure of this, let us consider heat and matter transfer once again, abandoning, as far as possible, the most rough assumptions.

Let molecules move in all directions, with any velocity, and experience their last collision at arbitrary distance from near the section under consideration. From the entire flux of molecules passing through this section, we first separate those moving towards it with a speed v inside a solid angle $d\Omega$ which is inclined at angle θ to the x axis (Fig. 1.49). From these molecules we select those which suffered their last collision at a distance R from the section. How many such molecules pass through the chosen unit section per unit time? The flux is equal to $v_x dn = v \cos \theta n dW$; however, the probability dW that we are dealing with molecules starting at a distance R with the speed v is defined by the product of probabilities $dW(\mathbf{v})dW(R)$. Here $dW(R)$ is the distribution in free path lengths (1.15.13), and $dW(\mathbf{v}) = g(v)d\mathbf{v}$ is the ordinary Maxwell distribution with the density

$$g(v) = \left(\frac{2\pi kT}{m}\right)^{-3/2} \exp\left(-\frac{mv^2}{2kT}\right), \quad (1.16.12)$$

where $T(x)$ is a function of the point where the collision occurred.

So the magnitude of the flux depends on the temperature at the point where the particle starts from and on the density there $n(x)$. The fluxes of particles

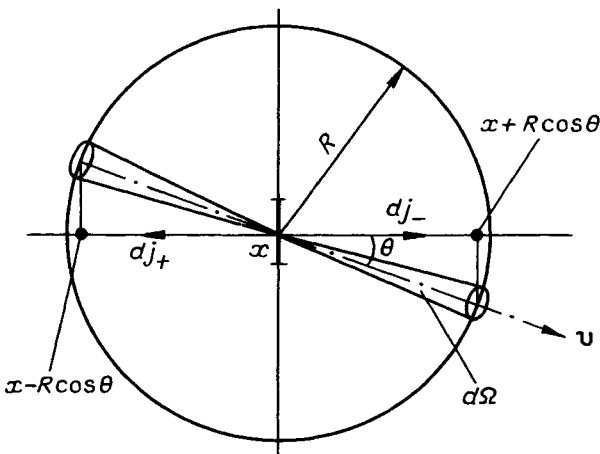


Figure 1.49 Opposite fluxes of particles moving with the same speed away from the points of last collision equidistant from section x .

from two opposite points lying on a sphere with radius R (see Fig. 1.49) differ only in the magnitude of the multiplier ng :

$$dj_- = v \cos \theta (ng)_- dv dW(R), \quad (1.16.13a)$$

$$dj_+ = v \cos \theta (ng)_+ dv dW(R) \quad (1.16.13b)$$

The subscripts $+$ and $-$ mean that the value of ng is taken, respectively, at the points $x + R \cos \theta$ and $x - R \cos \theta$, where the last collisions before the "finishing line" took place. It is of interest that $dj_- \neq dj_+$ even at $n = \text{const}$, provided that there is temperature inhomogeneity. By virtue of the difference between g_- and g_+ , the flux of high energy particles moves from hot points to cold ones, while low energy particles move from cold to hot points. The resulting flux of particles with the given velocity is as follows

$$dj = dj_- - dj_+ = v \cos \theta [(ng)_- - (ng)_+] dv dW(R). \quad (1.16.14)$$

The partial flux dj can differ from zero even when the total is zero (i.e. $j = \int dj = 0$). This ensures heat transfer from hot points to cold ones in the absence of diffusion.

If the starting points are offset by λ from the section and this distance may be considered small compared to the macroscopic scale, we can use the truncated expansion

$$(ng)_- - (ng)_+ = -2 \frac{d(ng)}{dx} R \cos \theta. \quad (1.16.15)$$

Substituting (1.16.15) into (1.16.14) gives

$$dj = -2v \frac{d(ng)}{dx} v^2 dv \cos^2 \theta d\Omega R dW(R). \quad (1.16.16)$$

This expression is easily integrated with respect to angles and free path lengths

$$dj = -2v \frac{d(ng)}{dx} 4\pi v^2 dv \overline{\cos^2 \theta} \ell = -\frac{\tau_0}{3} v^2 \frac{d(ng)}{dx} dv, \quad (1.16.17)$$

since, according to (1.15.14), $\ell = \int R dW(R) = v\tau_0$, and $\overline{\cos^2 \theta} = \int \cos^2 \theta d\Omega / 4\pi = \frac{1}{3}$.

Using a constant $\tau_c = 1/\nu$ instead of $\tau_0(v)$ and integrating over velocities in (1.16.17), we obtain

$$j = -\frac{1}{3} \frac{d}{dx} \left[n \int \tau_0(v) v^2 g(v) dv \right] = -\frac{\tau_c}{3} \frac{d(n\bar{v}^2)}{dx} = -\frac{\tau_c k}{m} \frac{d(nT)}{dx}. \quad (1.16.18)$$

Differentiating, we find

$$j = -D \frac{dn}{dx} - B \frac{dT}{dx}, \quad (1.16.19)$$

where

$$D = \frac{kT\tau_c}{m} = \frac{\bar{v}^2\tau_c}{3}, \quad B = \frac{k\tau_cn}{m}. \quad (1.16.20)$$

The second term in (1.16.19) describes the phenomenon known as *thermodiffusion*. It differs from ordinary diffusion in that the particles move from hot points to cold ones due to the higher velocity of motion rather than higher density.

Allowing another dependence $\tau_0(v)$ in (1.16.18) will result only in numerical changes to the conclusion. For example, in the case of the diffusion of light particles in a heavy gas $\tau_0 = [n\sigma v]^{-1} \equiv \lambda/v$, and on averaging over v , we get $D = \frac{1}{3}\bar{v}\lambda = \bar{v}^2\tau_c/3$ (i.e., $D \propto \bar{v}^2$, not v^2), just as in (1.16.8). Within the framework of the hard sphere model both results are reasonable, but in reality the dependence $\tau_0(v)$ should be found allowing for the actual intermolecular interaction, taking into account both repulsion and attraction.

Let us estimate the flux of heat, that is, thermal energy transferred by moving molecules. In the simplest case of monoatomic gas only kinetic energy is considered,* so at $\tau_0(v) = \tau_c$, we find using (1.16.17):

$$q = \int \frac{mv^2}{2} dj = -\frac{m\tau_c}{6} \frac{d(\bar{mv}^4)}{dx} = -\frac{5\tau_ck^2}{2m} \frac{d(nT^2)}{dx}.$$

Differentiating, we have

$$q = -\chi \frac{dn}{dx} - \kappa \frac{dT}{dx}, \quad (1.16.21)$$

where

$$\chi = \frac{5}{2} \frac{(kT)^2}{m} \tau_c, \quad \kappa = \frac{5k^2T\tau_cn}{m}. \quad (1.16.22)$$

It is seen that heat transfer is stimulated both by the temperature gradient and the concentration gradient, since energy is transferred together with the matter carrying it. This fact makes difficult a comparison between the result obtained

*For polyatomic molecules $q = \int [(mv^2/2) + i(kT/2)] dj$ where i = total number of excited degrees of freedom except translational ones.

and the simple estimate of thermal conductivity given above. The latter was found under the additional condition $n = \text{const}$, while Eq. (1.16.21) describes the more general and usual situation. For example, it arises when heat exits a house through a double window frame, the inner glass of which is at room temperature T_i , while the outer one at the outside temperature T_e (see Fig. 1.47). The pressure at all points of the air layer between the glasses is constant (normal). In the ideal gas approximation

$$p = nkT = \text{const} \quad \text{or} \quad \frac{1}{n} \frac{dn}{dx} = -\frac{1}{T} \frac{dT}{dx}, \quad (1.16.23)$$

that is, the concentration gradient is proportional to the temperature gradient although opposite in sign. Eliminating it from (1.16.21) with the use of (1.16.23), we obtain the Fourier law for a stationary flux

$$q = -\left[\kappa - \chi \frac{B}{D}\right] \frac{dT}{dx} = -\mathcal{H} \frac{dT}{dx}, \quad (1.16.24)$$

where \mathcal{H} is the thermal conductivity in the ordinary sense. Substituting formulae (1.16.20) and (1.16.22) into (1.16.24), we can see that \mathcal{H} differs from κ in (1.16.22) just by a factor of 2:

$$\mathcal{H} = \kappa - \chi \frac{B}{D} = \frac{5k^2 T \tau_c n}{2m} = \frac{5\pi k \bar{v}}{16\sqrt{2}\sigma}. \quad (1.16.25)$$

The change in corpuscular density from the hot to the cold glass does not essentially affect the heat conductivity of the gas. Comparison of its magnitude with the approximate estimate (1.16.3) where $M = N_0 m$, $C_V = \frac{3}{2} k N_0$ shows that they differ only by a numerical factor. In view of the uncertainty in \bar{v} in (1.16.3), this is of no fundamental significance. The most important features of the process, the dependence of \mathcal{H} on temperature and its independence of density, are quite satisfactorily represented by the simplest calculation.

Heat Transfer

To demonstrate the significance of the above results let us apply them to the calculation of the heat flux through the double window frame. As the temperatures inside and outside the house vary rather slowly, the process may be regarded as being stationary, but the temperature-dependence of the thermal conductivity must be essentially taken into account:

$$\mathcal{H} = AT^{1/2}, \quad A = \frac{5\sqrt{\pi}}{8\sigma\sqrt{m}} k^{3/2}. \quad (1.16.26)$$

This expression is used in Eq. (1.16.24) which can now be treated as a differential equation for the $T(x)$ -dependence:

$$-\sqrt{T} \frac{dT}{dx} = \frac{q}{A}, \quad (1.16.27)$$

where q is a constant to be defined later. Solving (1.16.27), we find

$$T^{3/2} = C - \frac{3}{2} \frac{q}{A} x. \quad (1.16.28)$$

The boundary conditions are given by the temperatures of the internal and external glasses:

$$T(0) = T_i; \quad T(L) = T_e. \quad (1.16.29)$$

The first condition serves to determine the integration constant in (1.16.28): $C = T_i^{3/2}$. Then, using the second condition, one can calculate the flux itself

$$q = \frac{2}{3} A \frac{T_i^{3/2} - T_e^{3/2}}{L}. \quad (1.16.30)$$

In this final expression the heat flux is expressed directly in terms specified by the experimental conditions: T_i , T_e , L . If $\mathcal{H}(T)$ were other than (1.16.26) this expression could be different.

The independence of thermal conductivity on density deserves special consideration. This fact is really paradoxical and points to a limited applicability of the results obtained. Indeed, how it can be explained that the decrease in the number of particles involved in energy transfer does not affect heat transfer? In normal gas this is attributed to the fact that the increasing length of the free path compensates for the decrease in molecular density. However, one can exhaust a gas from a vessel until vacuum is reached. Obviously, in this case the heat conduction will go to zero due to the absence of heat carriers. However, the mere existence of such an alternative cannot be inferred from the results obtained: $\mathcal{H} = \text{const}$ whatever the degree of the gas rarefaction.

Ultrarefined Gas

In view of the above reasoning, it is necessary to discuss the limits of application of the whole approach, based on the concept of local equilibrium. It was supposed that each point within a microregion of the scale λ may be considered as almost at equilibrium, with its own local characteristics of state: temperature and density. However, is this always true? Remember that $\lambda = 1/n\sigma = kT/p\sigma$; therefore, by decreasing the pressure we can make the path length a macroscopic quantity which exceeds considerably the vessel's size. In this situation,

the molecules will collide against the walls more often than with other molecules. From a kinetic standpoint, such an ultrarefined gas (physical vacuum) behaves quite differently to dense gases.

It should be noted that collisions with the walls are not necessarily elastic. Moreover, the molecules may be adsorbed onto a wall, leveling the energy with it. If the wall is warmer than the gas, the molecules take away some energy, and give it up in the opposite case. The heat exchange between gas and environment proceeds owing to adsorption–desorption processes. In order to heat a gas, we need only heat up the walls of the vessel.

The external heat exchange promotes attainment and maintenance of equilibrium in ultrarefined gas. The “stirring” property of such a system is so depressed that equilibrium is more rapidly established by the interaction with the exterior medium. This fact has an essential effect on all transfer phenomena. The concept of local equilibrium becomes meaningless. Since molecules move freely in the vessel, heat is transferred directly from one wall to another, rather than in the relay fashion (from molecule to molecule), as before.

Let us assume that from j molecules colliding against the wall per second, αj adhere to it. Under stationary conditions the same number of molecules evaporate each second taking with them the mean energy corresponding to the temperature of the surface. Also, there are $(1 - \alpha)j$ particles in the reflected flux whose energy remains unchanged due to elastic collisions with the wall. In such a model there are two groups of particles between the walls moving in opposite directions (Fig. 1.50). The total flux and density are correspondingly

$$j = j_1^+ + j_2^+ = j_1^- + j_2^- \quad \text{and} \quad n = n_1^+ + n_2^+ + n_1^- + n_2^- . \quad (1.16.31)$$

Here the signs denote the direction of motion, and the indices label which wall the molecules are in equilibrium with. Obviously, the heat flux is

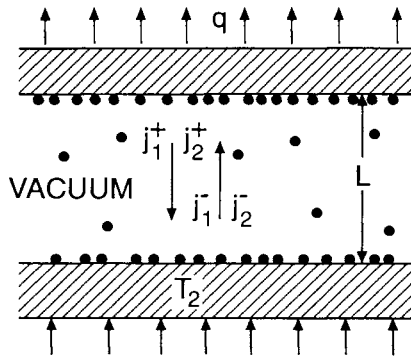


Figure 1.50 Opposite fluxes in an ultrarefined gas carrying out the heat transfer.

$$q = \frac{C_V}{N_0} [T_2 (j_2^- - j_2^+) + T_1 (j_1^- - j_1^+)], \quad (1.16.32)$$

In order to calculate q , one has to determine the relative magnitude of all fluxes. It is clear that the molecules with the “foreign” temperature only appear in the reflected flux $j_1^- = (1 - \alpha)j_1^+$, while those with the native one are either reflected or desorbed: $j_2^- = (1 - \alpha)j_2^+ + \alpha j$. Hence, it follows from the balance considerations that

$$\begin{cases} j_2^- = j_2^+ + \alpha j_1^+ ; & \begin{cases} j_2^+ = (1 - \alpha)j_2^- ; \\ j_1^+ = j_1^- + \alpha j_2^- . \end{cases} \end{cases}$$

The system on the left refers to the lower wall (Fig. 1.50), while that on the right to the upper one. Thus

$$(1 - \alpha)j_2^- = j_2^+ = j_1^- = (1 - \alpha)j_1^+ . \quad (1.16.33)$$

Each of the fluxes consists solely of particles moving “forth” (they return in another flux). So, unlike (1.4.12), we have

$$j_i^\pm = \frac{1}{2} n_i^\pm \bar{v}_i, \quad i = 1, 2, \quad (1.16.34)$$

Generally speaking, all n_i^\pm are different.

The difference in density between the opposing fluxes can be readily illustrated by the following experiment. Joining two vessels filled with rarefied gas at temperatures T_1 and T_2 by a short tube, one can see that eventually the fluxes in the tube in both directions become equal to one another: $j_1^+ = j_2^-$. In view of (1.16.34), this is only possible at $n_2/n_1 = \bar{v}_1/\bar{v}_2$, since the gas density is related to its pressure, so $p_2/p_1 = T_2\bar{v}_1/T_1\bar{v}_2 = (T_2/T_1)^{1/2}$, that is, the pressure in the joined vessels together ceases to be the same, which is just what was observed.

Using (1.16.33) and (1.16.34) in (1.16.31), we get

$$j = (2 - \alpha)j_2^- = (2 - \alpha)j_1^+ = \frac{n}{2} \frac{\bar{v}_1 \cdot \bar{v}_2}{\bar{v}_1 + \bar{v}_2} . \quad (1.16.35)$$

On substitution of (1.16.33) into (1.16.32) and in view of the above result, we can easily obtain

$$q = \frac{C_V \alpha}{N_0 (2 - \alpha)} \cdot \frac{n}{2} \frac{\bar{v}_1 \cdot \bar{v}_2}{\bar{v}_1 + \bar{v}_2} (T_2 - T_1) . \quad (1.16.36)$$

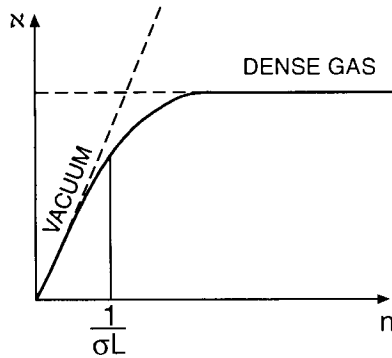


Figure 1.51 Density-dependence of the effective thermal conductivity κ .

The quantity

$$\mathcal{H} = \frac{C_V \alpha}{N_0 (2 - \alpha)} \cdot \frac{nL}{2} \cdot \frac{\bar{v}_1 \cdot \bar{v}_2}{\bar{v}_1 + \bar{v}_2} \quad (1.16.37)$$

has the meaning and dimension of thermal conductivity and is linear in the density of the remaining molecules.

This result holds when $\lambda \gg L$. With increasing of density the sign of the inequality is reversed, and local equilibrium is restored. Only then the previous estimate of \mathcal{H} (1.16.25) becomes valid. Thus the estimate independent of the gas density holds in the limited density range $n \gg 1/\sigma L$ (Fig. 1.51).

Current in Gases

Although at room temperature and atmospheric pressure any gas is a dielectric, there is always a small equilibrium concentration of charges brought about by heat ionization of molecules. When the electric conductivity of a gas becomes observable, the concentration of ions in the unit volume is still much less than the density of neutral particles. Note that this concentration can exceed the equilibrium one, if it is created by external sources: penetrating radiation or emission of electrons from a cathode. Whatever their origin, the charges which find themselves in the spark-gap respond to the applied field and drift in the direction of the force acting upon them. Moving with velocity w , they transfer electricity between electrodes, thus making the gas a conductor.

When electric conduction is unipolar, that is, when all carriers have the same sign, the current density

$$i = e w n, \quad (1.16.38)$$

where n is the concentration of ions, and e is the absolute magnitude of their charge. If the drift speed w is directly proportional to the field

$$w = uE, \quad (1.16.39)$$

then Ohm's law holds

$$i = \sigma E. \quad (1.16.40)$$

The conductivity is

$$\sigma = eun, \quad (1.16.41)$$

where u is the mobility of the current carriers. To prove Ohm's law, it is sufficient to assume that ions completely change the direction of their motion in each collision. Because of this, the mean velocity after collision is equal to zero as in Eq. (1.15.42). In other words, on the average, each collision makes the ion stop, and its acceleration in the next free path starts afresh. That is why charge drift is uniform, despite quadratic increase of the free path with time typical for uniformly accelerated motion (Fig. 1.52).

Indeed, the free path in the direction of the field averaged over initial velocity directions,

$$\bar{x} = \bar{v}_x t + \frac{eE}{2m} t^2 = \frac{eE}{2m} t^2,$$

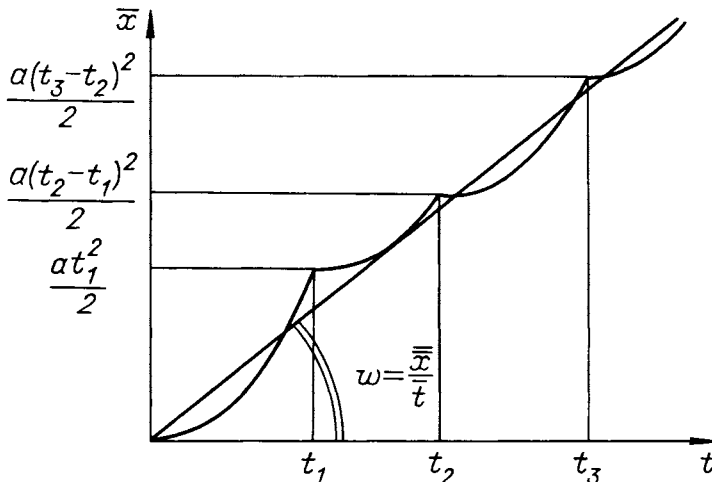


Figure 1.52 Averaged ion drift (straight line) accomplished by a sequence of free paths in an external electric field (polygonal line).

should also be averaged over the distribution of free path times (1.15.15):

$$\bar{x} = \frac{eE}{2m} \int_0^{\infty} t^2 dW(t) = \frac{eE\tau_0^2}{m}.$$

Now it is clear that the drift speed is proportional to the field

$$w = \int \frac{\bar{x}}{\tau_0} dW(v) = u E, \quad (1.16.42)$$

and the mobility of carriers is equal to

$$u \approx \frac{e\tau_c}{m} = \frac{e\lambda}{m\sqrt{8kT/\pi\mu}}. \quad (1.16.43)$$

Naturally, the lighter the charge carriers and the lower the density of the gas they pass through, the greater the mobility.

These qualitative conclusions were verified experimentally by Rutherford, although the measured mobility was found to be less by an order of magnitude than the expected result

$$u = \frac{e\tau_c}{m} = \frac{5 \cdot 10^{-10} \cdot 3 \cdot 10^{-9}}{300 \cdot 10^{-22}} \approx 50 \text{ cm}^2/(\text{V} \cdot \text{sec}) \quad (1.16.44)$$

This anomaly is partly due to an inappropriate estimation of the ion mass. As a rule, owing to their charge, the gas ions attract some neutral particles and form associates which move as a unit. Such ions have greater mass, and therefore are less mobile. Another source of error is the rough nature of the model of hard spheres. The charged particle is the source of a long-range Coulomb field. This affects the ion's trajectories far beyond the limits of their own diameter, that is, in fact, collisions occur at greater distances than one can infer on simple geometric grounds. To put it another way, the effective cross-section of an ion exceeds the sizes of the neutral molecules. Consequently, the frequency of collisions is greater, and the interval between them τ_c is less than was assumed in (1.16.44). These peculiarities of charged particles gave a stimulus for the refinement of electric conduction theory which proved to be quite satisfactory for ions of any substance and both signs.

The single but very important exception from the rule is the case where charge is carried by free electrons. This mechanism of electric conduction was taken to explain the extremely high mobility of negative carriers in some experiments (up to $10^4 \text{ cm}^2/\text{V} \cdot \text{sec}$). In inert gases and strong fields the electrons adhere weakly to molecules and become free, undergoing only elastic collisions. In this case the charge mobility becomes much greater, because the electron's mass is less than that of a negative ion by a factor of 10^5 . On

closer examination of formula (1.16.43), it is seen that the mobility increases by a factor of $\sqrt{M/m} \approx 200$, and this was verified experimentally.

However, this is not all. When free electrons take the role of carriers, the character of their movement through the gas changes. Due to the sharp difference in mass, the energy exchange between electrons and molecules resulting from collisions is hampered. The share of energy transferred from light to heavy particles in collisions is determined by the ratio of their masses. This can easily be seen if one tries to play cherry stones against billiard balls. The energy $\Delta\epsilon$ lost by an electron upon collision accounts for just a small fraction $q = \Delta\epsilon/\epsilon = m/M = 10^{-5}$ of the total energy ϵ it carries. Thus the local equilibrium principle which formed the basis of the previous consideration is violated. Collisions are unable to correct the electron's energy in such a way as to make it correspond to the local temperature of the points where the collisions occur. On the contrary, moving through the gas along the field, the electron accumulates gradually the energy imparted to along the free path. Only an insignificant share of this energy is converted into heat at collisions.

Although unable to take away all the electron's energy, collisions essentially affect the direction of its motion. Owing to this, the work executed by the field accelerates the motion of electrons uniformly in all directions, thus establishing a distribution similar to the Maxwell one. However, the *electron temperature* T_e appearing in this distribution is greater than the local temperature T of the gas. It is determined by the mean electron energy $\bar{\epsilon} = \frac{3}{2}kT_e$.

As long as the energy of electrons is fairly small the electron temperature increases linearly approaching the anode:

$$\frac{3}{2}kT_e = \frac{mv^2}{2} \approx eEx. \quad (1.16.45)$$

However, this rise of temperature cannot continue indefinitely, since upon each collision a q th portion of the electron's energy is lost. At higher ϵ , it is no longer a small value compared with the additional energy acquired in free path. Eventually, ϵ ceases to increase, and all the energy taken from the field is converted to heat transferred to the surroundings.

Accumulation of energy by a drifting electron is described by the equation

$$\frac{d\epsilon}{dt} = eEw - \frac{q}{\tau_c}[\epsilon - \epsilon_0],$$

where $\epsilon_0 = \frac{3}{2}kT$. If the second term is neglected, then $\epsilon = eEwt = eEx$, as in (1.16.45). On the other hand, in the stationary regime $d\epsilon/dt = 0$, while

$$\epsilon = \epsilon_0 + \frac{eEw\tau_c}{q} \approx \frac{eEw\tau_c}{q},$$

if electrons become hot enough. Using (1.16.42) and (1.16.43), we obtain

$$\epsilon = \frac{mw^2}{q} = \frac{m\bar{v}^2}{2},$$

or

$$w = \left(\frac{q}{2}\bar{v}^2\right)^{1/2}.$$

As is seen, the drift speed is less than the root mean square velocity by a factor of $\sqrt{q/2}$. Revealing the meaning of w with the help of Eqs. (1.16.42) and (1.16.43), we find

$$\frac{e\lambda}{m\bar{v}}E = \sqrt{\frac{q}{2}\bar{v}^2},$$

and

$$\frac{3}{2}kT_e = \frac{m\bar{v}^2}{2} \approx \frac{e\lambda E}{\sqrt{q}}. \quad (1.16.46)$$

Thus the kinetic energy of an electron in a stationary drift is $q^{-1/2}$ times as great as the work executed by the field in one free path. The electron temperature T_e exceeds considerably the temperature of the environment, and it is T_e that should be substituted for T in formula (1.16.43) to estimate the electrons' mobility

$$u = (e\lambda\sqrt{q}/mE)^{1/2}. \quad (1.16.47)$$

So it turns out that, due to the dependence of the electron temperature on the field, the direct proportionality between w and E is replaced by the relation

$$w = uE = (e\lambda E\sqrt{q}/m)^{1/2}. \quad (1.16.48)$$

Thus the notion of mobility becomes less significant, as this quantity is no longer a constant. Under normal conditions, for a field of 10 V/cm, $u \sim 10^3 \text{ cm}^2/\text{V} \cdot \text{sec}$, $T_e \sim 1000 \text{ K}$, and the kinetic energy of electrons is about 0.1 eV.

Formulae (1.16.45) and (1.16.46) describe two opposite limits. The former accounts for the electron acceleration interval where losses are very low, while the latter the stationary regime where the gain and expenditure of energy compensate one another. On its way from the cathode to anode, the electron passes from one region to another. Obviously, the boundary is the point where, according to both approximate estimates, the electron temperature is the same: $(e\lambda E)/\sqrt{q} = eEx_0$. Thus

$$x_0 = \frac{\lambda}{\sqrt{q}} \quad (1.16.49)$$

is approximately one hundred times greater than the free path length. At normal pressure, it is still a small value: $x_0 \sim 10^{-2}$ cm. So, under normal conditions, the electron drift is stationary over almost the entire discharge gap, except in a very narrow layer. However, at pressures a thousand times less than atmospheric, the acceleration interval extends to macroscopic sizes. If the electrodes are separated by a distance of the order of several centimeters, the stationary regime is not reached at all. As is seen from formula (1.16.45), in this case the electron temperature is measured merely by the distance covered. Thus any *a priori* prescribed energy may be imparted to the electrons by installing a grid near the cathode within the acceleration interval. The energy of the electrons which reach the grid will be specified by the difference in potential between the grid and the cathode.

So, the violation of local equilibrium results in the coexistence of two gases in the spark-gap: molecular and electron, each having its own temperature. The difference in temperature is maintained and controlled by the field: the source of energy accumulation. Thus one can easily increase the field to such a degree that the energy of heat motion of electrons will be sufficient for excitation, and ultimately for ionization of neutral particles of the matter. Atoms and molecules excited upon collisions with electrons can radiate the acquired energy in the visible range. In principle, the operation of gas-filled tubes which remain relatively cool, despite the daylight they create, is based just on this phenomenon. At high electron temperatures, ionization of molecules also becomes possible. The chain ionization results in an avalanche increase of current carriers. Positive ions also contribute to gas conductivity. Among other things, they bombard the cathode knocking additional electrons out of it. Thus at a definite potential difference, the "breakdown" of a gas may take place—a sudden conversion into a highly ionized conducting matter (*plasma*).